Problems in Nonlinear Diffusion

Thesis by
Thomas P. Witelski

In Partial Fulfillment of the Requirements
for the Degree of
Doctor of Philosophy

California Institute of Technology
Pasadena, California

1995

(Submitted April 21, 1995)

Acknowledgements

I would like to thank my advisor, Professor Donald S. Cohen, for sharing his years of experience with me and for introducing me to many aspects of the field of applied mathematics. My research was supported by a National Science Foundation graduate fellowship.

Abstract

A variety of effects can occur from different forms of nonlinear diffusion or from coupling of diffusion to other physical processes. I consider two such classes of problems; first, the analysis of behavior of diffusive solutions of the generalized porous media equation, and second, the study of stress-driven diffusion in solids. The porous media equation is a nonlinear diffusion equation that has applications to numerous physical problems. By combining classical techniques for the study of similarity solutions with perturbation methods, I have examined some new initial-boundary value problems for the porous media equation, including "stopping" and "merging" problems. Using matched asymptotic expansions and boundary layer analysis, I have shown that the initial deviations from similarity solution form in these problems are asymptotic beyond all orders. Applications of these studies to the Cahn-Hilliard and Fisher's equations are also considered. In my examination of stress-driven diffusion, I consider models for the behavior of systems in the emerging technological field of viscoelastic diffusion in polymer materials. Using asymptotic analysis, I studied some of the non-traditional effects, shock formation in particular, that occur in initial-boundary value problems for these models. Phase-interface traveling waves for "Case II" diffusive transport were also studied, using phase plane techniques.

Contents

List of Figures

Chapter 1

Chapter 5

Part I

Similarity solutions for nonlinear diffusion

Introduction

Here we study similarity solutions of problems for nonlinear diffusion equations. For these special solutions, the governing partial differential equation can be reduced to a more tractable ordinary differential equation. Using perturbation methods and matched asymptotic expansions it will be shown how these similarity solutions can be employed to construct solutions for more general problems involving the full partial differential equation. In the first section, the method of inverse similarity solutions for the porous media diffusion equation is discussed. The influence of boundary conditions and merging solutions of similarity type are analyzed for this class of problem. In the second section, this approach is extended to study merging traveling wave solutions in a porous-Fisher's equation model for population dynamics. Finally, we consider the consequences of non-invertible inverse similarity solutions that occur for nonlinear forward-backward heat equations in the Cahn-Hilliard model.

Chapter 1

The stopping problem for the porous media equation

1.1 Introduction

The general nonlinear diffusion equation

$$\frac{\partial u}{\partial t} = \frac{\partial}{\partial x}\left(D(u)\frac{\partial u}{\partial x}\right), \tag{1.1}$$

specialized to the case $D(u) = u^n$ $(n > 0)$ is called the porous media equation

$$\frac{\partial u}{\partial t} = \frac{\partial}{\partial x}\left(u^n\frac{\partial u}{\partial x}\right). \tag{1.2}$$

This model can be used to describe diffusive behavior in many physical applications [2], [5], [19], [22], [28]. We illustrate two of these applications below. The mathematical properties of certain classes of solutions of (1.2) have been

studied extensively [3], [4], [20], [21]. It is well-known that if the diffusion coefficient $D(u)$ vanishes at $u = 0$, then (1.1) has solutions with compact support and well-defined interfaces that move with finite velocity – this is also the case for (1.2).

We formulate an initial-boundary value problem for (1.2) on a finite domain that admits a similarity solution of this form for a finite interval of time. When the solution reaches the edge of the finite domain, the solution's further evolution will come under the influence of the boundary condition. The focus of this report is to analyze the ability of a fixed boundary to "stop" an expanding similarity solution. The solution of the "stopping problem" will be an analytic description of the short-time affect of the boundary on the similarity solution. This approach is motivated by suggestions to generalize the use of similarity solutions made by Barenblatt [6], [17]. In developing this description we will construct an asymptotic solution for a linear problem and show how the approach generalizes to nonlinear problems. Finally, the techniques used to solve the stopping problem will be extended to describe interface-merging dynamics for the porous media equation.

1.2 Derivations of the model

The porous media equation is a model that occurs in many physical problems [4], [22]. To illustrate this point we present derivations of the model for problems in porous-media diffusion and for gravity-dominated spreading of thin layers of viscous liquids.

Following Aronson's presentation [4], we consider the flow of a gas through

a porous medium. The conservation of mass for this system is given by

$$\varepsilon \frac{\partial \rho}{\partial t} + \nabla \cdot (\rho \mathbf{u}) = 0, \tag{1.3}$$

where ε is the porosity of the medium and ρ,$\mathbf{u}$ are the density and velocity of the diffusing gas. A popular model for the velocity in porous media is given by Darcy's law

$$\mathbf{u} = -\frac{\kappa}{\mu} \nabla P, \tag{1.4}$$

where κ is the permeability of the medium, μ is the viscosity of the gas and P is the local pressure. This system is closed using the equation of state for an isentropic gas,

$$P = P_0 \rho^\gamma, \tag{1.5}$$

where γ is a constant related to the specific heats of the gas. Combining these equations to eliminate $\mathbf{u}$ and P yields the porous media equation

$$\frac{\partial \rho}{\partial t} = D \nabla \cdot (\rho^\gamma \nabla \rho), \tag{1.6}$$

where $D = \frac{\kappa \gamma P_0}{\mu \varepsilon}$.

Alternately, following Buckmaster's presentation [9], we derive the equation governing a layer of incompressible, viscous liquid spreading over a level surface, neglecting surface tension. Consider the case where we have a drop of liquid with upper surface $z = h(x, y)$ spreading on the dry surface $z = 0$.

The momentum balance for the drop is

$$\frac{D\mathbf{u}}{Dt} = -\frac{1}{\rho}\nabla P + \nu\nabla^2\mathbf{u} - \mathbf{g}, \tag{1.7}$$

where ν is the kinematic viscosity and $\mathbf{g}$ is the acceleration due to gravity. Using approximations from lubrication theory, we may take the pressure to be

$$P = -\rho g(z - h), \tag{1.8}$$

and reduce (1.7) to

$$\frac{\partial^2\mathbf{u}}{\partial z^2} = \frac{g}{\nu}\nabla h(x, y). \tag{1.9}$$

Applying no-slip boundary conditions at $z = 0$ ($\mathbf{u} = \mathbf{0}$), and free-slip conditions at the drop's surface $z = h$ ($\mathbf{u}_z = 0$) yields

$$\mathbf{u} = \frac{g}{\nu}\nabla h\left(\tfrac{1}{2}z^2 - hz\right). \tag{1.10}$$

Integrating the velocity over the height of the drop yields the local mass flux

$$\mathbf{q} = \int_0^h \rho\mathbf{u}\, dz = -\frac{\rho g}{3\nu}h^3\nabla h. \tag{1.11}$$

Then, writing the conservation of mass,

$$\rho\frac{\partial h}{\partial t} + \nabla\cdot\mathbf{q} = 0, \tag{1.12}$$

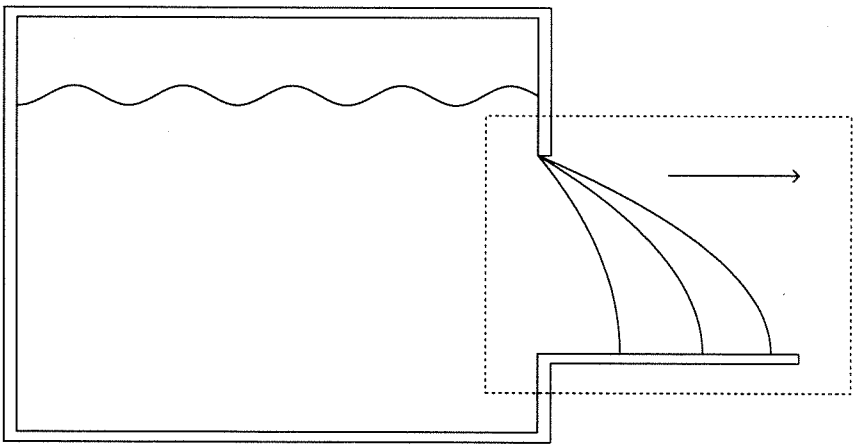

Figure 1: Liquid pouring out of a tank – a physical situation corresponding to initial-boundary value problem (1.14a–c).

yields the porous media equation

$$\frac{\partial h}{\partial t} = D\nabla \cdot (h^3 \nabla h), \tag{1.13}$$

where $D = \frac{g}{3\nu}$.

Many of the qualitative properties of solutions of (1.2) are the same for all $n > 0$. While much of our analysis will be done for a modified model with $n = 1$ [17], [23], we use Buckmaster's model with $n = 3$ to fix physical ideas. We will address some of the differences in the analysis and the nature of solutions for the cases $n < 1$ and $n > 1$ later, but now we formulate a problem for the porous media equation that will lead to the "stopping" phenomenon.

1.3 The initial-boundary value problem

We consider the one-dimensional initial-boundary value problem for the porous media equation

$$u_t = (u^n u_x)_x, \tag{1.14a}$$

on the finite domain $0 < x < 1$ for $t > 0$ with $n > 0$, boundary conditions

$$u(0,t) = 1, \qquad u(1,t) = 0, \tag{1.14b}$$

and initial condition

$$u(x,0) = 0. \tag{1.14c}$$

In the context of spreading viscous liquids, this problem describes the behavior, in the region of the spout, of a liquid pouring out of a large tank (see Figs. 1, 2).

It has been shown that (1.14a) has well-defined non-negative compact-support solutions [4]. Beyond the leading-edge of the region of support, or the interface, the solution vanishes identically (see Fig. 3). Before the leading-edge hits the boundary at $x = 1$, the boundary condition there is trivially satisfied; hence we can find a similarity solution of the form

$$u(x,t) = (U(z))^+, \qquad z = x/\sqrt{t}, \tag{1.15}$$

where $(w)^+ \equiv \max(w, 0)$ and $U(z)$ satisfies the ordinary differential equation

$$-\frac{1}{2} z U'(z) = (D(U)U'(z))'. \tag{1.16}$$

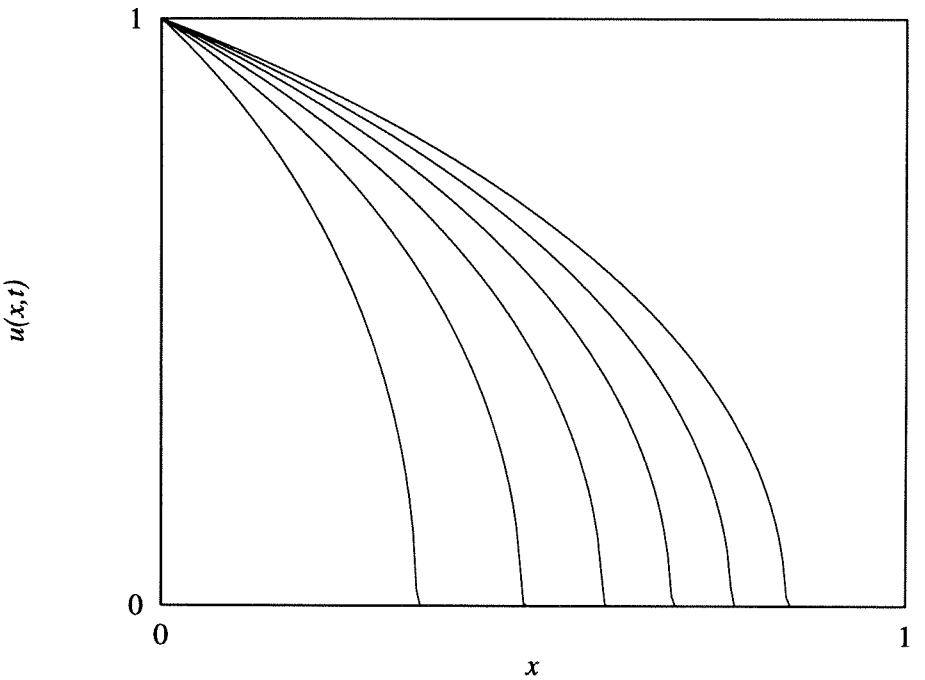

Figure 2: The behavior of the solution $u(x,t)$ for short times.

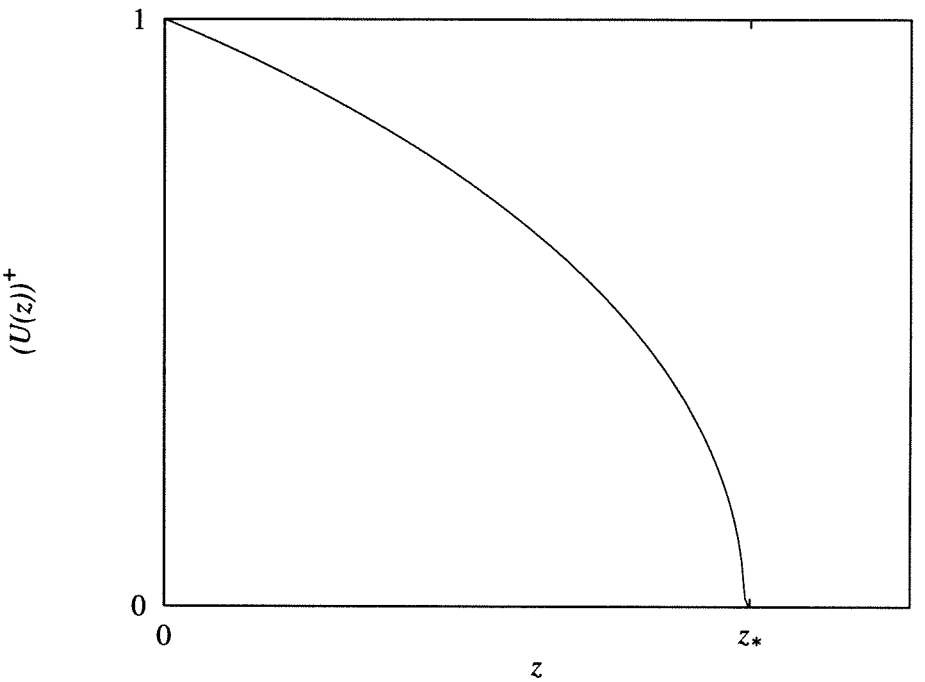

Figure 3: The compact-support similarity solution $(U(z))^+$.

To uniquely specify the desired similarity solution, we give two conditions. First, transforming the boundary condition at $x = 0$ yields $U(0) = 1$. Secondly, we integrate (1.16) over the region of support to yield a statement of global conservation of mass. We denote the interface position by z_*, where $U(z_*) = 0$ by continuity of the solution. Additionally, requiring the flux, $-D(U)U'(z)$, to vanish at z_* [5], [25] yields

$$-\frac{1}{2}\int_0^{z_*} U(z)\,dz = D(1)U'(0), \tag{1.17}$$

which is an equation for the unknown interface position z_*. Observe that the position of the leading edge is $x_*(t) = z_*\sqrt{t}$ which moves with velocity $v_*(t) = z_*/\sqrt{4t}$, which is finite for $t > 0$. For diffusion coefficients with $D(0) > 0$, (1.17) still applies [26], but the region of support is no longer compact, $z_* \to \infty$, and the well-known result of infinite propagation speed for classical diffusion is recovered.

If we integrate (1.16) from z_* to some indefinite position z and use the chain rule to write z as a function of U, that is $z = z(U)$, then [8], [27]

$$D(U) = -\frac{1}{2}z'(U)\int_0^U z(u)\,du. \tag{1.18}$$

This is a formula that yields the diffusion coefficient corresponding to a given similarity solution. Later, we will use (1.18) to construct a model problem for a modified porous media equation with an explicit closed-form solution. For now, we return to the analysis of (1.14a).

The compact-support similarity solution is valid for times up till the in-

terface $x_*(t)$ hits the right boundary $x = 1$. At that time, $t_* = 1/z_*^2$, $z = z_* x$ and we may determine the final similarity solution $\mathcal{U}(x) \equiv U(x/\sqrt{t_*})$ by solving the scaled ordinary differential equation

$$-\frac{1}{2} z_*^2 x \mathcal{U}'(x) = \left(D(\mathcal{U})\mathcal{U}'(x)\right)', \tag{1.19}$$

subject to the boundary condition $\mathcal{U}(0) = 1$ and

$$-\frac{1}{2} z_*^2 \int_0^1 \mathcal{U}(x)\, dx = D(1)\mathcal{U}'(0). \tag{1.20}$$

Observe that for times $t > t_*$, the similarity solution will not be a solution of the boundary value problem (1.14a–c) since the boundary condition $u(1,t) = 0$ can no longer be satisfied. The solution can no longer continue expanding to the right; it is stopped behind the boundary at $x = 1$ (see Fig. 4). We may describe the "stopped" behavior with the solution of the initial-boundary value problem

$$u_t = (u^n u_x)_x, \tag{1.21a}$$

on $0 < x < 1$ with boundary conditions

$$u(0,t) = 1, \qquad u(1,t) = 0, \tag{1.21b}$$

for $t > t_*$ with initial condition

$$u(x,t_*) = \mathcal{U}(x). \tag{1.21c}$$

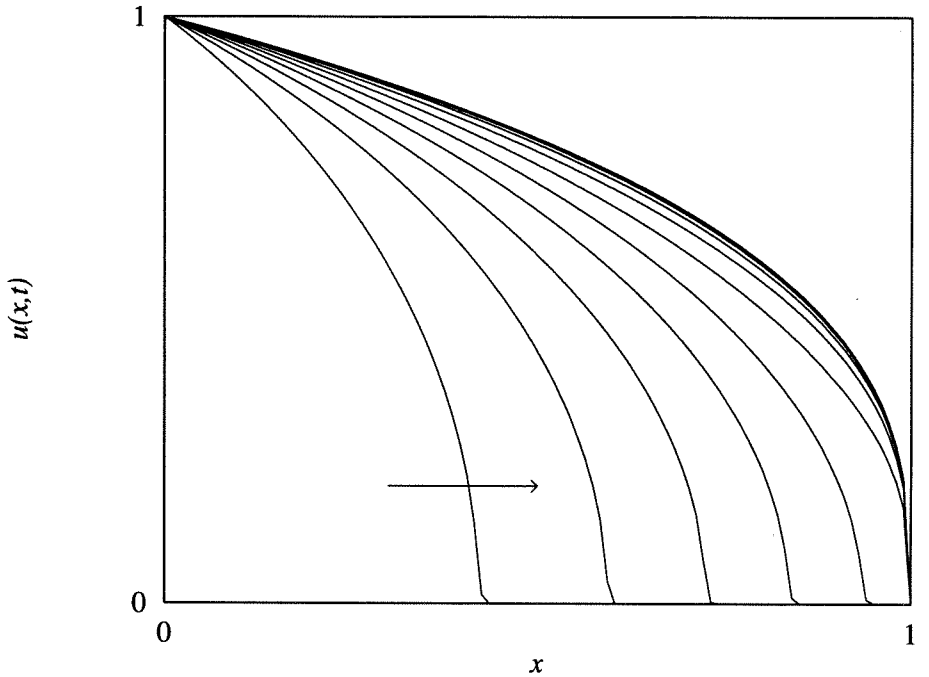

Figure 4: The stopping behavior of $u(x,t)$.

In the following sections we will more carefully examine the nature of "stopping" and develop techniques for studying short-time behavior of solutions to initial-boundary value problems like (1.21a–c).

1.4 The stopping problem

In this section we will expand our discussion of some of the interesting aspects of the stopping problem. In our problem, a moving similarity solution is stopped by a fixed boundary and then the solution evolves there. This is in some ways complementary to Kath's description of the waiting-time problem [22], where a solution evolves for a time before it begins to move.

It is instructive to note that we may reformulate our initial-boundary value problem (1.14a–c) as the moving boundary problem

$$u_t = (u^n u_x)_x, \qquad 0 < x < s(t), \tag{1.22a}$$

$$u(0,t) = 1, \qquad \left.\begin{array}{c} u^n u_x = 0, \\ u = 0, \end{array}\right\} \text{ at } x = s(t), \tag{1.22b}$$

$$u(x,0) = 0, \tag{1.22c}$$

with the prescribed interface

$$s(t) = x_*(t) \equiv \begin{cases} z_* \sqrt{t} & 0 < t < t_*, \\ 1 & t > t_*. \end{cases} \tag{1.22d}$$

For times $t < t_*$, (1.22a–d) has a unique similarity solution that loses this structure for $t > t_*$. Observe that the interface $x_*(t)$ is a continuous function, but it is not smooth. We will study how the kink in $x_*(t)$ at t_* yields effects that propagate into the interior of the domain, where we expect the solution to be very smooth. This behavior is comparable to the reflection of an expansion fan by a wall in the study of gas dynamics.

Another approach to studying this behavior is to reformulate the problem in inverse variables to directly examine the level sets, or contours of constant u. In the study of diffusive problems, this technique is called the isotherm migration method (IMM) [15], [16]. If we consider the similarity ordinary differential equation (1.16) in terms of inverse variables, that is $z = z(U)$

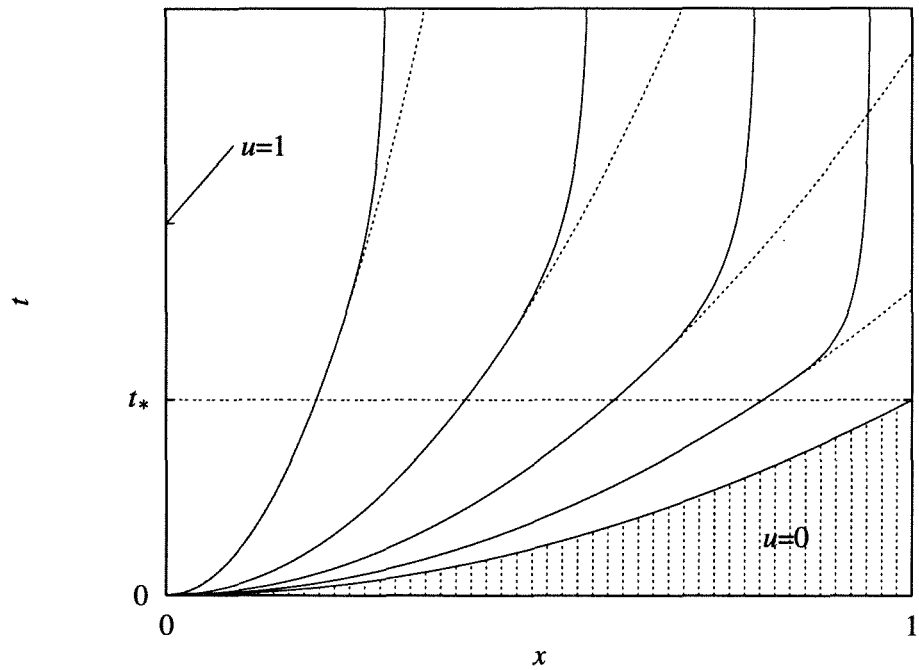

Figure 5: The level sets of the solution (solid) and the similarity solution (dashed).

rather than $U = U(z)$ then we derive the equation

$$\frac{1}{2}z(U) = -\frac{d}{dU}\left(D(U)\left(\frac{dz}{dU}\right)^{-1}\right), \tag{1.23}$$

and the corresponding partial differential equation

$$\frac{\partial x}{\partial t} = -\frac{\partial}{\partial u}\left(D(u)\left(\frac{\partial x}{\partial u}\right)^{-1}\right). \tag{1.24a}$$

This is an equation that describes the motion of the isotherms $x(u,t)$ for all values of u for $0 < u < 1$. The initial and boundary conditions corresponding to problem (1.14a–c) for (1.24a) are

$$x(1,t) = 0, \qquad x(0,t) = x_*(t), \tag{1.24b}$$

$$x(u,0) = 0. \tag{1.24c}$$

Simple numerical discretizations of (1.24a–c) yield very accurate level sets (see Fig. 5). Comparison of the numerical solution with the similarity solution $X(U,t) = z(U)\sqrt{t}$, where $z(U)$ is given by (1.23), shows that there is a smooth transition from the similarity solution for $t < t_*$ to the stopped state for $t > t_*$. In the interior of the domain, the isotherms are smooth curves for all time. We observe that the isotherms diverge from the similarity solution for $t > t_*$ more rapidly as we approach the interface $x_*(t)$.

To analyze the character of the stopped state we will use singular perturbation expansions to yield the short-time asymptotic behavior of the solution. This study will show that for a short time after the solution has formally

stopped, it may still be represented by the similarity solution with an additional correction from a boundary layer. This approach will also be used to characterize the dynamics of the interface in a problem describing merging viscous fluids. In the next section we will study a simple linear problem so that we may find the limitations of the techniques that will consequently be applied to the nonlinear initial-boundary value problem (1.21a–c).

1.5 A linear problem - the heat equation

Here we develop a representation of the solution, for short times, of an initial-boundary value problem for the heat equation. Our representation is asymptotically accurate as $t \to 0$ and clearly separates the influences of initial and boundary conditions on the solution. In the following sections we will show that this approach generalizes to nonlinear problems.

We consider the initial-boundary value problem for the heat equation

$$u_t = u_{xx}, \tag{1.25a}$$

on the finite domain $0 < x < 1$ for $t > 0$, with boundary conditions

$$u(0,t) = 0, \qquad u(1,t) = 0, \tag{1.25b}$$

and smooth initial condition

$$u(x,0) = u_0(x). \tag{1.25c}$$

We are most interested in the behavior for short times $t = 0^+$, hence we introduce the stretched time $\tau = t/\epsilon$, where $0 \ll \epsilon < 1$ is an artificial small parameter, then (1.25a) becomes

$$u_\tau = \epsilon u_{xx}. \tag{1.26}$$

We will use matched asymptotic expansions in ϵ to write a solution of (1.25a–c). The parameter ϵ is called an artificial parameter since it was introduced by an arbitrary scaling and can just as easily be completely eliminated. Artificial parameter expansions can be shown to be nonuniformly convergent [12], [14], [24]. Hence, our solution will be good only for a limited time, but for the study of the stopping problem this will be sufficient to determine the interesting behavior. We now solve (1.26) by constructing an outer solution to satisfy the initial conditions and boundary layers to correct for the applied boundary conditions.

1.5.1 Outer solution

We may obtain the outer solution to (1.26) using a regular perturbation expansion of the form

$$\underline{u}(x,\tau) = \sum_{n=0}^{\infty} \frac{u_n(x)}{n!} \epsilon^n \tau^n, \tag{1.27}$$

which yields

$$u_{n+1}(x) = u_n''(x), \qquad n = 0, 1, 2, \ldots \tag{1.28}$$

and after applying the initial condition, we find that

$$\underline{u}(x,\tau) = \sum_{n=0}^{\infty} \frac{u_0^{(2n)}(x)}{n!}\,\epsilon^n \tau^n. \tag{1.29}$$

Observe that this is a Taylor series in time t with coefficients that contain the spatial dependence. In general, this outer solution will not satisfy the boundary conditions at $x = 0$, and $x = 1$, hence we need to place boundary layers there.

1.5.2 Boundary layers

The stretched variable in the boundary layers scales like $O(\epsilon^{1/2})$ and we recover the full heat equation for the inner problems:

$$\begin{aligned} x = 0 \;:&\quad u_\tau = u_{\tilde{x}\tilde{x}}, \quad 0 < \tilde{x} < \infty, \qquad x = \epsilon^{1/2}\tilde{x}, \\ x = 1 \;:&\quad u_\tau = u_{\overline{x}\overline{x}}, \quad -\infty < \overline{x} < 0, \quad x = 1 + \epsilon^{1/2}\overline{x}. \end{aligned} \tag{1.30}$$

We shall look for a uniformly convergent solution $u(x,t)$ that is the sum of the outer solution (1.29) and corrections due to the boundary layers, $U^L(\tilde{x},\tau)$ and $U^R(\overline{x},\tau)$,

$$u(x,t) = \underline{u}(x,\tau) + U^L(\tilde{x},\tau) + U^R(\overline{x},\tau). \tag{1.31}$$

Note that the boundary layer corrections vanish as $(|\tilde{x}|, |\overline{x}|) \to \infty$ in the interior of the domain, so

$$u(x,t) \sim \begin{cases} \underline{u}(x,\tau) + U^L(\tilde{x},\tau) & |\overline{x}| \to \infty, \\ \underline{u}(x,\tau) + U^R(\overline{x},\tau) & |\tilde{x}| \to \infty. \end{cases} \tag{1.32}$$

This is the only approximation that is made in the analysis of this problem. We consider the situation at $x = 0^+$ in detail; the analysis for the right boundary layer is exactly analogous. Using a Taylor series, we expand the outer solution (1.29) in terms of the inner variables to get

$$\underline{u}(\tilde{x},\tau) = \sum_{n=0}^{\infty}\sum_{m=0}^{\infty} \frac{u_0^{(2n+m)}(0)}{m!\; n!}\, \epsilon^{n+\frac{m}{2}} \tilde{x}^m \tau^n. \tag{1.33}$$

Substituting the uniform solution (1.32) into (1.30) yields an initial-boundary value problem for the boundary layer correction on $0 < \tilde{x} < \infty$

$$U^L_\tau = U^L_{\tilde{x}\tilde{x}}, \tag{1.34a}$$

$$U^L(0,\tau) = -\sum_{n=0}^{\infty} \frac{u_0^{(2n)}(0)}{n!}\, \epsilon^n \tau^n, \qquad U^L(\tilde{x}\to\infty,\tau)\to 0, \tag{1.34b}$$

$$U^L(x,0) \equiv 0. \tag{1.34c}$$

We then expand U^L in a perturbation series

$$U^L(\tilde{x},\tau) = \sum_{n=0}^{\infty} \epsilon^n U_n(\tilde{x},\tau), \tag{1.35}$$

where at each order U_n satisfies

$$U_{n\tau} = U_{n\tilde{x}\tilde{x}}, \tag{1.36a}$$

$$U_n(0,\tau) = -\frac{u_0^{(2n)}(0)}{n!}\, \tau^n, \qquad U_n(\tilde{x}\to\infty,\tau)\to 0. \tag{1.36b}$$

$$U_n(\tilde{x},0) = 0. \tag{1.36c}$$

At each order in ϵ, this problem has a similarity solution of the form

$$U_n(\tilde{x},\tau) = \tau^n y_n(\tilde{z}), \qquad \tilde{z} = \tilde{x}/\sqrt{4\tau}, \tag{1.37}$$

where $y_n(\tilde{z})$ satisfies the ordinary differential equation

$$y'' + 2\tilde{z}y' - 4ny = 0. \tag{1.38}$$

If we let $m = 2n$ then we obtain the differential equation for integrals of the error function [1]

$$w'' + 2\tilde{z}w' - 2mw = 0, \tag{1.39}$$

which has the solution that vanishes as $z \to \infty$

$$w(\tilde{z}) = I_m(\tilde{z}) \equiv 2^m\Gamma\left(\frac{m}{2}+1\right)\,\mathrm{i}^m\mathrm{erfc}(\tilde{z}), \tag{1.40}$$

where $I_m(0) = 1$. Note that $\mathrm{i}^m\mathrm{erfc}(\tilde{z})$ is a standard notation where i refers to an integral operator, not the complex number i. These functions can be generated from the recursion relation

$$\mathrm{i}^m\mathrm{erfc}(\tilde{z}) = -\frac{\tilde{z}}{m}\mathrm{i}^{m-1}\mathrm{erfc}(\tilde{z}) + \frac{1}{2m}\mathrm{i}^{m-2}\mathrm{erfc}(\tilde{z}), \qquad m = 1,2,3,\ldots \tag{1.41a}$$

where

$$\mathrm{i}^0\mathrm{erfc}(\tilde{z}) = \mathrm{erfc}(\tilde{z}), \qquad \mathrm{i}^{-1}\mathrm{erfc}(\tilde{z}) = \frac{2}{\sqrt{\pi}}\mathrm{e}^{-\tilde{z}^2}. \tag{1.41b}$$

Solving at each order, we find that

$$U_n(\tilde{x},\tau) = -\frac{u_0^{(2n)}(0)}{n!}\,\tau^n I_{2n}\left(\frac{\tilde{x}}{\sqrt{4\tau}}\right). \tag{1.42}$$

Using these solutions, we write a uniformly-convergent-in-space solution to the original problem (1.25a–c) that is good for short times

$$\begin{aligned} u(x,t) = &\sum_{n=0}^{\infty} \frac{u_0^{(2n)}(x)}{n!}\,t^n \\ &- \sum_{n=0}^{\infty} \frac{u_0^{(2n)}(0)}{n!}\,t^n I_{2n}\left(\frac{x}{\sqrt{4t}}\right) - \sum_{n=0}^{\infty} \frac{u_0^{(2n)}(1)}{n!}\,t^n I_{2n}\left(\frac{1-x}{\sqrt{4t}}\right), \end{aligned} \tag{1.43}$$

where the first sum is the outer solution and the following sums are the corrections due to the left and right boundary layers respectively. Observe that (1.43) is valid even when $u_0(x)$ does not satisfy the boundary conditions at $x = 0$, $x = 1$. This solution may be interpreted as being composed of pieces coming from related problems: a Cauchy initial-value problem (the outer solution), and two initial-boundary value problems on semi-infinite domains (the left and right boundary layers). Further analysis of (1.43) is pursued in the next section in order to provide insight into the nature of the representation.

1.5.3 An example

We now carry out a detailed analysis of (1.25a–c) with the specific initial condition

$$u_0(x) = x(1-x). \tag{1.44}$$

The asymptotic solution, (1.43), for this initial condition is

$$\mathcal{U}(x,t) = x(1-x) - 2t + \mathcal{V}(x,t), \tag{1.45}$$

where the boundary layer contribution is given by

$$\mathcal{V}(x,t) = 8t\left(\mathrm{i}^2\mathrm{erfc}\left(\frac{x}{\sqrt{4t}}\right) + \mathrm{i}^2\mathrm{erfc}\left(\frac{1-x}{\sqrt{4t}}\right)\right). \tag{1.46}$$

We now compare (1.45) with two representations of the exact solution of (1.25a–c). Using the Laplace transform method [11], we find that

$$u_{\mathcal{L}}(x,t) = x(1-x) - 2t + v(x,t), \tag{1.47}$$

where

$$v(x,t) = 8t\sum_{k=0}^{\infty}(-1)^k\left(\mathrm{i}^2\mathrm{erfc}\left(\frac{x+(k+\frac{1}{2})}{\sqrt{4t}}\right) + \mathrm{i}^2\mathrm{erfc}\left(\frac{1-x+(k+\frac{1}{2})}{\sqrt{4t}}\right)\right). \tag{1.48}$$

Alternately, using elementary separation of variables, the Fourier series solution is

$$u_{\mathcal{F}}(x,t) = \frac{8}{\pi^3}\sum_{k=0}^{\infty}\frac{\mathrm{e}^{-(2k+1)^2\pi^2 t}}{(2k+1)^3}\sin(2k+1)\pi x. \tag{1.49}$$

By studying certain properties of the solution we will illustrate the virtues of our asymptotic representation.

First, we see that (1.45) is a closed-form representation as opposed to the infinite series in the exact solution. Indeed, comparing $\mathcal{V}(x,t)$ with $v(x,t)$

we note that the asymptotic solution replaces two infinite series of $\mathrm{i}^2\mathrm{erfc}$'s by just two $\mathrm{i}^2\mathrm{erfc}$'s! The asymptotic accuracy of $\mathcal{U}(x,t)$ for $t \to 0^+$ can be shown from the agreement of the Laplace transforms of v and $\mathcal{V}$ as $s \to \infty$ [10],

$$\hat{v}(x,s) = \frac{2\cosh\sqrt{s}(x-\frac{1}{2})}{s^2\cosh\frac{1}{2}\sqrt{s}}, \qquad \hat{\mathcal{V}}(x,s) = \frac{4\cosh\sqrt{s}(x-\frac{1}{2})}{s^2 e^{\sqrt{s}/2}}, \tag{1.50}$$

and $\hat{\mathcal{V}} \sim \hat{v}$ as $s \to \infty$. Our representation also does not suffer problems from nonuniformly convergence of series: consider the calculation of $u_t(x,t)$ at $t = 0$. We know that the exact solution should have $u_t = 0$ at $x = 0$ and $x = 1$ for all times since u is prescribed to be a constant on the boundaries. However, from the Fourier series solution

$$\left.\frac{\partial u_{\mathcal{F}}}{\partial t}\right|_{t=0} = -2\left(\frac{4}{\pi}\sum_{k=0}^{\infty}\frac{\sin(2k+1)\pi x}{2k+1}\right) = -2, \tag{1.51}$$

where the above sine series is a nonuniformly-convergent representation of $u \equiv 1$. Consequently we see that the behavior near $x = 0$ and $x = 1$ for $t \to 0$ is not well-handled by this representation of the solution. In contrast, from the asymptotic solution

$$\begin{aligned}\frac{\partial \mathcal{U}}{\partial t} = -2 + 8\left(\mathrm{i}^2\mathrm{erfc}\left(\frac{x}{\sqrt{4t}}\right) + \mathrm{i}^2\mathrm{erfc}\left(\frac{1-x}{\sqrt{4t}}\right)\right) + \\ \frac{2}{\sqrt{t}}\left(x\mathrm{i}^1\mathrm{erfc}\left(\frac{x}{\sqrt{4t}}\right) + (1-x)\mathrm{i}^1\mathrm{erfc}\left(\frac{1-x}{\sqrt{4t}}\right)\right),\end{aligned} \tag{1.52}$$

which agrees with (1.51) on $0 < x < 1$ as $t \to 0$ and also correctly captures the behavior of the solution on the edges of the domain in the boundary

layers.

The eventual breakdown in validity of our artificial parameter expansion can be tied to the fact that the boundary layers spread like $O\left(\sqrt{t}\right)$ as t increases. As described earlier, the only approximation made in the derivation of the asymptotic solution is that the boundary layer contributions vanish in the interior of the domain. Moreover, we have assumed that the contribution from the boundary layer on the far side of the domain is zero in applying the boundary conditions. In either the limit of an infinite domain, $L \to \infty$, or of small time, $t \to 0^+$, this contribution will be transcendentally small, but on a finite domain there will be an error for $t > 0$. The asymptotic behavior of a boundary layer term $I_{2n}(\tilde{z})$ is

$$I_{2n}(\tilde{z}) \sim \frac{n!}{\sqrt{\pi}\tilde{z}^{2n+1}} \mathrm{e}^{-\tilde{z}^2}, \qquad \tilde{z} \to \infty. \tag{1.53}$$

Hence the behavior of the error for short times is

$$I_{2n}\left(\frac{L}{\sqrt{4t}}\right) \sim \frac{4^{n+1/2} n!}{\sqrt{\pi} L^{2n+1}} t^{n+1/2} \exp\left(-\frac{L^2}{4t}\right), \qquad t \to 0. \tag{1.54}$$

For short times, the exponential is the controlling factor, independent of n, and as $t \to 0$ the error is negligible beyond all orders. We will now consider a nonlinear stopping problem where we will find that a similar boundary layer influences the short-time evolution of the solution.

1.6 Solution of the stopping problem

We will now apply the techniques developed above to study stopping in a nonlinear initial-boundary value problem of the form (1.14a–c). Consider the generalized porous media equation

$$u_t = f(u)_{xx}, \tag{1.55a}$$

on the finite domain $0 < x < 1$ for $t > 0$, with boundary conditions

$$u(0,t) = 1, \qquad u(1,t) = 0, \tag{1.55b}$$

and initial condition

$$u(x,0) = 0, \tag{1.55c}$$

where the chemical potential function $f(u)$ [13] is

$$f(u) = \frac{u^2}{4}\left(1 - \frac{u}{3}\right), \tag{1.55d}$$

where the diffusion coefficient is given by $D(u) \equiv f'(u)$. Note that for (1.55d), $D(u) = O(u)$ as $u \to 0$, so we are considering a modified porous media equation with $n = 1$.

This modified equation is very convenient to study since it possesses a closed-form similarity solution. For arbitrary diffusion coefficients $D(u)$, the similarity solution of (1.55a) can only be obtained from numerical calculations or a perturbation expansion [5] and will be difficult to work with analytically. However, if we write a suitable analytic similarity solution $U(z)$,

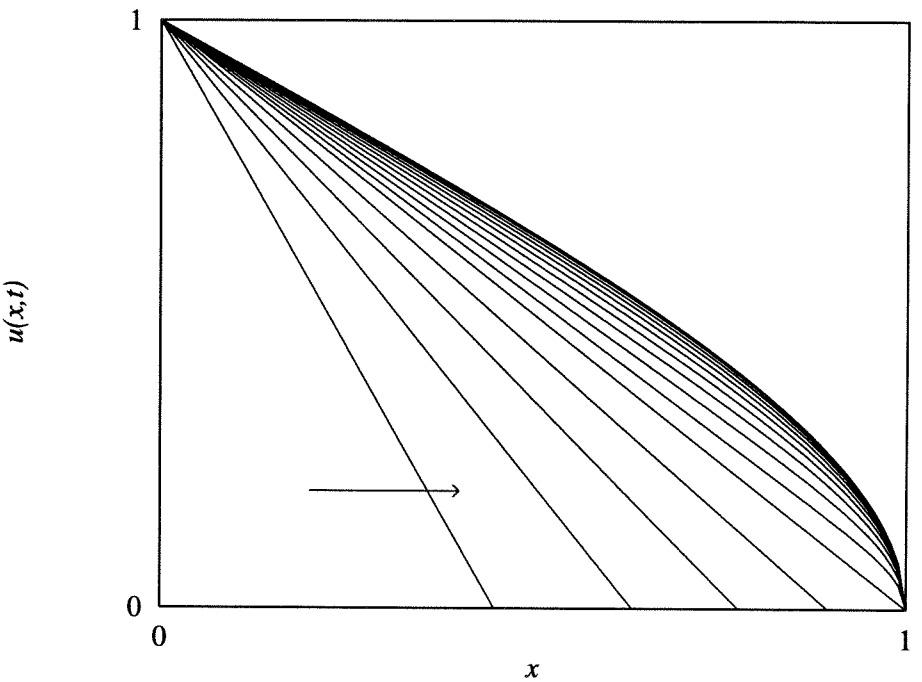

Figure 6: The solution of (1.55a–d).

then we may determine the diffusion coefficient $D(U)$ from (1.18) such that our given $U(z)$ is a solution of (1.55a). By picking a function that approximates the numerical solution of a problem with a given $D(u)$, we may write a modified equation that reproduces the behavior of the solution to arbitrary accuracy. This powerful technique is well known in the modeling of infiltration and sorption problems for porous media diffusion [8], [27]. In our case, we have picked (1.55d) in order to simplify the analysis so that we may focus attention on the phenomenon occurring in the boundary layer. Equation (1.55a,d) has the simple closed-form solution (see Fig. 6)

$$u(x,t) = (U(z))^+ \equiv (1-z)^+, \qquad z = x/\sqrt{t}. \tag{1.56}$$

This solution has interface position $z_* = 1$, hence from the discussion in section 3, stopping occurs for times greater than $t_* = 1$.

We now consider the stopped initial-boundary value problem (1.21a–c) for (1.55a) for $t > 1$ with the initial condition

$$u(x,1) = U(x) = 1 - x. \tag{1.57}$$

We introduce a stretched time τ to focus on the behavior at $t = 1^+$,

$$t = 1 + \epsilon\tau, \tag{1.58}$$

yielding

$$u_\tau = \epsilon f(u)_{xx}, \tag{1.59}$$

where $0 < \epsilon \ll 1$. We search for an outer solution of (1.59) in terms of a regular perturbation expansion

$$\underline{u}(x,\tau) = \sum_{n=0}^{\infty} \epsilon^n u_n(x,\tau), \tag{1.60}$$

which yields the series of problems

$$\begin{array}{lll} O(1) & u_{0\tau} = 0, & u_0(x,\tau) = 1 - x, \\ O(\epsilon) & u_{1\tau} = f(u_0)_{xx}, & u_1(x,\tau) = \frac{1}{2}x\tau. \\ & \cdots & \end{array} \tag{1.61}$$

To $O(\epsilon)$, our outer solution is

$$\underline{u}(x,\tau) = 1 - x + \frac{1}{2}\epsilon x\tau + O(\epsilon^2). \tag{1.62}$$

This can be seen to form the beginning of the expansion of the similarity solution (1.56) for $\epsilon\tau \ll 1$,

$$\begin{aligned} \underline{u}(x,\tau) &= 1 - x(1+\epsilon\tau)^{-1/2} \\ &= 1 - x\left(1 - \frac{1}{2}\epsilon\tau + \frac{3}{8}\epsilon^2\tau^2 + O(\epsilon^3\tau^3)\right). \end{aligned} \tag{1.63}$$

Hence, we actually know the outer solution to all orders since (1.56) is an exact solution of (1.55a) for all times (neglecting boundary conditions). Like the outer solution of the linear problem (1.29), (1.64) is completely determined by the initial condition. If our problem were on an unbounded domain, then this would be the solution of a Cauchy problem; for boundary value prob-

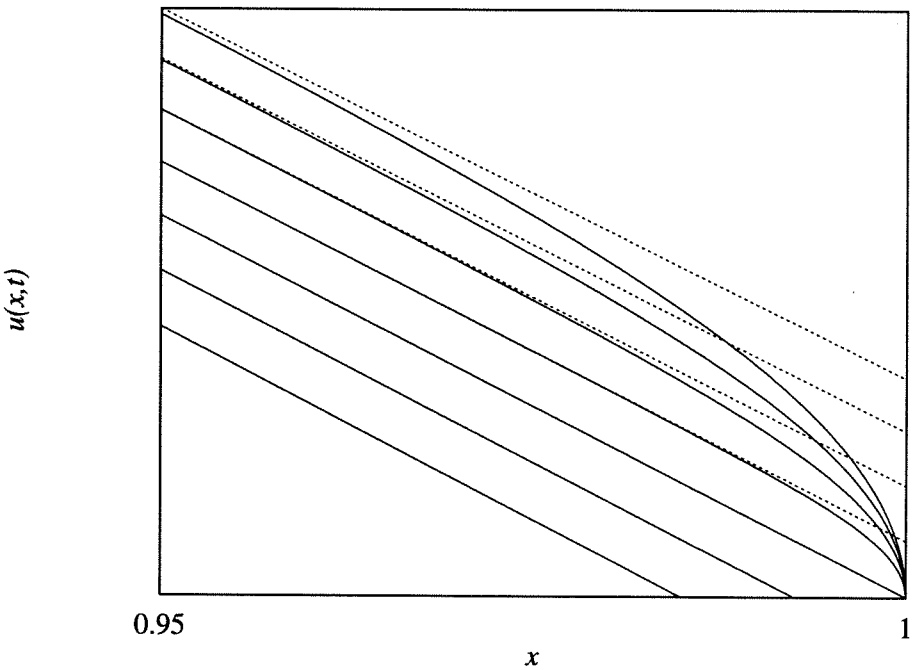

Figure 7: The behavior of the solution in the boundary layer at $x = 1$ compared with the outer similarity solution (dashed).

lems on finite domains this solution must be combined with boundary layer corrections as was done in the previous sections. Solution (1.56) satisfies the boundary condition at $x = 0$ for all times, so we only need a boundary layer at $x = 1$ (see Fig. 7).

Observe that at time τ the value of the outer solution at $x = 1$ is $\underline{u} = \frac{1}{2}\epsilon\tau + O(\epsilon^2)$, therefore we know that u is $O(\epsilon)$ in the right boundary layer. Therefore, rescale

$$u = \epsilon\tilde{u}, \tag{1.64}$$

yielding

$$\tilde{u}_\tau = f(\epsilon\tilde{u})_{xx} = \frac{1}{4}\left(\epsilon^2\tilde{u}^2 + O(\epsilon^3)\right)_{xx}. \tag{1.65}$$

Rescaling the independent variable, we find that the width of the boundary layer is $O(\epsilon)$

$$x = 1 + \epsilon\tilde{x}, \tag{1.66}$$

and to leading order we obtain the porous media equation with $n = 1$

$$\tilde{u}_\tau = \frac{1}{4}\left(\tilde{u}^2\right)_{\tilde{x}\tilde{x}}, \tag{1.67}$$

for $-\infty < \tilde{x} < 0$, $\tau > 0$. At $\tilde{x} = 0$, the boundary layer must satisfy the boundary condition $u = 0$, and by expanding the outer solution in terms of the boundary layer variables, we find that

$$\tilde{u}(\tilde{x} \to -\infty, \tau) \to \frac{1}{2}\tau - \tilde{x} + O(\epsilon). \tag{1.68}$$

This problem has a similarity solution of the form

$$\tilde{u}(\tilde{x}, \tau) = \tau y(\tilde{z}), \qquad \tilde{z} = \tilde{x}/\tau, \tag{1.69}$$

where $y(\tilde{z})$ satisfies

$$y - \tilde{z}y' = \frac{1}{4}\left(y^2\right)'', \tag{1.70a}$$

$$y(0) = 0, \qquad y(\tilde{z} \to -\infty) \to -\tilde{z} + \frac{1}{2}. \tag{1.70b}$$

Let $y(\tilde{z}) = -\tilde{z} + \frac{1}{2} + w(\tilde{z})$, where $w(\tilde{z})$ satisfies

$$(\tilde{z} - \frac{1}{2} - w)w'' + (2 - 2\tilde{z} - w')w' + 2w = 0, \tag{1.71a}$$

$$w(\tilde{z} \to -\infty) \to 0, \qquad w(0) = -\frac{1}{2}. \tag{1.71b}$$

To determine the asymptotic behavior of $w(\tilde{z})$ as $\tilde{z} \to -\infty$ we may approximate (1.71a) by the linear equation

$$w'' - 2w' + \frac{2}{\tilde{z}}w \sim 0. \tag{1.72}$$

Using the WKBJ method [7] to write $w(\tilde{z}) = \mathrm{e}^{s(\tilde{z})}$ we find that

$$w(\tilde{z}) \sim C\tilde{z}^{-1}\mathrm{e}^{2\tilde{z}} \qquad \tilde{z} \to -\infty. \tag{1.73}$$

Therefore, the asymptotic solution is

$$u(x,t) \sim \left(1 - \frac{x}{\sqrt{t}}\right)^{+} + (t-1)w\left(\frac{x-1}{t-1}\right), \qquad t \to 1^{+}, \tag{1.74}$$

and the correction due to the boundary condition is

$$O\left(\frac{(t-1)^2}{x-1}\exp\left[2\frac{x-1}{t-1}\right]\right), \tag{1.75}$$

which is transcendentally small for $x < 1$ as $t \to 1^{+}$. Hence, we have shown that the similarity solution is valid for short times past $t = 1$ with a boundary-condition correction that is negligible beyond all orders as $t \to 1^{+}$ (see Fig. 7). Moreover, (1.74) is appealing since it clearly separates the influence of the

boundary from the rest of the solution. This form of the solution will offer us some insight into a merging process that is studied in the next section.

1.7 Dynamics of merging interfaces in one dimension

In this section we will extend the results derived above to describe interactions of similarity solutions. Generally, similarity solutions only exist for a small class of problems. We will consider a problem whose solution does not have a similarity structure, but for short times we show how to construct a uniform asymptotic solution from combinations of similarity solutions and a nonlinear interaction term.

In the context of viscous flows, we will be describing the short-time behavior of two merging streams in one-dimension (see Fig. 8). We will consider a problem for the generalized porous media equation used in the previous section (1.55a,d) on the finite domain $0 < x < 1$ with boundary conditions

$$u(0,t) = 1, \qquad u(1,t) = 1. \tag{1.76}$$

Observe that the nonlinear diffusion equation (1.55a) admits the following invariant transformations:

$$\begin{aligned} x &\to -x && \text{reflection in space,} \\ x &\to x + h && \text{translation in space,} \\ t &\to t + k && \text{translation in time.} \end{aligned} \tag{1.77}$$

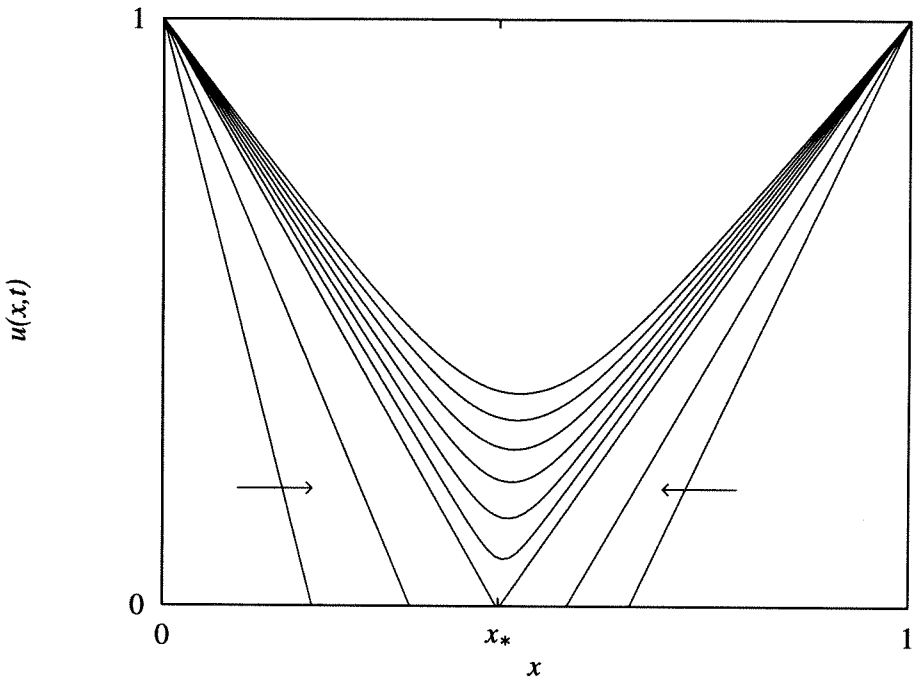

Figure 8: A problem for merging streams.

Using these transformations, we can generalize the similarity solution (1.56). For example,

$$u_0(x,t) = U\left(\frac{x}{\sqrt{t+k_0}}\right) \tag{1.78}$$

describes a similarity solution expanding to the right that started from the initial condition $u_0(x,0) = \left(1 - x/\sqrt{k_0}\right)^+$. Likewise,

$$u_1(x,t) = U\left(\frac{1-x}{\sqrt{t+k_1}}\right) \tag{1.79}$$

is a similarity solution expanding to the left from the boundary condition $u_1(1,t) = 1$ with the initial condition $u_1(x,0) = \left(1 - (1-x)/\sqrt{k_1}\right)^+$.

While the regions of support of $u_0(x,t)$ and $u_1(x,t)$ are disjoint, there is no interaction between them and we may write the exact solution to (1.55a,d), (1.76) as

$$\underline{u}(x,t) = \max(u_0(x,t), u_1(x,t)). \tag{1.80}$$

Nonlinear interactions begin when the regions of support first intersect at

$$(x_*, t_*) = \left(\frac{k_0 + (1-k_1)}{2},\ x_*^2 - k_0\right), \tag{1.81}$$

(see Fig. 9). For short times t_*^+, we assume that the nonlinear interactions are localized in the neighborhood of x_* and, just as in the stopping problem, we determine the scalings for inner problem to be

$$x = x_* + \epsilon\tilde{x}, \qquad t = t_* + \epsilon\tau, \tag{1.82a}$$

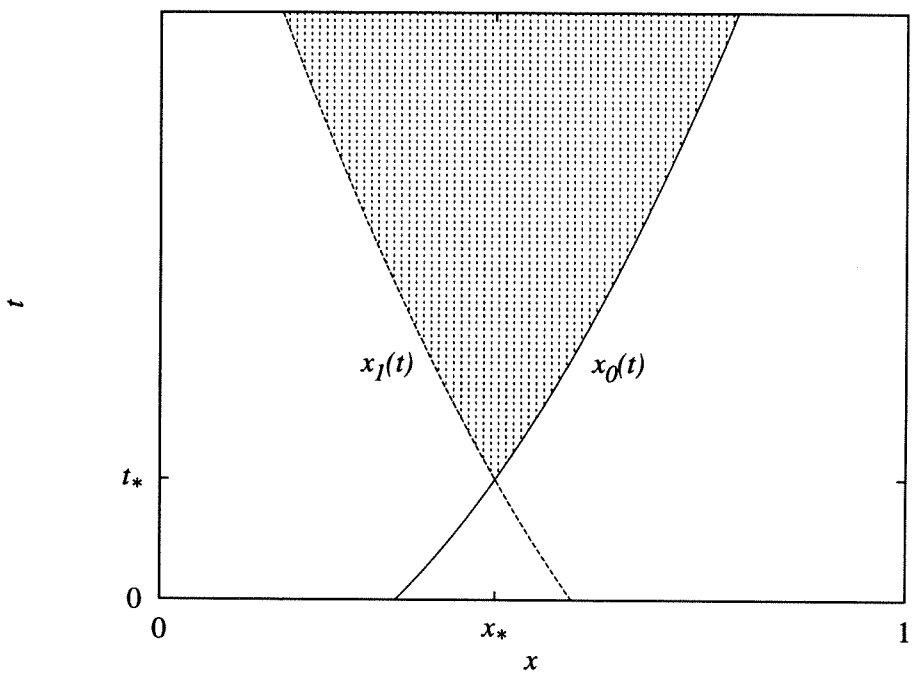

Figure 9: The interfaces of the similarity solutions $u_0(x,t)$ and $u_1(x,t)$ and the region of interaction (shaded) in the x–t plane.

$$u = \epsilon\tilde{u}, \tag{1.82b}$$

so that

$$\tilde{u}_\tau = \frac{1}{4}\left(\tilde{u}^2\right)_{\tilde{x}\tilde{x}} + O(\epsilon), \tag{1.82c}$$

where $-\infty < \tilde{x} < \infty$. Expanding the outer solution in terms of the inner variables, we obtain the boundary conditions to leading order for $\tilde{u}$

$$\tilde{u} \to \begin{cases} \frac{\tau}{2x_*^2} - \frac{\tilde{x}}{x_*} & \tilde{x} \to -\infty, \\ \frac{\tau}{2(1-x_*)^2} + \frac{\tilde{x}}{1-x_*} & \tilde{x} \to \infty. \end{cases} \tag{1.82d}$$

Like the boundary layer problem for the stopping problem, this problem for $\tilde{u}$ has a similarity solution of the form

$$\tilde{u}(\tilde{x}, \tau) = \tau y(\tilde{z}), \qquad \tilde{z} = \tilde{x}/\tau, \tag{1.83}$$

where $y(\tilde{z})$ satisfies

$$y - \tilde{z}y' = \frac{1}{4}\left(y^2\right)'', \tag{1.84a}$$

$$y \to \begin{cases} \frac{1}{2x_*^2} - \frac{\tilde{z}}{x_*} & \tilde{z} \to -\infty, \\ \frac{1}{2(1-x_*)^2} + \frac{\tilde{z}}{1-x_*} & \tilde{z} \to \infty. \end{cases} \tag{1.84b}$$

For times $t > t_*$, the behavior of the approximate solution offers an interesting view of the physical merging process. The outer solution $\underline{u}(x,t)$ describes two isolated streams that flow through each other with no interactions (see Fig. 10). This solution is incorrect due to the lack of conservation

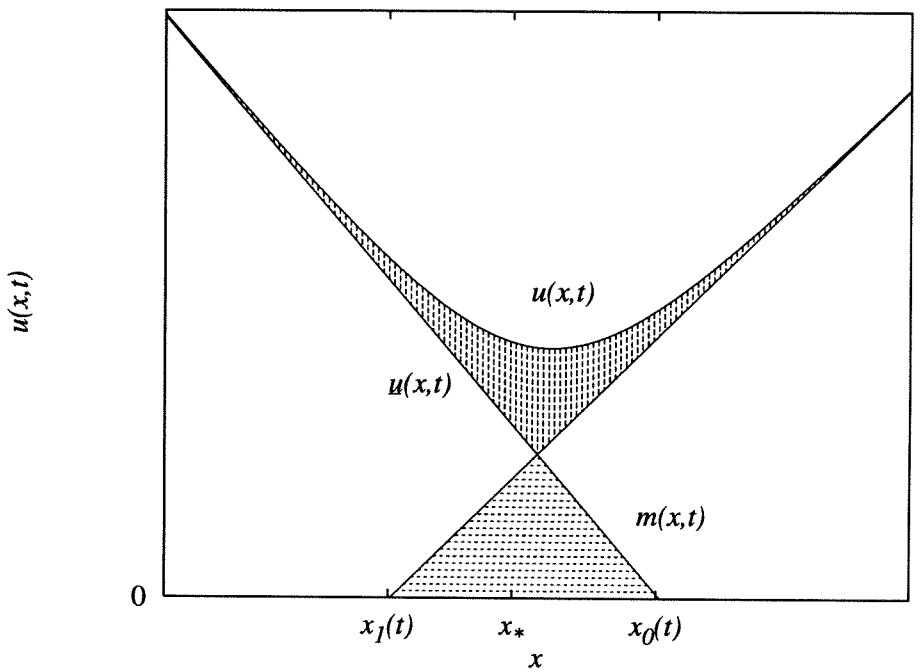

Figure 10: To conserve mass the regions above/below the outer solution must have equal areas.

of mass in the region of overlap, where the mass defect is given by

$$m(t) = \int_{x_1(t)}^{x_0(t)} m(x,t)\,dx, \tag{1.85}$$

where

$$m(x,t) \equiv \min(u_0(x,t), u_1(x,t)), \tag{1.86}$$

with the interfaces for $u_0(x,t)$ and $u_1(x,t)$

$$x_0(t) = \sqrt{t+k_0}, \qquad x_1(t) = 1 - \sqrt{t+k_1}, \tag{1.87}$$

where $x_0(t) > x_1(t)$ for $t > t_*$ and $m(t) \equiv 0$ for $t < t_*$. To conserve mass, the nonlinear interaction solution in the internal layer at x_* must balance this mass defect to leading order, that is

$$m(t) = \int_{-\infty}^{\infty} \epsilon\tilde{u}(\tilde{x},\tau) - \underline{u}(x,t)\,d\tilde{x}. \tag{1.88}$$

Observe however, that away from the interaction region, $m(x,t) = 0$ and the similarity solutions given by the outer solution $\underline{u}(x,t)$ are still locally exact solutions. These physical considerations lead to a physical criterion for judging if the asymptotics yield a good approximation of the true solution; while $m(x,t)$, and presumably the corresponding nonlinear interaction, is localized compared to the length of the domain, the approximation should be good. When the spatial extent of the interaction at x_* becomes significant, then solving an infinite domain shock layer problem for $y(z)$ (1.84a,b) is no longer valid since the effect of the boundary conditions (1.76) on the

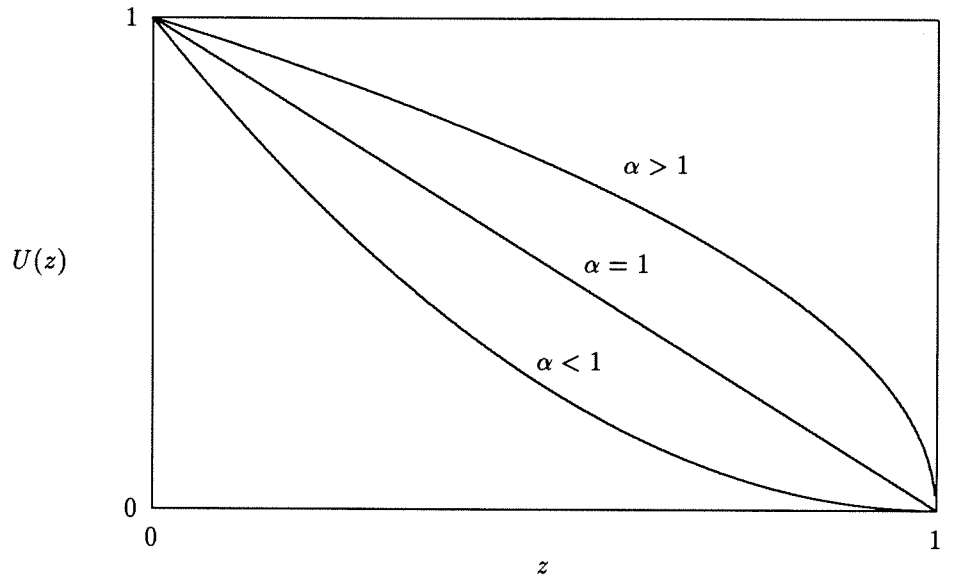

Figure 11: Similarity solutions to the porous media equation for $\alpha < 1$, $\alpha = 1$, and $\alpha > 1$.

finite domain will become important. This situation was observed in the examination of the "far boundary layer" error for the heat equation (section 5).

1.8 Further considerations

We conclude with a discussion of approaches to generalize the analysis given above. The porous media equation will be examined for general $n > 0$ and also for the two-dimensional case.

Above, we have studied the stopping problem for a modified porous media equation with $D(u) = O(u)$, that is, the case $n = 1$. For the general case $D(u) = O(u^\alpha)$, $\alpha > 0$, there are some significant differences in the analysis.

If we assume a similarity solution of the form

$$u(x,t) = (U(z))^+, \qquad U(z) \equiv (1-z)^{1/\alpha}, \qquad z = x/\sqrt{t}, \tag{1.89}$$

then, from (1.18), we obtain $D(u) = O(u^\alpha)$. For $\alpha = 1$ the solution has finite slope at the interface; for $\alpha < 1$ zero slope; and for $\alpha > 1$ infinite slope (see Fig. 11). For the analysis of section 6 to $O(\epsilon)$ there is no trouble for $\alpha \leq 1$. For $\alpha > 1$, we will encounter divergent terms in the direct expansion of the outer solution (1.61). To avoid this difficulty, we can either use the similarity solution (1.89) as the complete outer solution, or attack the problem in inverse variables. While for $\alpha > 1$, $U(z)$ has an infinite slope at the interface $z_* = 1$, in inverse variables, $z(U) = 1 - U^\alpha$ is a nice, differentiable function. Recalling (1.24a), the inverse partial differential equation corresponding to (1.55a) is

$$\frac{\partial x}{\partial \tau} = -\epsilon \frac{\partial}{\partial u}\left(D(u) \left(\frac{\partial x}{\partial u} \right)^{-1} \right), \tag{1.90}$$

and we may expand $x(u,t)$ in a regular perturbation series

$$\underline{x}(u,t) = \sum_{n=0}^{\infty} \epsilon^n x_n(u,t). \tag{1.91}$$

Using either approach, we will determine that in the boundary layer at $x = 1$, $u = O(\epsilon^{1/\alpha})$, and

$$\tilde{u}_\tau = \frac{\alpha}{2} \left(\tilde{u}^{\alpha+1} \right)_{\tilde{x}\tilde{x}}, \tag{1.92}$$

where

$$u = \epsilon^{1/\alpha} \tilde{u}, \qquad x = 1 + \epsilon \tilde{x}. \tag{1.93}$$

This boundary layer problem has the similarity solution

$$\tilde{u}(\tilde{x},\tau) = \tau^{1/\alpha} y(\tilde{z}), \qquad \tilde{z} = \tilde{x}/\tau, \tag{1.94}$$

where $y(\tilde{z})$ satisfies

$$\frac{1}{\alpha} y - \tilde{z} y' = \frac{\alpha}{2} \left(y^{\alpha+1}\right)'', \tag{1.95a}$$

$$y(\tilde{z} \to -\infty) \to \left(-\tilde{z} + \frac{1}{2}\right)^{1/\alpha}, \qquad y(0) = 0. \tag{1.95b}$$

Observe that the similarity variable for the boundary layer problem is given by $\tilde{z} = \tilde{x}/\tau$ for all α; hence the spreading of the boundary-condition influence like $O(t)$ is a generic property of the porous media equation in one dimension.

Application of this analysis can be extended to the porous media equation in several dimensions

$$u_t = \nabla \cdot (u^n \nabla u). \tag{1.96}$$

Consider the Barenblatt similarity solution of (1.96) in two dimensions [18], [22]

$$\mathcal{U}(x,y,t;E) = \frac{1}{t^{1/(n+1)}} \left(\left[E - \frac{n(x^2+y^2)}{4(n+1)t^{1/(n+1)}} \right]^+ \right)^{1/n}, \tag{1.97}$$

where E is a parameter. In Buckmaster's model $\mathcal{U}(x,y,t;E)$ would describe a finite drop of fluid on a surface, spreading under the influence of gravity. We might consider the Cauchy initial-value problem for two merging drops

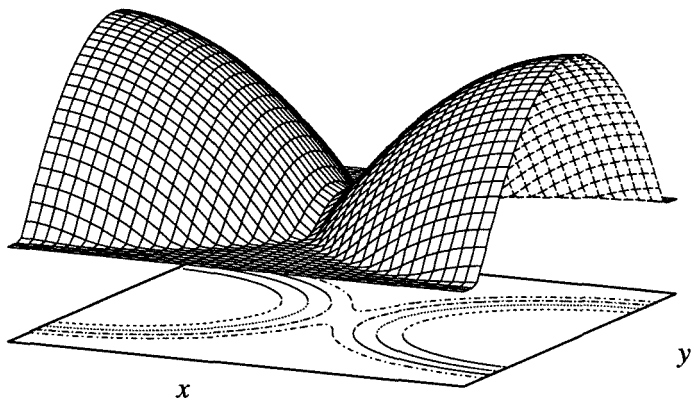

Figure 12: Merging drops in two dimensions.

given by the initial condition

$$u_0(x,y) = \max(u_0(x,y,0), u_1(x,y,0)), \tag{1.98}$$

$$u_0(x,y,t) = \mathcal{U}(x - x_0, y - y_0, t + k_0; E_0), \tag{1.99}$$

$$u_1(x,y,t) = \mathcal{U}(x - x_1, y - y_1, t + k_1, E_1). \tag{1.100}$$

We expect the qualitative features of the solution to this problem to be similar, however the details to the analysis will be much more difficult due to added geometric considerations and the fact that the nonlinear interaction will be governed by a partial differential equation. Numerical simulations support the generalization of the outer solution

$$\underline{u}(x,y,t) = \max(u_0(x,y,t), u_1(x,y,t)), \tag{1.101}$$

for short-times after merging in the two-dimensional case (see Fig. 12).

1.9 Appendix: long-time behavior of the stopping problem

Above, we considered the "stopping problem" – the one-dimensional initial-boundary value problem for the porous media equation

$$u_t = (u^n u_x)_x, \tag{1.102a}$$

on the finite domain $0 < x < 1$ for $t > 0$ with $n > 0$, with boundary conditions

$$u(0,t) = 1, \qquad u(1,t) = 0, \tag{1.102b}$$

and initial condition

$$u(x,0) = 0. \tag{1.102c}$$

The solution to this problem was developed in terms of a compact support similarity solution for times up to a critical stopping time t_*. Moreover, using singular perturbations, a solution for short times after t_* was constructed using matched asymptotic expansions. Here, we complete the analysis of (1.102a-c) by giving a description of the behavior of the solutions for long times, $t \to \infty$.

As $\to \infty$, we expect the solution u to approach a steady-state. The steady-state solution $\overline{u}(x)$ of (1.102ab) satisfies

$$\left(\overline{u}^n \overline{u}_x\right)_x = 0, \tag{1.103a}$$

and

$$\overline{u}(0) = 1, \qquad \overline{u}(1) = 0. \tag{1.103b}$$

The unique solution of this problem is

$$\overline{u}(x) = (1-x)^{1/(n+1)}. \tag{1.104}$$

If our solution at time t, $u(x,t)$, is a function in some sense close to the steady-state, we may express it as the sum of the steady-state and higher

order deviation terms

$$u(x,t) = \overline{u}(x) + \delta v(x,t) + O(\delta^2), \tag{1.105}$$

where δ is a small parameter. This ansatz allows us to study the evolution of the solution using linearized stability analysis.

Substituting (1.105) into (1.102a) and retaining terms to leading order in δ yields

$$\frac{\partial v}{\partial t} = \frac{\partial^2}{\partial x^2}\left(\overline{u}^n v(x,t)\right) + O(\delta). \tag{1.106}$$

Using separation of variables, we search for a solution of the linearized problem in the form

$$v(x,t) = \sum_{k=0}^{\infty} f_k(x) g_k(t). \tag{1.107}$$

We find that $g_k(t) = e^{-\lambda_k^2 t}$ and that $f_k(x)$ satisfies the boundary value problem

$$(1-x)^2 f''(x) - \frac{2n}{n+1}(1-x)f'(x) + \left(\lambda^2(1-x)^{\frac{n+2}{n+1}} - \frac{n}{(n+1)^2}\right) f(x) = 0, \tag{1.108a}$$

$$f(0) = 0, \qquad f(1) = 0, \tag{1.108b}$$

where the eigenvalue λ^2 is the exponential rate of decay of the linearized deviation from the steady-state. We can put (1.108b) in a more standard

form with the change of variables $s = 1 - x$, $y(s) = f(x)$,

$$\left(s^{\frac{2n}{n+1}} y'(s)\right)' + \left(\lambda^2 s^{\frac{n}{n+1}} - \frac{n}{(n+1)^2} s^{-\frac{2}{n+1}}\right) y(s) = 0. \tag{1.109}$$

Equation (1.109) subject to the boundary conditions $y(0) = 0$, $y(1) = 0$ is a self-adjoint eigenvalue problem. It can also be written in the form

$$s^2 y''(s) + \frac{2n}{n+1} s y'(s) + \left(\lambda^2 s^{\frac{n+2}{n+1}} - \frac{n}{(n+1)^2}\right) y(s) = 0, \tag{1.110}$$

which is related to Bessel's equation and has solutions

$$y(s) = s^p J_\nu \left(\frac{\lambda}{q} s^q\right), \tag{1.111}$$

where

$$p = \frac{1-n}{2n+2}, \qquad q = \frac{n+2}{2n+2}, \qquad \nu = \frac{n+1}{n+2}, \tag{1.112}$$

where the J_ν is the Bessel function of fractional order ν and the eigenvalues satisfy

$$J_\nu \left(\frac{\lambda_k}{q}\right) = 0 \qquad \text{for } k = 0, 1, 2, \ldots. \tag{1.113}$$

Therefore, we can write $v(x,t)$ as a generalized Fourier-Bessel series expansion

$$v(x,t) = \sum_{k=0}^{\infty} a_k e^{-\lambda_k^2 t} (1-x)^p J_\nu(\lambda_k (1-x)^q / q). \tag{1.114}$$

In the limit that $t \to \infty$, we may neglect the higher order terms $k = 1, 2, \ldots$ in (1.114) and higher order terms in (1.105) as we approach steady-state.

Hence

$$u(x,t) \sim \overline{u}(x) + a_0 e^{\lambda_0^2 (t-t_*)} (1-x)^p J_\nu(\lambda_0 (1-x)^q/q), \qquad t \to \infty. \quad (1.115)$$

Chapter 2

Merging traveling waves for the porous-Fisher's equation

2.1 Introduction

Wavelike propagation of properties is a phenomenon that is observed in countless biological and chemical systems. In biology, studies of population dynamics are often based on models that show properties spreading in traveling waves [12], [13]. Similarly, in many chemical systems, such as the Belousov-Zhabotinskii (BZ) reaction and combustion problems [13], a "reaction front" propagates with constant velocity into regions of unreacted materials. All of these problems are described by mathematical models called reaction-diffusion equations. We will construct a reaction-diffusion model for a population dynamics system and show how the case of two merging populations can be examined.

The simplest and most well-known reaction-diffusion model is Fisher's equation [4], [9], [12], given in one dimension by

$$\frac{\partial u}{\partial t} = \frac{\partial^2 u}{\partial x^2} + u(1-u), \qquad 0 \leq u(x,t) \leq 1, \tag{2.1}$$

which is a partial differential equation that describes the evolution of a population density function $u(x,t)$. Fisher's original work modeled the spreading of a gene throughout a population [12]. The terms on the right-hand side of (2.1) represent the effects of diffusion and local nonlinear reaction on the population respectively. Equation (2.1) has two homogeneous steady-state solutions; $u \equiv 0$, $u \equiv 1$. These solutions describe spatially-uniform empty and full populations respectively. In the absence of spatial variations, Fisher's equation reduces to the logistic ordinary differential equation

$$\frac{du}{dt} = u(1-u), \tag{2.2}$$

where the nonlinear reaction term $F(u) = u(1-u)$ is called the Pearl-Verhulst model [6], [13]. This model describes growth processes and the stabilization of a saturated finite-density population. Kolmogorov, Petrovksy and Piscounoff (KPP) [9] showed that, for a general class of reaction functions $F(u)$, Fisher's equation yields the same behavior as the Pearl-Verhulst model. We will take reaction terms $F(u)$ from this general class and focus on making an improved population dynamics model by modifying the diffusive term in (2.1) [1], [15].

In the absence of the reaction term, Fisher's equation reduces to the

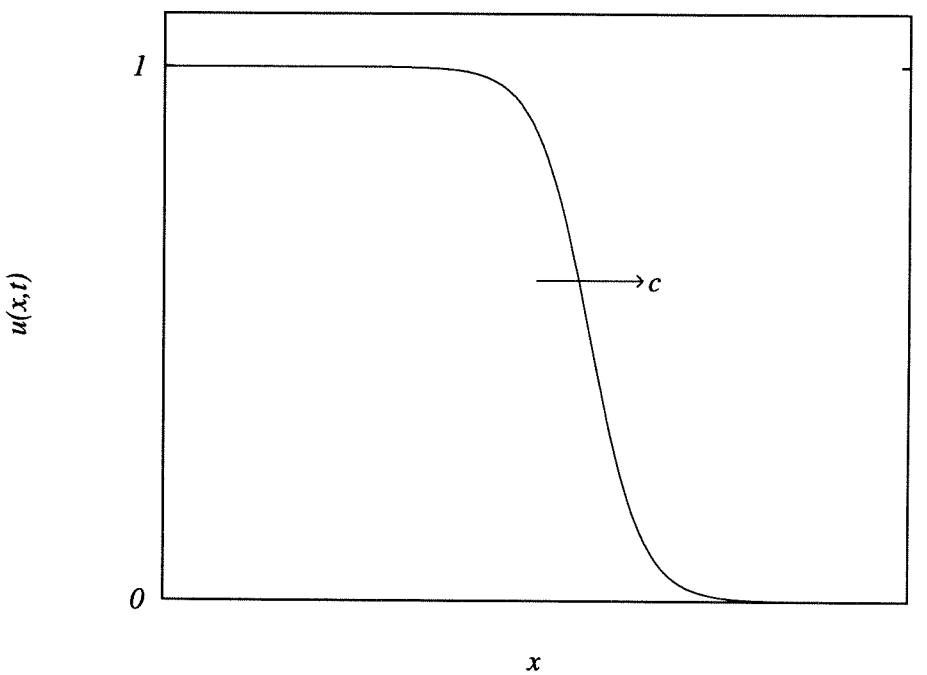

Figure 1: A traveling wave solution of Fisher's equation.

classical model of diffusive processes, the heat equation,

$$\frac{\partial u}{\partial t} = \frac{\partial^2 u}{\partial x^2}. \tag{2.3}$$

This equation describes the spreading out of a population composed of individuals that move about at random [7], [11], [12]. The interaction of diffusion and reaction terms in Fisher's equation yields steady-profile traveling wave solutions (see Fig. 1)

$$u(x,t) = U(z), \qquad z = x - ct, \tag{2.4}$$

in which fronts move with constant velocity c and do not change shape as they propagate. These fronts connect regions where $u = 1$ to regions where $u = 0$. Such traveling wave solutions describe locally saturated populations expanding into empty regions. We will now derive an improved model of the diffusive effects in population dynamics by considering a revised description of the motion of individuals.

Following Gurney and Nisbet [7], we study a population made up of individuals whose motions are governed by a simple drive: to avoid overcrowding. The spatial distribution of a fixed-size population is governed by the conservation law

$$\frac{\partial u}{\partial t} = -\nabla \cdot \mathbf{J}, \tag{2.5}$$

where $\mathbf{J}$ is the local population flux vector. We model the flux as having contributions from random, diffusive motion and from the tendencies of in-

dividuals to avoid crowded regions

$$\mathbf{J} = -D\nabla u + u\mathbf{v}, \tag{2.6}$$

where D is a constant diffusion-coefficient and $\mathbf{v}$ is a density-dependent velocity vector. To represent our model, we take $\mathbf{v}$ to be opposite the direction of maximal density increase

$$\mathbf{v} \propto -\nabla u, \tag{2.7}$$

this is the "directed motion" model of Gurney and Nisbet [7]. A generalization of their model is to have the velocity scaled by an increasing function of density

$$\mathbf{v} = -Eg(u)\nabla u, \tag{2.8}$$

where E is a constant of proportionality. Hence, local density and local gradients both contribute to the anti-crowding impulse. The flux may then be written as

$$\mathbf{J} = -D\nabla u - EG(u)\nabla u, \tag{2.9}$$

where $G(u) = ug(u)$. The relative sizes of D and E determine the magnitudes of the diffusive and directed-motion contributions to the flux. We will consider a population where directed-motion is the dominant effect $E = 1$, $D \ll E$. Then we have

$$\frac{\partial u}{\partial t} = \nabla \cdot (G(u)\nabla u) + O(D), \tag{2.10}$$

which is a generalized porous media equation [16]. Weak diffusive effects can

be added to this model, but the results will only be minor modifications to the solution of (2.10).

The porous media equation with $G(u) = u^\alpha$, $\alpha > 0$,

$$\frac{\partial u}{\partial t} = \frac{\partial}{\partial x}\left(u^\alpha \frac{\partial u}{\partial x}\right), \tag{2.11}$$

is a model describing diffusive processes in many physical systems [8], [10], [16]. Murray [12] describes how this nonlinear diffusion model has been used to represent "population pressure" in biological systems. The mathematical properties of solutions of (2.11) have also been extensively studied [2]. The most significant features are "compact support" and "finite speed of propagation." Non-negative compact support solutions can be written as

$$u(x,t) = (U(x,t))^+, \tag{2.12}$$

where

$$(w)^+ \equiv \max(w,0) = \begin{cases} w & w > 0, \\ 0 & \text{else}, \end{cases} \tag{2.13}$$

and $U(x,t)$ is a smooth function [8]. These population distributions have distinct boundaries, called interfaces, beyond which the population density is identically zero. Solutions of the heat equation (2.3) do not have distinct boundaries; rather, they have populations which extend over the whole domain. Solutions of the porous media equation spread with a finite interface speed. This is also a desirable feature for our model since it corresponds to a finite speed for the motion of individuals in the population. The properties of compact support and finite propagation speed can be shown to be related,

and they also extend to the generalized porous media equation [16].

We will study population dynamics for a generalized directed-motion porous-Fisher's equation [1]

$$\frac{\partial u}{\partial t} = \nabla \cdot (u^{\alpha} \nabla u) + u(1 - u^{\alpha}). \tag{2.14}$$

Using combinations of traveling wave solutions of (2.14), we will describe the behavior of merging populations. In the BZ reaction, circular traveling wave solutions ("target patterns") are often observed [5], [12]. A simple model for the BZ reaction in two dimensions can be reduced to an axisymmetric Fisher's equation [12]

$$\frac{\partial u}{\partial t} = \frac{\partial^2 u}{\partial r^2} + \frac{1}{r}\frac{\partial u}{\partial r} + u(1 - u). \tag{2.15}$$

As described by Murray, (2.15) does not formally allow steady-profile traveling wave solutions of the form (2.4). However, for large radii, $R = \delta^{-1} \gg 1$, where $\delta \to 0$ is a small parameter, we may introduce the change of variables $r = R + \tilde{r}$ to yield

$$\frac{\partial u}{\partial t} = \frac{\partial^2 u}{\partial \tilde{r}^2} + u(1 - u) + \frac{\delta}{1 + \delta \tilde{r}}\frac{\partial u}{\partial \tilde{r}}. \tag{2.16}$$

As $\delta \to 0$, we solve (2.16) using a regular perturbation expansion of the form

$$u(\tilde{r}, t) \sim u_0(\tilde{r}, t) + \delta u_1(\tilde{r}, t) + \ldots. \tag{2.17}$$

To leading order, (2.16) becomes the one-dimensional Fisher's equation

$$\frac{\partial u_0}{\partial t} = \frac{\partial^2 u_0}{\partial \tilde{r}^2} + u_0(1 - u_0) + O(\delta), \tag{2.18}$$

and hence has the leading order axisymmetric traveling wave solution $u_0(\tilde{r}, t) = U(\tilde{r} - ct)$. In three dimensions, the spherical wave case can similarly be reduced to the study of the one-dimensional Fisher's equation. The focus of our study is to analyze the interaction of two expanding populations. By considering the porous-Fisher's equation in one-dimension, we hope to describe the fundamental behavior of merging target patterns in the BZ reaction [5] and more generally, the dynamics of merging populations.

The following section will be a mathematical analysis of this problem. For the global structure of the population distribution, we will make use of traveling wave solutions of the form (2.4), (2.12) found by Newman [12], [13], [14]. Our focus will be the study of the local interactions near the merging interfaces (see Fig. 2). Using perturbation theory and the method of matched asymptotic expansions, we will be able to describe the dominant physical effects for the short-time merging behavior.

2.2 The merging problem

We study the porous-Fisher's equation on $-\infty < x < \infty$:

$$\frac{\partial u}{\partial t} = \frac{\partial}{\partial x}\left(u^\alpha \frac{\partial u}{\partial x}\right) + u(1 - u^\alpha), \tag{2.19}$$

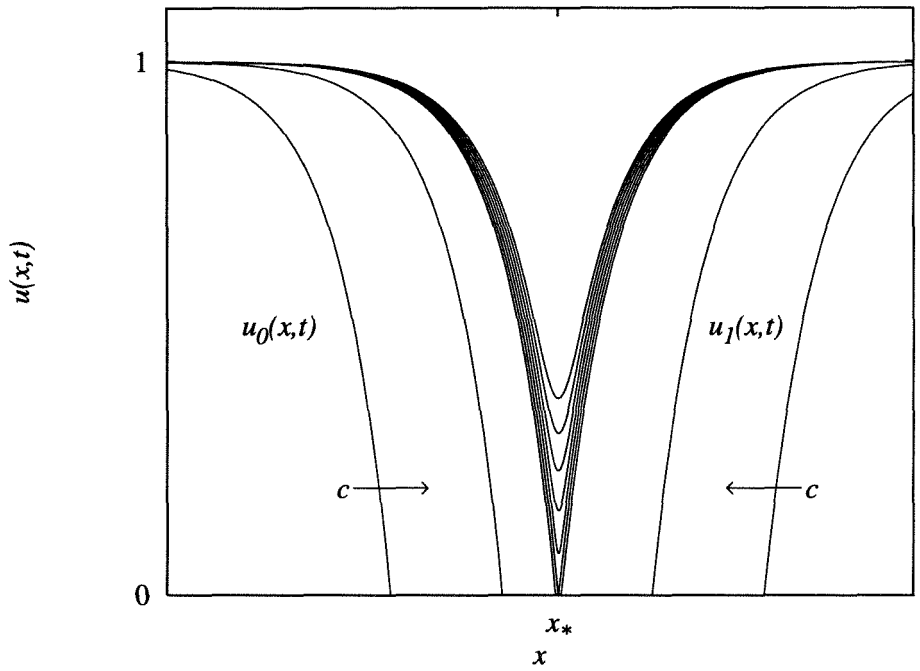

Figure 2: Merging fronts in the porous-Fisher's equation.

for $\alpha > 0$. After reviewing some properties of traveling waves for this equation, we will construct a problem describing merging populations and then solve it using perturbation theory.

Traveling wave solutions of (2.19) of the form $u(x,t) = U(x-ct)$ satisfy the nonlinear ordinary differential equation

$$-cU'(z) = (U^{\alpha}U'(z))' + U(1-U^{\alpha}). \tag{2.20}$$

The corresponding ordinary differential equation for the classical Fisher's equation (2.1) has traveling wave solutions for a continuous range of velocities c. Newman [14] has showed that for the porous-Fisher's equation, there is a unique traveling wave solution

$$u(x,t) = (U(z))^{+} = \left(\left(1 - \exp\left[\frac{\alpha z}{\sqrt{\alpha+1}}\right]\right)^{1/\alpha}\right)^{+}, \qquad z = x - ct, \tag{2.21}$$

with velocity

$$c = \frac{1}{\sqrt{\alpha+1}}. \tag{2.22}$$

Observe that the partial differential equation (2.19) remains unchanged under the following transformations

$$\begin{aligned} x &\to -x && \text{reflection in space,} \\ x &\to x + h && \text{translation in space,} \\ t &\to t + k && \text{translation in time.} \end{aligned} \tag{2.23}$$

Using these transformations, we can generalize the traveling wave solution

(2.21). For example,

$$u_0(x,t) = (U(x - x_0 - ct))^+ \tag{2.24}$$

is a shifted traveling wave moving to the right, starting from position $x = x_0$ at time $t = 0$. Likewise,

$$u_1(x,t) = (U(x_1 - x - ct))^+ \tag{2.25}$$

is a reflected traveling wave moving to the left, starting from position $x = x_1$ at time $t = 0$. Using these two solutions, we now produce a description for merging populations.

While the populations represented by $u_0(x,t)$ and $u_1(x,t)$ remain separated (see Fig. 2), there will be no interaction between them and the overall population distribution is

$$\underline{u}(x,t) = \max(u_0(x,t), u_1(x,t)). \tag{2.26}$$

This equation describes two populations moving toward each other; the two populations first meet at

$$(x_*,\ t_*) = \left(\frac{x_0 + x_1}{2},\ \frac{x_1 - x_0}{2c}\right). \tag{2.27}$$

Hence, if the initial population distribution at time $t = 0$ is given by

$$u^0(x) = \max(u_0(x,0), u_1(x,0)), \tag{2.28}$$

then $\underline{u}(x,t)$ will be the exact solution for times $0 \leq t \leq t_*$. In fact, we can consider a large class of initial conditions similar to (2.28) representing initially widely-separated populations, since KPP showed that each such population will eventually approach a traveling wave profile $U(z)$ [9].

At time t_*, the populations begin to merge and interactions take place. For $t > t_*$, $\underline{u}(x,t)$ is no longer an exact solution; it requires a correction in the neighborhood of x_*. Equation (2.26) incorrectly predicts that at x_* the populations will "pass through" each other with no interactions (see Fig. 3). While near x_*, $\underline{u}(x,t)$ is not accurate, away from x_*, it correctly describes the behavior of the bulk of the population. In our asymptotic solution of (2.19), $\underline{u}(x,t)$ is called the outer solution since it describes the solution away from the critical point x_*. We will show that the correction needed to describe the interaction of the merging populations, called the inner solution, is initially localized to a small neighborhood of x_*.

We will study (2.19) for short times after the merger at $t = t_*$, so we rescale time as

$$t = t_* + \epsilon\tau, \tag{2.29}$$

where $\epsilon \ll 1$ is a small parameter. Observe that at x_*, $u(x,t)$ at time τ is $U(-\epsilon c\tau)$, and from (2.21) we have that

$$u = O(\epsilon^{1/\alpha}). \tag{2.30}$$

Therefore, we rescale the dependent variable as

$$u = \epsilon^{1/\alpha}\tilde{u}, \tag{2.31}$$

and the distinguished limit yields the scaling in x to be

$$x = x_* + \epsilon\tilde{x}, \tag{2.32}$$

yielding the partial differential equation

$$\tilde{u}_\tau = (\tilde{u}^\alpha \tilde{u}_{\tilde{x}})_{\tilde{x}} + \epsilon\tilde{u}(1 - \epsilon\tilde{u}^\alpha). \tag{2.33}$$

Expanding $\tilde{u}(\tilde{x}, \tau)$ in a regular perturbation series as $\epsilon \to 0$,

$$\tilde{u}(\tilde{x}, t) \sim \tilde{u}_0(\tilde{x}, t) + \epsilon\tilde{u}_1(\tilde{x}, t) + \ldots, \tag{2.34}$$

yields the leading-order porous media equation

$$\frac{\partial \tilde{u}_0}{\partial \tau} = \frac{\partial}{\partial \tilde{x}}\left(\tilde{u}_0^\alpha \frac{\partial \tilde{u}_0}{\partial \tilde{x}}\right) + O(\epsilon). \tag{2.35}$$

Therefore we observe that in the neighborhood of x_*, the population-merging dynamics are diffusion dominated; the reaction terms do not affect the solution to leading order.

Expanding the outer solution in terms of the inner variables, we obtain the matching boundary conditions to leading order for $\tilde{u}$

$$u(x, t) \to \begin{cases} U(\epsilon(\tilde{x} - c\tau)) & \tilde{x} \to -\infty, \\ U(-\epsilon(\tilde{x} + c\tau)) & \tilde{x} \to \infty, \end{cases} \tag{2.36}$$

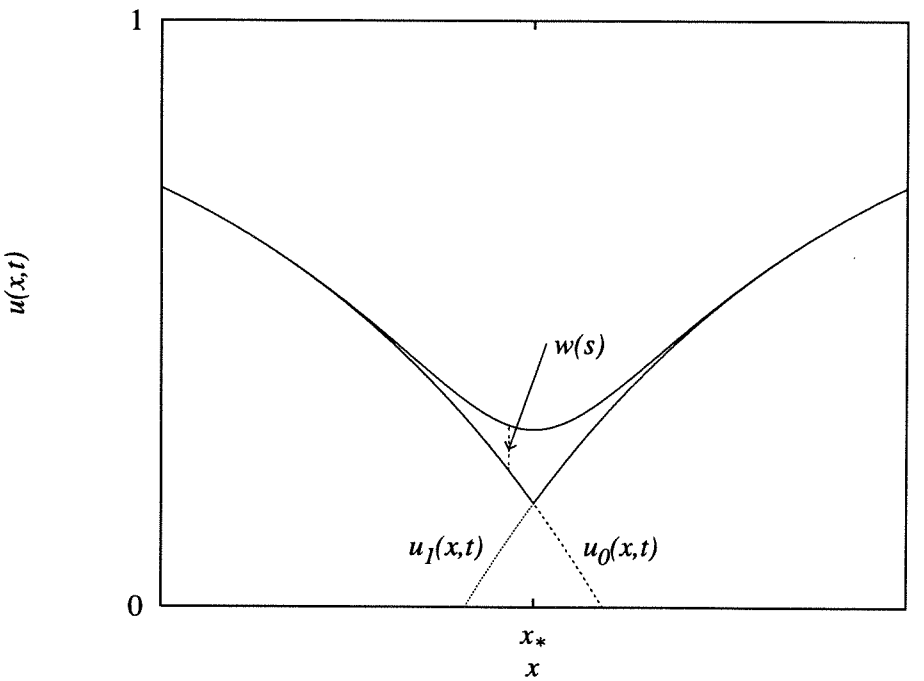

Figure 3: Details of the merging-dynamics perturbation expansion.

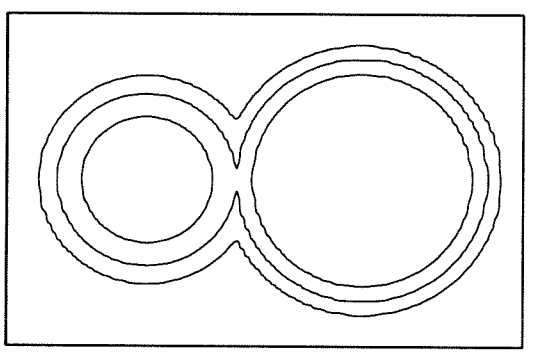

Figure 4: Circular merging fronts in the porous-Fisher's equation.

and, from (2.21)

$$\tilde{u}(x,t) \to \left(\frac{\alpha\tau}{\sqrt{\alpha+1}}\right)^{1/\alpha} \begin{cases} (c-\tilde{x}/\tau)^{1/\alpha} & \tilde{x} \to -\infty, \\ (c+\tilde{x}/\tau)^{1/\alpha} & \tilde{x} \to \infty. \end{cases} \tag{2.37}$$

This problem for $\tilde{u}(\tilde{x},\tau)$ has a similarity solution of the form

$$\tilde{u}(\tilde{x},\tau) = \tau^{1/\alpha} y(\tilde{s}), \qquad \tilde{s} = \tilde{x}/\tau, \tag{2.38}$$

where $y(\tilde{s})$ satisfies the ordinary differential equation on $-\infty < \tilde{s} < \infty$

$$\frac{1}{\alpha} y - \tilde{s} y'(\tilde{s}) = (y^{\alpha} y'(\tilde{s}))', \tag{2.39}$$

with boundary conditions

$$y(\tilde{s}) \to \left(\frac{\alpha}{\sqrt{\alpha+1}}\right)^{1/\alpha} \begin{cases} (c-\tilde{s})^{1/\alpha} & \tilde{s} \to -\infty, \\ (c+\tilde{s})^{1/\alpha} & \tilde{s} \to \infty. \end{cases} \tag{2.40}$$

We present the analysis for the case $\alpha = 1$, corresponding to the simple directed-motion model and the Pearl-Verhulst reaction term, for which the algebra becomes straight-forward. From considerations of (2.39), (2.40), we note that $y(\tilde{s})$ must be an even function of $\tilde{s}$, so we may consider the problem for (2.39) on $-\infty < \tilde{s} < 0$ with boundary condition $y'(0) = 0$. Let

$$y(\tilde{s}) = \frac{1}{2} - \frac{\tilde{s}}{\sqrt{2}} + w(\tilde{s}), \tag{2.41}$$

where $w(\tilde{s})$ represents the nonlinear correction needed to describe the merging dynamics (see Fig. 3) and satisfies the nonlinear ordinary differential

equation

$$\left(\frac{\tilde{s}}{\sqrt{2}} - \frac{1}{2} - w\right) w'' + (\sqrt{2} - \tilde{s} - w')w' + w = 0, \tag{2.42}$$

with boundary conditions

$$w(\tilde{s} \to -\infty) \to 0, \qquad w'(0) = \frac{1}{\sqrt{2}}. \tag{2.43}$$

To determine the asymptotic behavior of $w(\tilde{s})$ as $\tilde{s} \to -\infty$ we may approximate (2.42) by the linear equation

$$w'' - \sqrt{2}w' + \frac{\sqrt{2}}{\tilde{s}}w = 0. \tag{2.44}$$

Using the WKBJ method [3] to write $w(\tilde{s}) = \mathrm{e}^{\phi(\tilde{s})}$ we find that

$$w(\tilde{s}) \sim C\tilde{s}^{-1}\mathrm{e}^{\sqrt{2}\tilde{s}} \qquad \tilde{s} \to -\infty. \tag{2.45}$$

Hence we have shown that during the initial stages of the merging process, the effects of nonlinear interactions are exponentially localized to the interface region. The uniform asymptotic solution to (2.19),

$$u(x,t) \sim \max(u_0(x,t), u_1(x,t)) + (t - t_*)^{1/\alpha} w\left(\frac{x - x_*}{t - t_*}\right) \qquad t \to t_*^+, \tag{2.46}$$

is the sum of the outer traveling wave solution (2.28) and the nonlinear merging correction $w(\tilde{s})$. From (2.46), we observe that effects of the population-merging propagate from the interface back into the bulk of the populations with distance proportional to $O(t)$. Since the nonlinear interactions are ini-

tially localized, we note that the bulk of the population away from the interface continues moving with the same speed in a traveling wave profile, just as before the merger. Hence (2.28) correctly describes the outer solution even for short times after the merger. We note that this solution for the circular traveling wave case yields patterns for the front positions during merger that are very much like the "merging target patterns" observed in the BZ reaction (see Fig. 4).

Chapter 3

Similarity solutions of the reduced Cahn-Hilliard equation

3.1 Introduction

Formation of spatial structures in nonequilibrium mixtures through the process of phase separation has been the focus of many recent studies [1], [6], [19]. When a solution of two miscible components is rapidly brought to a thermodynamic state where the components can no longer exist as a uniform mixture, or "quenched," then it will spontaneously separate into two phases. We will examine certain aspects of the Cahn-Hilliard model for phase separation [8], [17]. While it was originally derived from classical thermodynamic considerations for a two-phase solution, the Cahn-Hilliard equation has become accepted as a model for various physical phenomena including pattern formation through phase transition [17], spinodal decomposition [13], [14],

and nucleation [8], [12].

We will study a problem for the Cahn-Hilliard equation in the limit of weak interfacial energy. Under these conditions, the Cahn-Hilliard equation reduces to a nonlinear diffusion equation, the reduced Cahn-Hilliard equation. After reviewing properties of an equilibrium solution to the Cahn-Hilliard equation, we will study a similarity solution of the reduced Cahn-Hilliard equation. From theoretical analysis and numerical simulations, it will be shown that this class of nonlinear diffusion equations admits weak solutions with shocks. The behavior of solutions to this nonlinear parabolic problem will be compared with wavelike behavior in hyperbolic systems of conservation laws and in Burger's equation.

3.2 The Cahn-Hilliard equation

Following Bates and Fife [6], we consider the Cahn-Hilliard equation in the form

$$\frac{\partial u}{\partial t} = \frac{\partial^2}{\partial x^2}\left(f(u) - \epsilon^2 \frac{\partial^2 u}{\partial x^2}\right), \tag{3.1}$$

where $0 < \epsilon \ll 1$ is a small parameter related to interfacial energy and $u(x,t)$ is the concentration of one of the two components in the system. This model can be derived from the energy functional [11]

$$\mathcal{F}[u] = \int \mathcal{E}[u]\, dx, \tag{3.2}$$

where the energy density $\mathcal{E}[u]$ is given by

$$\mathcal{E}[u] = F(u) + I(u_x), \tag{3.3}$$

where $F(u)$ is the free-energy density and $I(u_x)$ is the interfacial energy. The chemical potential [11] may be derived from (3.2), for systems with Dirichlet or Neumann boundary conditions on μ [19], as

$$\frac{\delta \mathcal{F}}{\delta u} = \int \mu[u]\, dx, \tag{3.4}$$

where

$$\mu[u] = f(u) - I''(u_x)u_{xx}, \tag{3.5}$$

with

$$f(u) \equiv F'(u). \tag{3.6}$$

We shall call $f(u)$ the reduced chemical potential. The diffusive flux is given by the negative gradient of the chemical potential, and we define the diffusion coefficient to be

$$D(u) \equiv f'(u) = F''(u). \tag{3.7}$$

Additionally, the interfacial energy can be modeled by

$$I(u_x) = \frac{1}{2}\epsilon^2 u_x^2. \tag{3.8}$$

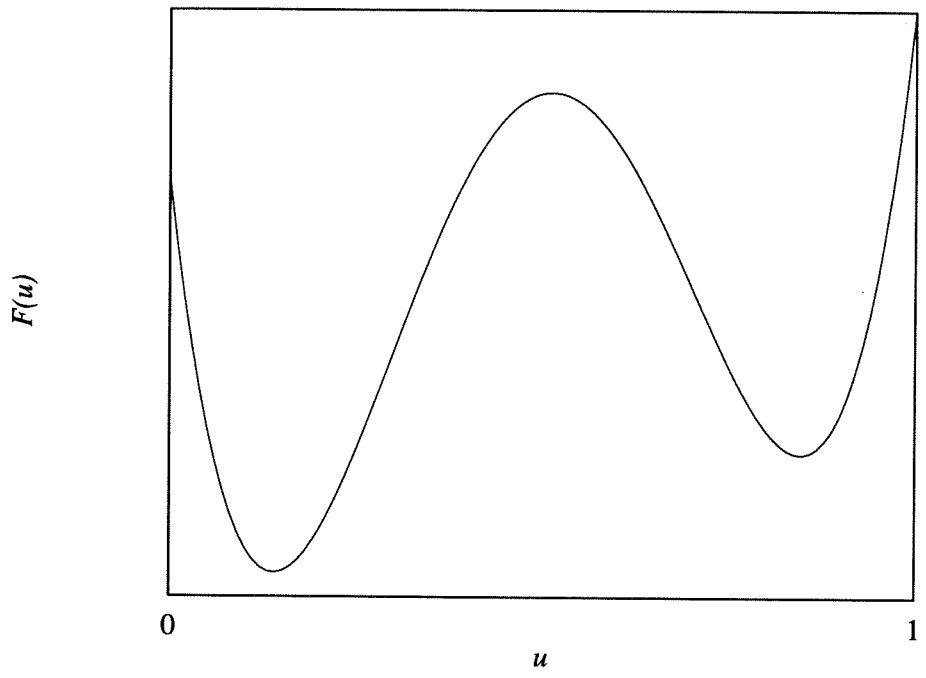

Figure 1: A double-well free-energy density $F(u)$.

With these definitions, the conservation law for u can be generally written as

$$u_t = \mu_{xx}, \tag{3.9}$$

or as (3.1) for our particular choice of μ.

For the study of phase separation, $F(u)$ is modeled by a double-well potential with two stable states (see Fig. 1). This form of the free-energy density yields a diffusion coefficient that becomes negative over a range of u. We will call diffusion coefficients with this property Cahn-Hilliard diffusion coefficients. The concentrations where $D(u) = 0$ are called spinodal points, u_a and u_b, and the range $u_a < u < u_b$ where $D(u) < 0$ is the spinodal or

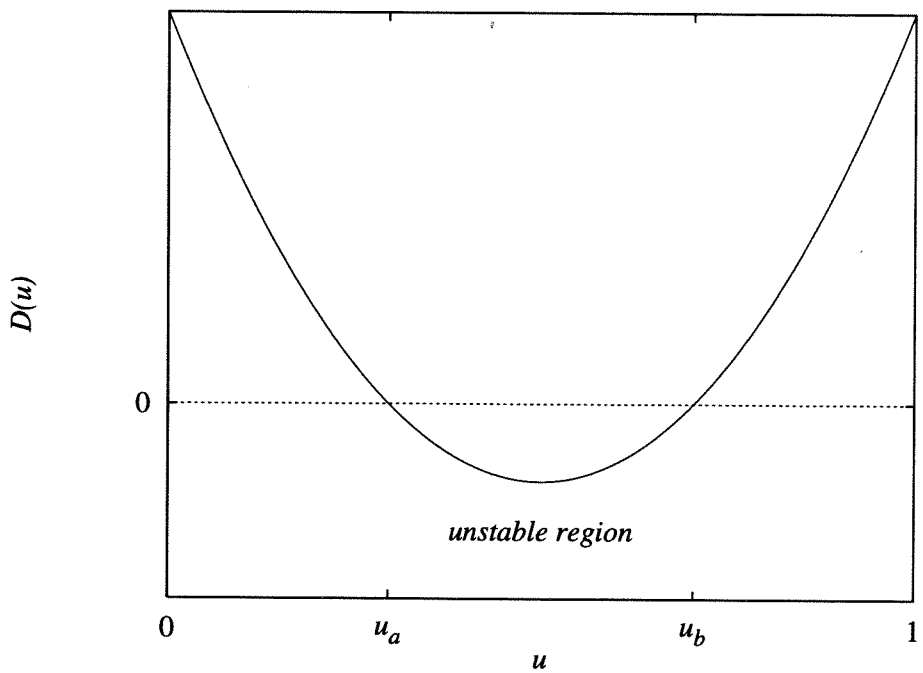

Figure 2: A Cahn-Hilliard diffusion coefficient $D(u)$.

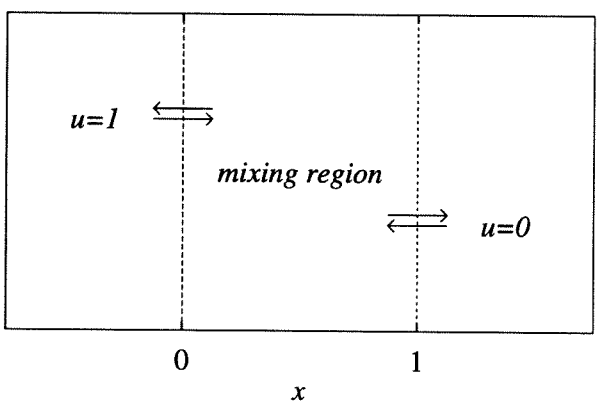

Figure 3: The physical problem studied here.

unstable region [1], [13] (see Fig. 2). The higher-order gradient term in (3.1) that gives the contribution to the energy due to an interface is needed to regularize fronts that form in this region in general solutions. Linearized analysis in the unstable region suggests that (3.1) is an ill-posed problem without this regularization [12], [14]. The focus of this report is to study a particular, well-defined solution of (3.1) in the absence of regularization. Close parallels exist between this special solution and the "breaking-wave" solution of the inviscid Burger's equation. Our solution will be a weak solution of (3.1), with $\epsilon = 0$, that contains a shock. The effect of regularization is to smooth out the shock according to the form of the interfacial energy.

Away from a sharp interface, we may approximate solutions to (3.1) using a regular perturbation expansion in ϵ for the outer solution

$$u(x,t) = \overline{u}(x,t) + \epsilon u_1(x,t) + \epsilon^2 u_2(x,t) + O(\epsilon^3). \tag{3.10}$$

Expanding (3.1) to leading order in ϵ yields the reduced Cahn-Hilliard equation

$$\overline{u}_t = f(\overline{u})_{xx} + O(\epsilon), \tag{3.11}$$

which can be written as a nonlinear diffusion equation

$$\overline{u}_t = (D(\overline{u})\overline{u}_x)_x, \tag{3.12}$$

where $D(\overline{u})$ is given by (3.7) from the appropriate form of $F(\overline{u})$.

We will study a Dirichlet problem for (3.12). The corresponding Dirichlet problem for the Cahn-Hilliard equation can be used to represent the behavior

of a mixture that is initially uniform $u = 0$ (the pure second component) separated by a semi-permeable membrane from a uniform reservoir of $u = 1$ (see Fig. 3). First we will consider the steady-state problem, and then using similarity solutions, we will describe a dynamic solution to the time-dependent Cahn-Hilliard equation.

3.3 The equilibrium problem

We introduce some of the properties of the Cahn-Hilliard equation through the examination of a steady-state problem. Consider the solution to the steady-state boundary-value problem for the Cahn-Hilliard equation on $0 < x < 1$

$$(f(u) - \epsilon^2 u_{xx})_{xx} = 0, \tag{3.13a}$$

$$u(0) = 1, \qquad u(1) = 0, \tag{3.13b}$$

$$u_{xx}(0) = 0, \qquad u_{xx}(1) = 0. \tag{3.13c}$$

These boundary conditions on u, u_{xx} correspond to Dirichlet conditions on the chemical potential μ and describe the physical problem given in the previous section. Integrating (3.13a) twice yields

$$f(u) - \epsilon^2 u_{xx} = ax + b, \tag{3.14}$$

where a and b are constants of integration. If we assume that $u(x)$ is a smooth function, so gradients are $O(1)$, then to leading order we may neglect the $O(\epsilon^2)$ term. Both boundary conditions (3.13b) are satisfied by the resulting

multi-valued implicit outer solution (see Fig. 4)

$$x(u) = \frac{f(u) - f(1)}{f(0) - f(1)}. \tag{3.15}$$

Returning to the full problem (3.13a), we have now determined a and b to yield

$$f(u) - \epsilon^2 u_{xx} = (f(0) - f(1))x + f(1). \tag{3.16}$$

The multivalued outer solution cannot satisfy this differential equation for $\epsilon > 0$, and we conclude that a shock layer must be inserted to form an admissible single-valued solution. Therefore, we will assume the existence of a sharp interface, or shock, of width $O(\epsilon)$ at some position x_s, to be determined. The inner problem in stretched variables in the neighborhood of the shock is

$$f(\tilde{u}) - \tilde{u}_{\tilde{x}\tilde{x}} = c + O(\epsilon), \tag{3.17}$$

where

$$\tilde{x} = \frac{x - x_s}{\epsilon}, \qquad c = (f(0) - f(1))x_s + f(1). \tag{3.18}$$

The general leading order solution to (3.17) is

$$\tilde{x} - \tilde{x}_0 = -\int_{u_0}^{\tilde{u}} \frac{dU}{\sqrt{2(F(U) - cU)}}, \tag{3.19}$$

where $\tilde{x}_0$,u_0 are constants of integration, and

$$F(u) = \int_0^u f(U)\, dU, \qquad \tilde{u}(\tilde{x}_0) = u_0. \tag{3.20}$$

To match to the outer solution, we require that $\tilde{u}$ approach constant values, say $\tilde{u}(\tilde{x} \to -\infty) \to u_2$ and $\tilde{u}(\tilde{x} \to \infty) \to u_1$, as $|\tilde{x}| \to \infty$. From (3.17), this results in the conditions

$$f(u_1) = c, \qquad f(u_2) = c. \tag{3.21}$$

In order that the integral (3.19) diverge as $\tilde{u} \to u_1$ and $\tilde{u} \to u_2$, we require that the denominator of the integrand vanish at these points. This condition can be written as the equal area rule [19] (see Fig. 5)

$$\int_{u_2}^{u_1} (f(u) - c)\, du = 0. \tag{3.22}$$

To uniquely specify the shock layer solution, we take $\tilde{x}_0 = 0$ and require that the shock layer agree pointwise with the multivalued outer solution at $x = x_s$ ($\tilde{x} = 0$). Therefore, define u_s as the value on the middle branch of (3.15) such that $x(u_s) = x_s$, and take $u_0 = u_s$. Equations (3.21) and (3.22) are a system of three equations for the unknowns u_1, u_2, and c. The solution of this system yields the shock position from (3.18) as

$$x_s = \frac{c - f(1)}{f(0) - f(1)} = x(u_s), \tag{3.23}$$

and by comparing (3.23) with (3.15), we note that $c = f(u_s)$.

For particular choices of the reduced chemical potential function $f(u)$ it is possible that the shock position determined by the equal-are rule will fall outside of the domain $0 < x < 1$ and hence will not be admissible. To study such a case, and for other general considerations, we consider a problem for

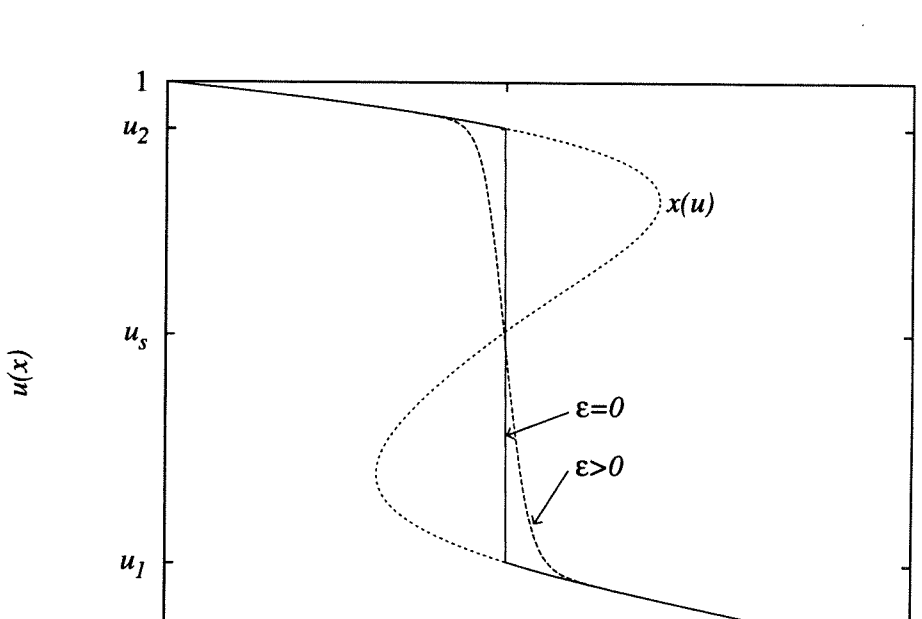

Figure 4: The equilibrium solution.

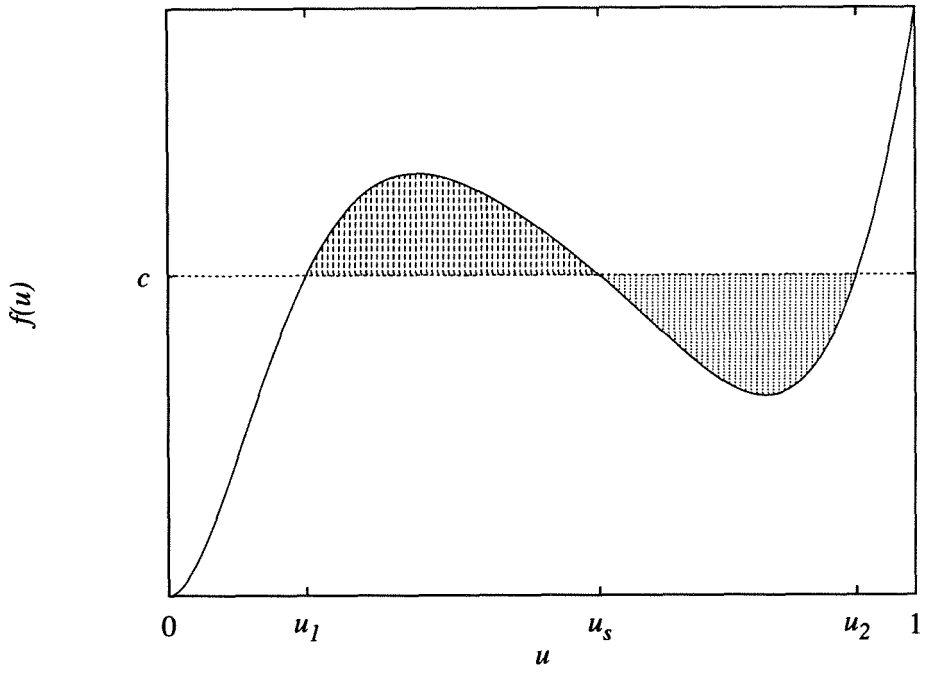

Figure 5: The equal-area rule.

the time-dependent Cahn-Hilliard equation.

3.4 The dynamic problem

We will consider the initial-boundary value problem for the Cahn-Hilliard equation on $0 < x < 1$ for $t > 0$

$$u_t = (f(u) - \epsilon^2 u_{xx})_{xx}, \tag{3.24a}$$

$$u(0) = 1, \qquad u(1) = 0, \tag{3.24b}$$

$$u_{xx}(0) = 0, \qquad u_{xx}(1) = 0. \tag{3.24c}$$

$$u(x, 0) = 0. \tag{3.24d}$$

As above, we will use the method of matched asymptotic expansions to construct a solution of this problem. For this problem, the shock layer analysis is very similar to that in the equilibrium case, so we address this point before proceeding to the study of the outer solution, which will be the focus of the remainder of this article.

3.5 The dynamic shock layer

As in the equilibrium case, to determine the fine structure of the solution at a sharp interface, we use stretched variables to obtain an inner problem. Consider an inner expansion centered at the unknown shock position $x_s =$

$s(t)$, which will be determined later by the outer solution,

$$\tilde{x} = \frac{x - s(t)}{\epsilon}. \tag{3.25}$$

Under this change of variables, (3.24a) for $u = \tilde{u}(\tilde{x}, t)$ becomes

$$\epsilon^2 \tilde{u}_t - \epsilon s'(t)\tilde{u}_{\tilde{x}} = (f(\tilde{u}) - \tilde{u}_{\tilde{x}\tilde{x}})_{\tilde{x}\tilde{x}}. \tag{3.26}$$

To leading order we get

$$A\tilde{x} + B = f(\tilde{u}) - \tilde{u}_{\tilde{x}\tilde{x}}, \tag{3.27}$$

where A and B are constants of integration, possibly functions of time, and are determined from matching to the outer solution. As in the equilibrium case, as $|\tilde{x}| \to \infty$, to match to a smooth outer solution $\tilde{u}$ must approach constant values, hence $A = 0$, and

$$B = f(\tilde{u}) - \tilde{u}_{\tilde{x}\tilde{x}}. \tag{3.28}$$

This is the same equation as for the steady-state shock (3.17), and therefore we obtain the same equal-area rule (3.22) for shock placement to leading order.

We will now study the outer problem for (3.24a) which will give the overall structure of the solution as well as determining the motion of the shock layer. The analysis of this problem is considerably simplified for outer solutions of similarity form. For particular forms of $F(u)$, these will be

exact solutions of (3.24a–d). Hence, in the next section we will use similarity solution techniques to reduce to outer problem (3.12) to a nonlinear ordinary differential equation.

3.6 The outer solution - similarity solutions of diffusion equations

As described earlier, away from the shock, we expand in a regular perturbation series to obtain the leading order nonlinear diffusion equation

$$u_t = f(u)_{xx}. \tag{3.29}$$

We will consider similarity solutions of this equation. The properties of similarity solutions used in the study of diffusive systems [9], [21] will be reviewed in this section.

We consider the initial-boundary value problem for the general nonlinear diffusion equation in one-dimension $0 < x < \infty$ for $t > 0$

$$u_t = (D(u)u_x)_x, \tag{3.30a}$$

with boundary conditions

$$u(0,t) = 1, \qquad u(x,t) \to 0 \text{ as } x \to \infty, \tag{3.30b}$$

and initial condition

$$u(x,0) = 0. \tag{3.30c}$$

If we define the diffusive flux as

$$q \equiv -D(u)\frac{\partial u}{\partial x}, \tag{3.31}$$

then we may write (3.30a) in conservation law form as

$$\frac{\partial u}{\partial t} + \frac{\partial q}{\partial x} = 0. \tag{3.32}$$

Searching for similarity solutions of (3.30a) of the form

$$u(x,t) = U(z), \qquad z = x/\sqrt{t}, \tag{3.33}$$

reduces it to the ordinary differential equation

$$\frac{1}{2}zU'(z) = -(D(U)U'(z))'. \tag{3.34}$$

The transformation to similarity variables yields a corresponding similarity flux

$$q(x,t) = t^{-1/2}Q(z), \tag{3.35}$$

where

$$Q(z) \equiv -D(U)U'(z). \tag{3.36}$$

With this definition (3.34) becomes

$$\frac{1}{2}zU'(z) = Q'(z). \tag{3.37}$$

Following Babu [5], we will consider this problem in inverse variables, that is $z = z(U)$ rather than $U = U(z)$. This change of variables is often used to make perturbation expansions of (3.34) more convenient [4], [5], but for our application this is an important step in the analysis. Using the chain rule, (3.37) yields

$$\frac{1}{2}z(U) = \frac{dQ}{dU}. \tag{3.38}$$

If we define the inverse-flux as

$$J(U) \equiv -\frac{1}{D(U)}\frac{dz}{dU} = \frac{1}{Q(z)}, \tag{3.39}$$

then we obtain

$$\frac{1}{2}z(U) = \frac{d}{dU}\left(\frac{1}{J(U)}\right), \tag{3.40}$$

which may be used to write the nonlinear ordinary differential equation for $z(U)$,

$$\frac{1}{2}zz'^2 = D(U)z'' - D'(U)z', \tag{3.41}$$

where the primes now denote differentiation with respect to U. For uniformly parabolic equations with $D(u) > 0$, (3.34) and (3.41) are equivalent representations.

If $D(0) = 0$ and $D(U) > 0$ for $U > 0$ then the diffusion equation is of porous media type. Similarity solutions of this class of equation are weak

solutions with compact support and are of the form

$$u(x,t) = (U(z))^+, \qquad z = x/\sqrt{t}, \tag{3.42}$$

where $(w)^+ \equiv \max(w, 0)$ and $U(z_*) = 0$ defines the leading edge of the region of support (see Fig. 6). Having a compact-support solution of the form (3.42) means that even though our original problem (3.24a–d) is a boundary value problem on a finite domain, a similarity solution will exist for a finite interval of time. For porous media equations, solving (3.41) becomes more convenient than solving (3.34) [5]. We determine z_* through a global conservation of mass

$$\frac{1}{2}\int_0^{z_*} zU'(z)\,dz = Q(z)\Big|_0^{z_*}. \tag{3.43}$$

Imposing the conditions that U is continuous and the flux vanishes at the leading edge yields

$$-\frac{1}{2}z'(1)\int_0^1 z(U)\,dU = D(1). \tag{3.44}$$

Note that (3.44) holds for general $D(U)$; if $D(0) > 0$ then the similarity solutions do not have compact support and $z_* \to \infty$ [20].

Similarly, if we integrate (3.34) from z_* to some indefinite position z and use the chain rule to write z as a function of U, $z = z(U)$, then [7], [21]

$$D(U) = -\frac{1}{2}z'(U)\int_0^U z(u)\,du. \tag{3.45}$$

This is a formula that yields the diffusion coefficient corresponding to a given similarity solution. We will now extend some of these ideas to study the

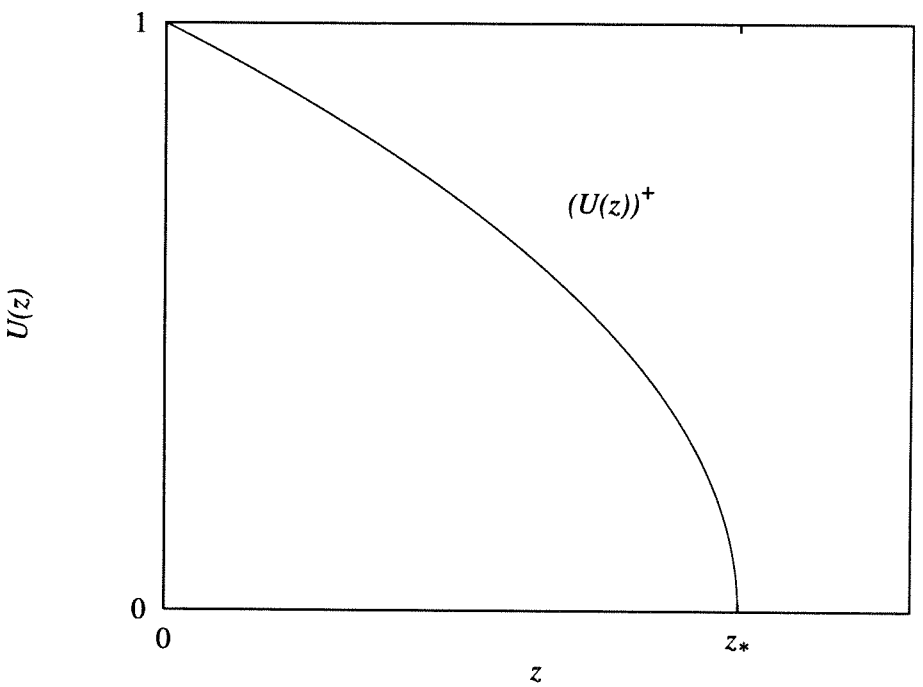

Figure 6: A compact-support similarity solution.

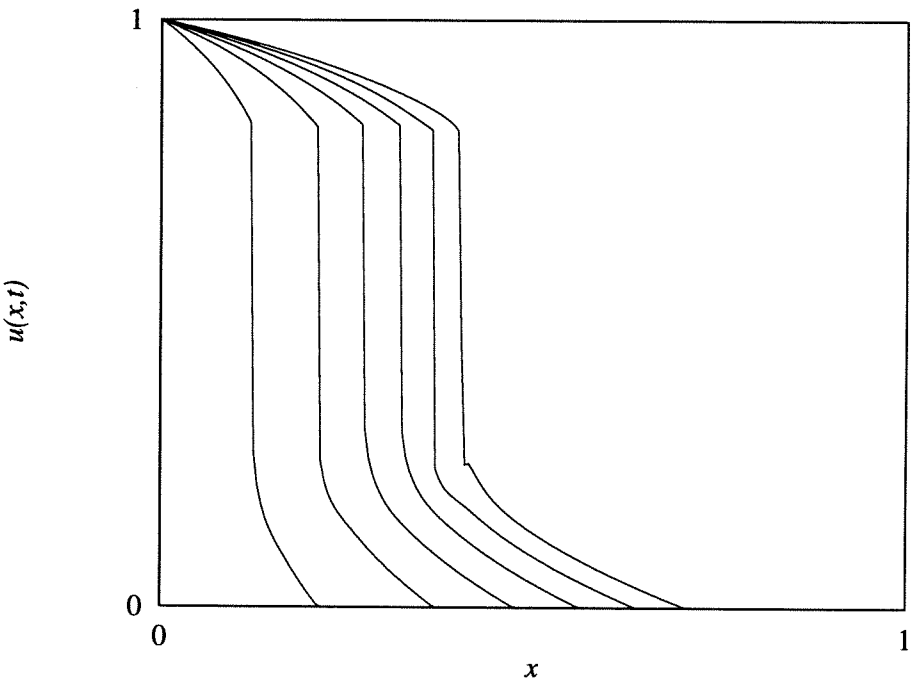

Figure 7: A numerical solution of (3.46a–c).

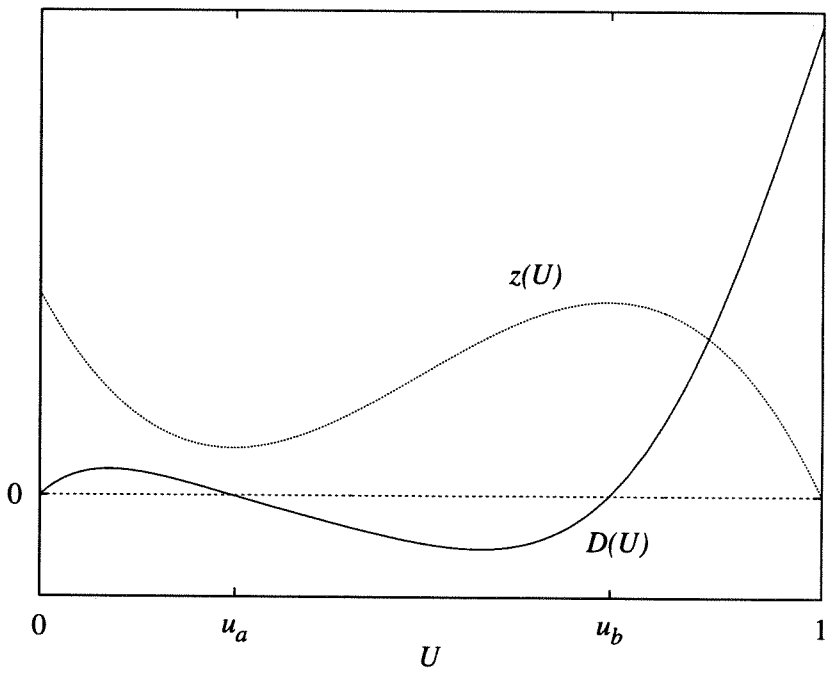

Figure 8: A Cahn-Hilliard $D(U)$ and a multi-valued similarity solution $z(U)$.

reduced Cahn-Hilliard equation, where $D(U)$ becomes negative.

3.7 Multivalued solutions

To gain some insight into the behavior of (3.30a), we conducted some preliminary numerical studies of the initial-boundary value problem on $0 < x < 1$ for $t > 0$

$$u_t = (D(u)u_x)_x, \tag{3.46a}$$

$$u(0, t = 1, \qquad u(1, t) = 0, \tag{3.46b}$$

$$u(x, 0) = 0, \tag{3.46c}$$

where $D(u)$ is a Cahn-Hilliard diffusion equation with $D(0) = 0$ to obtain compact-support similarity solutions. Using several finite difference schemes [2], [16], we obtained consistent results showing the existence of a compact-support similarity solution with an apparent shock in u (see Fig. 7). Solving (3.41) numerically with a Cahn-Hilliard diffusion coefficient, subject to the boundary condition $z(U = 1) = 0$ and (3.44), yields a nonmonotone solution. The solution $z = z(U)$ cannot be written as a single-valued function $U = U(z)$ and hence (3.34) cannot be used! The implication of having a Cahn-Hilliard diffusion coefficient is that the corresponding similarity solution will be multivalued! This behavior can be shown to be generic; if we assume a solution $z = z(U) \geq 0$ for a multivalued function $U(z)$, then we can make use of (3.45) to determine the corresponding $D(U)$. Since $z(U)$ is positive, so is its integral. Since $U(z)$ is multivalued, $z(U)$ is not monotone and $z'(U)$ changes sign, yielding a corresponding diffusion coefficient $D(U)$ which is negative in some range (see Fig. 8).

As in the theory of nonlinear waves [22], since the partial differential equation (3.46a) governs the evolution of a physical quantity such as density, concentration or temperature, a multivalued solution is not admissible. For waves, multivalued solutions can be replaced by weak solutions that contain discontinuities.

Recalling section 3, we can write the nonlinear diffusion equation in conservation form as

$$u_t + q_x = 0, \tag{3.47}$$

where the flux is given by

$$q = -f(u)_x. \tag{3.48}$$

In this form we may apply Whitham's derivation [22] of the condition for the motion of the shock $x_s = s(t)$ to yield

$$\frac{ds}{dt} = \frac{[q]}{[u]} = -\frac{[f(u)_x]}{[u]}, \tag{3.49}$$

where the brackets indicate the jump across the shock. This condition on the interface velocity was also derived by Pego [19] through the consideration of a Stefan problem for the reduced Cahn-Hilliard equation. We note that for our similarity solution $s(t) = z_s\sqrt{t}$ and (3.49) yields the equation for the shock position

$$\frac{1}{2}z_s = -\frac{[D(U)U']}{[U]}. \tag{3.50}$$

Equation (3.49) states that the motion of the interface is driven by a jump in the flux across the shock. This is a condition that is commonly used in the formulation of Stefan problems [9].

Similarly, using some of Whitham's considerations of weak solutions [22], we can argue that the reduced chemical potential $f(u)$ must be continuous across the shock. We may take the solution $U(z)$ of the equation

$$\frac{1}{2}zU'(z) = -f(U)'' \tag{3.51}$$

to be of the form

$$U(z) = \begin{cases} U_2(z) & 0 \le z < z_s \\ U_1(z) & z_s < z, \end{cases} \tag{3.52}$$

or, equivalently,

$$U(z) = U_2(z)H(z_s - z) + U_1(z)H(z - z_s), \tag{3.53}$$

where $H(z)$ is the Heaviside step function. Substituting (3.53) into the lefthand-side of (3.51) yields terms like

$$-\frac{1}{2}zU_2(z)\delta(z_s - z) + \cdots, \tag{3.54}$$

where $\delta(z)$ is the Dirac delta function. In order to balance this singularity, d^2f/dz^2 must act like a delta function, df/dz must act like a step function and hence $f(U)$ must be C^0 continuous at z_s,

$$[f(U)] = 0. \tag{3.55}$$

The motion of the shock in a first-order scalar conservation law is controlled by one condition at the shock, given by (3.49). For example, consider the generalized Burger's equation

$$u_t + q(u)_x = \epsilon u_{xx}, \tag{3.56}$$

where the flux is $q(u)$ and the viscosity is $0 < \epsilon \ll 1$. In the absence of viscosity we get the first order equation

$$u_t + q(u)_x = 0. \tag{3.57}$$

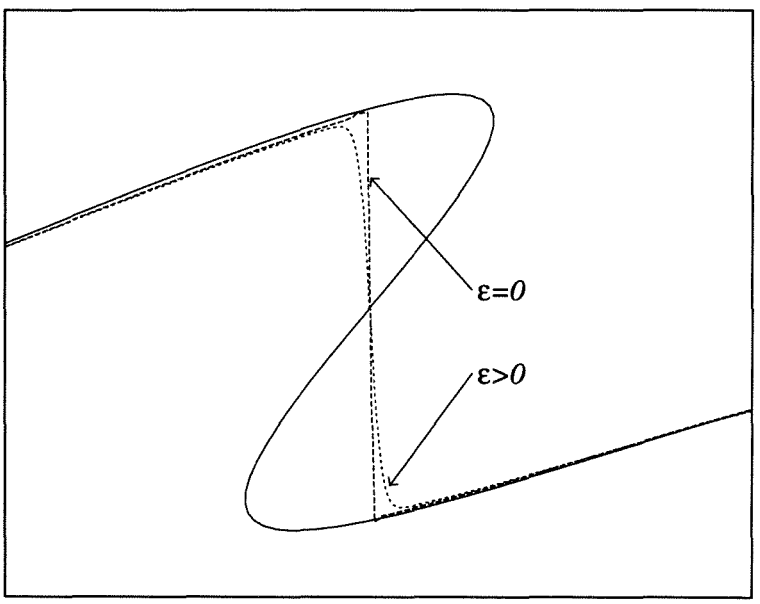

Figure 9: A breaking wave solution of Burger's equation.

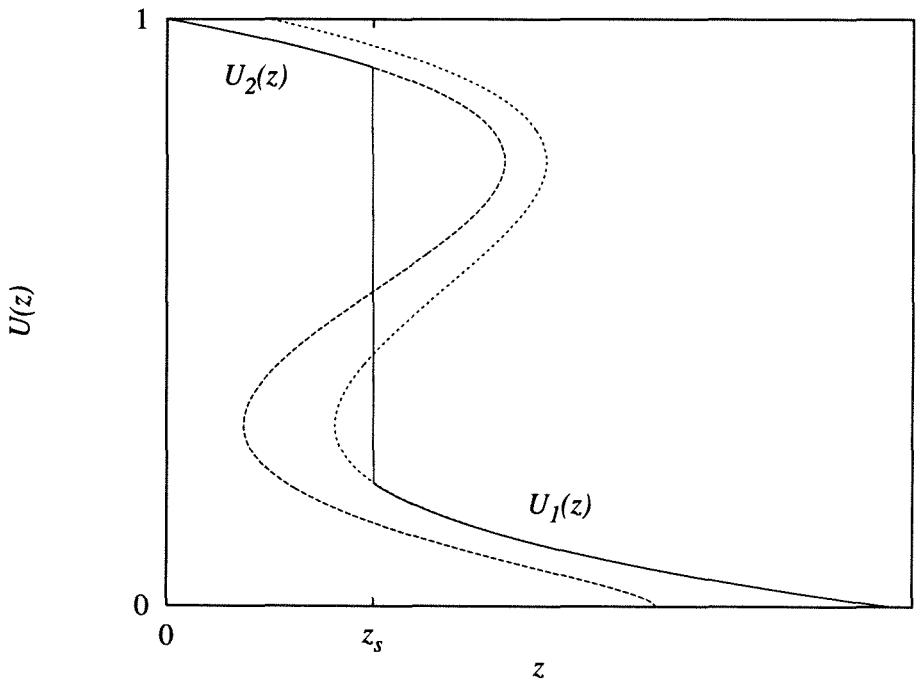

Figure 10: A reduced Cahn-Hilliard solution.

Solutions of this equation will generally become multivalued breaking waves. It is possible to insert a shock into these solutions to yield a weak solution that corresponds to a viscous solution of Burger's equation as $\epsilon \to 0$ (see Fig. 9). In the weak solution, a shock connects the upper and lower branches of the original multi-valued solution. The position of the shock is determined by the shock condition. If u is the conserved quantity in the system, then we get (3.49). If some function $P(u)$ is conserved, then, by multiplying (3.57) by $P'(u)$ we get

$$P(u)_t + Q(u)_x = 0, \tag{3.58}$$

where

$$Q(u) = \int^u q(v)P'(v)\,dv, \tag{3.59}$$

and we get the shock condition

$$\frac{ds^P}{dt} = \frac{[Q(u)]}{[P(u)]}, \tag{3.60}$$

where $s^P(t)$ is the shock position. Hence, by specifying the conserved quantity in the system a unique shock equation is determined.

Our problem for the reduced Cahn-Hilliard equation is in some ways more analogous to a hyperbolic system of conservation laws. The Euler equations for gas dynamics describe the transport of mass, momentum and energy. Solutions of this system of mathematical equations yield breaking waves which correspond to shock formation in the physical system. At a shock, the governing conditions, the Rankine-Hugoniot relations, require the conservation of the three transported quantities. Unlike a weak solution of a single con-

servation law, a weak solution of a hyperbolic system cannot generally be constructed from a shock connecting the upper and lower branches of a single breaking-wave solution. The solution of the system is in fact composed of different classical solutions ahead of and behind the shock, related to each other through the shock conditions. For the reduced Cahn-Hilliard equation, the weak solution is constructed from a shock that connects the upper branch of one multi-valued solution of (3.41) to the lower branch of another multi-valued solution of (3.41) (see Fig. 10).

Requiring that u is conserved and $f(u)$ is continuous does not uniquely specify a shock position for the the reduced Cahn-Hilliard equation. Consider finding a weak similarity solution of (3.51) of the form (3.52). U_1 and U_2 are solutions of a second order ordinary differential equation and hence they each have two unknown constants of integration. Additionally, the shock position z_s is unknown for a total of five unknown parameters in the weak solution. The boundary conditions (3.30b) for the nonlinear diffusion equation yield two conditions. The shock relations (3.50) and (3.55) give two more restrictions. One more condition is needed. The correct weak solution is selected by the form of the higher-order viscous terms in the equation. For the Cahn-Hilliard equation, the shock position is determined by the equal area rule derived in section 3. In numerical methods for solving the reduced Cahn-Hilliard equation (3.46a), the form of the higher order numerical viscosity in the discretization scheme determines the shock selection rule.

Acknowledgment I wish to thank Professor G. B. Whitham for many helpful discussions and suggestions about this project.

Part II

Stress-driven diffusion

Chapter 4

Shock formation in stress-driven diffusion

4.1 Introduction

Many chemical and biological systems can be described by coupled reaction-diffusion equations. These mathematical models generally describe the interaction of advection, molecular diffusion and nonlinear reactions in simple materials. However, many recent developments in emerging technologies require more sophisticated models to explain newly observed phenomena. Here we study one such model, called stress-driven diffusion, describing the behavior of polymeric materials.

Polymer materials are becoming commonly used in many industries including medicine and pharmaceuticals. Many nontraditional effects occur in these materials. Generically called "anomalous behavior," these effects

cannot be predicted from classical models. An example is the nature of the diffusive spreading of a penetrant liquid in a polymer film. Experimental studies of polymer sorption behavior show constant velocity spreading of the penetrant with a well-defined sharp interface. Classical diffusion models cannot yield such characteristics. As a result, numerous studies have focused on tying anomalous behaviors to the special material properties of polymers. Since polymers are very long molecules, some effects can have considerable characteristic times [30]. Consequently, incorporation of relaxation effects through viscoelastic models becomes important. Additionally, polymer materials can undergo a phase transition from a relatively inflexible "glassy" state to a more responsive "rubbery" state with corresponding changes in diffusion coefficients and relaxation times. We will study mathematical models that incorporate these effects.

We will review and extend the analysis of models for anomalous "case II" diffusion in polymers. After briefly reviewing a derivation of the governing equation given by Wu and Peppas [32], we will relate the model to equations proposed by Cohen et al. [10], [11], [12], [16], [17], [18], [19], [20] Finally, we will study some of the phenomena present in a new generalized stress-driven diffusion model.

4.2 Derivation of the model

In this section we present a simplified derivation of the equations describing a system composed of a penetrant liquid diffusing in a polymer film substrate. This presentation, based on [32], introduces many assumptions and neglects

several effects, but it yields the correct qualitative form for the equations of motion of the simple one-dimensional model. Rigorous formulation of the full three-dimensional requires careful consideration of many factors and is still an active area of research [1], [2], [3], [4]. Properties of the penetrant will be indicated by the subscript 1, while properties of the polymer will be indicated by the subscript 2. The densities ρ_1 and ρ_2 will be taken to be constants. The local material velocities are given by $\mathbf{u}_1$ and $\mathbf{u}_2$. The volume fractions of penetrant and polymer ϕ_1, ϕ_2 are the main quantities of interest. The penetrant and polymer volume fractions are related through

$$\phi_1 + \phi_2 = 1. \tag{4.1}$$

Initially, the polymer is dry, i.e. it contains no penetrant, so we have $\phi_1(\mathbf{X}) = 0$ and $\phi_2(\mathbf{X}) = 1$ at $t = 0$.

From thermodynamic arguments, Wu and Peppas [32] claim that the velocity of the penetrant is given by

$$\phi_1 \mathbf{u}_1 = -\overline{D}(\phi_1)\left(\nabla\phi_1 + \frac{k\phi_1}{(1-\phi_1)(1-2\chi\phi_1)}\nabla P\right), \tag{4.2}$$

where P is the osmotic pressure (or pressure due to the swelling of the polymer), $\overline{D}(\phi_1)$ is an inter-diffusion coefficient, $k = \overline{V}_1/RT$, and χ is called the Flory interaction parameter. By substituting the velocity model (4.2) in the statement of conservation of mass for the penetrant,

$$\frac{\partial}{\partial t}(\rho_1\phi_1) + \nabla\cdot(\rho_1\phi_1\mathbf{u}_1) = 0, \tag{4.3}$$

we obtain

$$\frac{\partial \phi_1}{\partial t} = \nabla \cdot \left[\overline{D}(\phi_1) \left(\nabla \phi_1 + \frac{k\phi_1}{(1-\phi_1)(1-2\chi\phi_1)} \nabla P \right) \right]. \tag{4.4}$$

Now, consider the conservation of momentum for the penetrant and the polymer

$$\rho_1 \frac{D_1 \mathbf{u}_1}{Dt} = -\nabla P_1 + \rho_1 \mathbf{p}_{12}, \tag{4.5}$$

$$\rho_2 \frac{D_2 \mathbf{u}_2}{Dt} = -\nabla P_2 + \rho_2 \mathbf{p}_{21} + \nabla \cdot \sigma, \tag{4.6}$$

where P_i are partial pressures, $\mathbf{p}_{ij}$ are momenta transferred to component i from component j and σ is the stress tensor of the polymer substrate. Summing (4.5, 4.6) yields

$$\rho_1 \frac{D_1 \mathbf{u}_1}{Dt} + \rho_2 \frac{D_2 \mathbf{u}_2}{Dt} = -\nabla (P_1 + P_2) + (\rho_1 \mathbf{p}_{12} + \rho_2 \mathbf{p}_{21}) + \nabla \cdot \sigma. \tag{4.7}$$

The following simplifications can be made to (4.7): the sum of the momenta transferred between components equals zero, and the sum of the partial pressures is the total pressure, $P = P_1 + P_2$. Additionally, we will neglect the inertial terms on the left of (4.7) to yield

$$\nabla P = \nabla \cdot \sigma. \tag{4.8}$$

Using (4.8), we may write (4.4) in the form

$$\frac{\partial \phi_1}{\partial t} = \nabla \cdot \left[\overline{D}(\phi_1) \left(\nabla \phi_1 + \overline{E}(\phi_1) \nabla \cdot \sigma \right) \right], \tag{4.9}$$

where the stress coefficient is

$$\overline{E}(\phi_1) = \frac{k\phi_1}{(1-\phi_1)(1-2\chi\phi_1)}. \tag{4.10}$$

It is now helpful to consider the elastic deformations of the polymer substrate. Since the polymer and penetrant have constant densities, when the penetrant enters the substrate, the polymer material must swell in size. If boundary conditions are being applied at the edges of the polymer material then we will have to solve a moving boundary problem. We can reduce this to a fixed-domain problem by changing to the material coordinates associated with the undeformed polymer substrate. The deformation tensor $\mathbf{F}$ is defined by

$$F_{ij} = \frac{\partial X_i}{\partial x_j}, \tag{4.11}$$

where X_i are the present deformed (or Eulerian) coordinates and x_j are the material (or Lagrangian) coordinates. The instantaneous volume ratio for deformed to undeformed states is given by the determinant of $\mathbf{F}$

$$J = |\mathbf{F}| = \frac{\text{deformed volume}}{\text{undeformed volume}} = \frac{1 = \phi_1 + \phi_2}{\phi_2} = \frac{1}{1-\phi_1}. \tag{4.12}$$

Therefore the change of variables to material coordinates, in one dimension, is

$$\frac{\partial}{\partial X} = (1-\phi_1)\frac{\partial}{\partial x}, \tag{4.13}$$

and (4.9) becomes

$$\frac{\partial \phi_1}{\partial t} = (1-\phi_1)\frac{\partial}{\partial x}\left[\tilde{D}(\phi_1)\left(\frac{\partial \phi_1}{\partial x} + \tilde{E}(\phi_1)\frac{\partial \sigma}{\partial x}\right)\right], \tag{4.14}$$

where

$$\tilde{D}(\phi_1) = (1-\phi_1)\overline{D}(\phi_1), \qquad \tilde{E}(\phi_1) = (1-\phi_1)\overline{E}(\phi_1). \tag{4.15}$$

The extension of model (4.14) to general multidimensional problems is still being studied since simple volume flux arguments like those in (4.12) are insufficient to yield the form of the deformation tensor and hence the coordinate transformation (4.13). Indeed, experiments have shown that complicated behavior, such as buckling instabilities, can occur in multidimensional problems. Another limitation of (4.14) stems from the coordinate transformation; to remain in the regime of validity of linearized elasticity, the relative deformations must be small. Hence we will allow the penetrant to take up only a small portion of the volume, $0 \leq \phi_1 \ll 1$. In the next section we will complete the description of the model by introducing a stress evolution equation.

4.3 Stress-driven diffusion

Here we will finish the formulation of our model and relate the above model to derivations done by Durning [7] and equations proposed by Cohen [10], [11], [12]. If we change dependent variables by

$$u = -\ln(1-\phi_1) \qquad \leftrightarrow \qquad \phi_1 = 1 - e^{-u}, \tag{4.16}$$

where $0 < \phi_1 < 1$ corresponds to $0 < u < \infty$. Then we get

$$\frac{\partial u}{\partial t} = \frac{\partial}{\partial x}\left[D(u)\left(\frac{\partial u}{\partial x} + E(u)\frac{\partial \sigma}{\partial x}\right)\right], \tag{4.17}$$

where $D(u)$ and $E(u)$ are given by

$$D(u) = \mathrm{e}^{-2u}\overline{D}(1 - \mathrm{e}^{-u}), \qquad E(u) = \mathrm{e}^{-u}\overline{E}(1 - \mathrm{e}^{-u}). \tag{4.18}$$

Observe that (4.17) is a nonlinear diffusion equation for u with an extra term in the flux to account for the effects of induced stress [12]. In the limit that $\phi_1 \ll 1$, to leading order we get

$$u \sim \phi_1, \qquad D(u) \sim \overline{D}(\phi_1), \qquad E(u) \sim \overline{E}(\phi_1), \tag{4.19}$$

and (4.17) is the leading-order approximation of the original diffusion equation (4.9). Hence, we conclude that in the low penetrant limit, $\phi_1 \to 0$, the swelling of the polymer is a higher-order effect and that the induced stress is primarily responsible for the observed phenomena. With this in mind we now focus our attention on models for the stress.

To close the description of the model, it is necessary to relate the induced stress to the penetrant concentration. In linear elasticity, the strain is given by $\varepsilon = \mathbf{F} - \mathbf{1}$. For our problem in one-dimension, this reduces to

$$\varepsilon = \frac{1}{1 - \phi_1} - 1 = \mathrm{e}^{u} - 1. \tag{4.20}$$

Having the strain in terms of u allows us to use the framework of stress-strain

models from viscoelasticity to describe the stress [6]. One simple model is the Maxwell model

$$\frac{\partial \sigma}{\partial t} + \beta\sigma = \lambda \frac{\partial \varepsilon}{\partial t}, \tag{4.21}$$

where λ is the elastic modulus and β is the ratio of the elasticity to the viscosity of the polymer. In general, β and λ will depend on the concentration of penetrant in the polymer. Consequently, we can write the solution to (4.21) for initially unstressed, dry polymer ($\sigma = 0$, $u = 0$ at $t = 0$) as the integral form

$$\sigma(x,t) = \int_0^t \mathrm{e}^{-\int_\tau^t \beta(u(x,s))\,ds} \lambda(u(x,\tau)) \mathrm{e}^{u(x,\tau)} u_t(x,\tau)\,d\tau, \tag{4.22}$$

and hence our penetrant diffusion model can be written as a single integro-differential equation

$$\frac{\partial u}{\partial t} = \frac{\partial}{\partial x}\left[D(u)\left(\frac{\partial u}{\partial x} + E(u)\frac{\partial}{\partial x}\int_0^t \mathrm{e}^{-\int_\tau^t \beta(u)\,ds} \lambda(u)\mathrm{e}^u u_t\,d\tau\right)\right]. \tag{4.23}$$

This form clearly points out the history-dependent nature of the stress. Durning and Fu [7] present a history-dependent model of the form

$$\frac{\partial u}{\partial t} = \frac{\partial}{\partial x}\left[D(u)\left(\frac{\partial u}{\partial x} + E(u)\frac{\partial}{\partial x}\left(G(u)\int_0^t \mathrm{e}^{-\int_\tau^t \beta(u)\,ds} \lambda(u)\mathrm{e}^u u_t\,d\tau\right)\right)\right]. \tag{4.24}$$

Note that this equation is equivalent to (4.17) coupled to the stress evolution equation

$$\frac{\partial \sigma}{\partial t} + \beta(u)\sigma = \left(\frac{G'(u)}{G(u)}\sigma + G(u)\right)\frac{\partial u}{\partial t}. \tag{4.25}$$

It is always possible to reduce the integro-differential form (4.23) to a coupled diffusion-stress evolution system. Generalizations of (4.23) can be derived through the use of more complicated stress-strain relations, such as the general Maxwell or Voigt models, or, equivalently, through considerations of modified forms of the memory integral (4.22). An alternate approach is to derive (4.23) from considerations of hereditary contributions to the chemical potential [12]. Some of the extensions of the integral form lead to a formulation of a "stress-like" quantity that cannot be rigorously derived from a standard viscoelastic model, hence we will denote the generalized stress by s to emphasize the generalization of

$$\sigma \to s. \tag{4.26}$$

These approaches lead to stress evolution equations of the general form

$$s_t + \beta(u, u_t)s = f(u, u_t, u_{tt}). \tag{4.27}$$

One such model is

$$\frac{\partial s}{\partial t} = \frac{\partial}{\partial t}\left(G(u)\frac{\partial u}{\partial t}\right), \tag{4.28}$$

which can be related to a generalized Maxwell model or derived from the elastic limit of (4.21) [32]. This viscous stress model yields the equation

$$\frac{\partial u}{\partial t} = \frac{\partial}{\partial x}\left[D(u)\left(\frac{\partial u}{\partial x} + E(u)\frac{\partial}{\partial x}\left(G(u)\frac{\partial u}{\partial t}\right)\right)\right]. \tag{4.29}$$

This equation has been studied as an approximation to (4.23) [7], [24], [31],

[32]. Later, we will study the traveling wave solution for (4.29). Here, however, we will focus on the behavior of first-order models for the stress.

4.4 Linear first-order stress models

We will consider a broad class of stress evolution equations that are linear in the stress and first order in time, given by

$$s_t + b(u)(s - S(u)) = (c(u)s + d(u))u_t. \tag{4.30}$$

It is hoped that this model is sufficiently general to describe a wide range of physical problems for general viscoelastic materials. Observe that if $S(u)$ and $c(u)$ are identically zero then (4.30) reduces to a Maxwell model. Similarly, note that (4.25) is of the form (4.30). In (4.30), $S(u)$ is the equilibrium induced stress as a function of the local concentration and $b(u)$ corresponds to the rate of relaxation to that equilibrium. The righthand side of (4.30) represents the instantaneous stress response with a general elastic modulus that can depend linearly on the stress state. It is possible to write the solution of (4.30) in an integral form similar to (4.22) and consequently express the model as a single integro-differential equation (4.23). However, for the following analysis it will be more convenient to use the coupled system of a diffusion equation (4.17) and a stress evolution equation (4.30). Our analysis will use perturbation methods in the limit of strong diffusion - where diffusive effects happen much faster than stress relaxation.

4.5 The problem

To focus attention on the role of the stress, we will consider a simplified diffusion model, (4.17) with D and E taken to be constants. This simplified problem does not capture all the properties of the full system, but it is very useful for understanding some of the qualitative effects of the stress. We will consider a problem representing a one-dimensional thin-film polymer membrane, initially dry and unstressed, separating two reservoirs of penetrant liquid at different concentrations. This model attempts to capture the stress-driven behavior induced by penetrant liquid causing a polymer film to undergo a phase separation into glassy and rubbery regions. The mathematical formulation is given by the initial-boundary value problem on $0 < x < 1$ for $t > 0$

$$\epsilon u_t = u_{xx} + s_{xx}, \tag{4.31a}$$

$$s_t + b(u)(s - S(u)) = (c(u)s + d(u))u_t, \tag{4.31b}$$

$$u(x = 0) = r, \qquad u(x = 1) = 1, \tag{4.31c}$$

$$u(t = 0) = 0, \qquad s(t = 0) = 0, \tag{4.31d}$$

where $0 < r < 1$, and $0 < \epsilon \ll 1$ is a small parameter corresponding to the diffusion coefficients being large, $O(\epsilon^{-1})$. We now solve this problem using perturbation theory and the method of matched asymptotic expansions to describe the short term diffusive spreading and the long term stress-driven evolution.

4.5.1 The initial layer

For $\epsilon \to 0$, we expect there to exist a short initial period where the solution evolves under the influence of the initial conditions. By rescaling time as

$$\tau = t/\epsilon, \tag{4.32}$$

the system (4.31a,b) becomes

$$u_\tau = u_{xx} + s_{xx}, \tag{4.33a}$$

$$s_\tau = (c(u)s + d(u))u_\tau - \epsilon b(u)(s - S(u)). \tag{4.33b}$$

We expand u and s using the regular perturbation series,

$$u(x,\tau) = \sum_{n=0}^{\infty} \epsilon^n U_n(x,\tau) = U_0(x,\tau) + \epsilon U_1(x,\tau) + \cdots, \tag{4.34a}$$

$$s(x,\tau) = \sum_{n=0}^{\infty} \epsilon^n S_n(x,\tau) = S_0(x,\tau) + \epsilon S_1(x,\tau) + \cdots. \tag{4.34b}$$

Substituting these expansions into (4.33a,b) and retaining the leading order terms yields

$$\frac{\partial U_0}{\partial \tau} = \frac{\partial^2 U_0}{\partial x^2} + \frac{\partial^2 S_0}{\partial x^2}, \tag{4.35a}$$

$$\frac{\partial S_0}{\partial \tau} = (c(U_0)S_0 + d(U_0))\frac{\partial U_0}{\partial \tau}. \tag{4.35b}$$

Observe that (4.35b) can be reduced to the ordinary differential equation

$$\frac{d\mathcal{S}}{dU_0} = c(U_0)\mathcal{S} + d(U_0), \tag{4.36}$$

by assuming S_0 to be a function of U_0, $S_0 = \mathcal{S}(U_0)$. Note that in the absence of forcing ($c(u) \equiv 0$, $d(u) \equiv 0$), the instantaneous stress $\mathcal{S}(U_0)$ would be identically zero and hence we would conclude that all stress responses are on a slow time-scale. We will study this case in an examination of the long-time evolution equation.

Solving (4.36) subject to the initial condition $U_0 = 0$, $S_0 = 0$ at $t = 0$ yields a unique solution for $\mathcal{S}(U_0)$ which may be substituted back into (4.35a) to yield the nonlinear diffusion equation

$$\frac{\partial U_0}{\partial \tau} = \frac{\partial}{\partial x}\left(\mathcal{D}(U_0)\frac{\partial U_0}{\partial x}\right), \tag{4.37}$$

with the diffusion coefficient

$$\mathcal{D}(U_0) = 1 + \mathcal{S}'(U_0). \tag{4.38}$$

Note that we may also write (4.37) as

$$\frac{\partial U_0}{\partial \tau} = \frac{\partial^2}{\partial x^2}\mathcal{W}(U_0), \tag{4.39}$$

where the initial chemical potential $\mathcal{W}$ is given by

$$\mathcal{W}(U_0) \equiv U_0 + \mathcal{S}(U_0). \tag{4.40}$$

Therefore, to leading order, the behavior of the concentration is purely diffusive in the initial layer. The stress serves to either increase or decrease the diffusivity, depending on the derivative of $\mathcal{S}(U_0)$. If $\mathcal{S}'(U_0) < -1$, then (4.37)

can form sharp interfaces [5].

The solution in the initial layer will be used as an initial condition for the outer solution governing the system for long times. For this matching procedure we seek the solution of (4.37) as $\tau \to \infty$. This steady-state solution is given in terms of the chemical potential as

$$\mathcal{W}(\underline{U_0}(x)) = \underline{w}(x), \tag{4.41}$$

where

$$\underline{w}(x) = \mathcal{W}(r)(1-x) + \mathcal{W}(1)x. \tag{4.42}$$

If $\mathcal{W}$ is invertible [5] then (4.42) will yield a smooth concentration profile as the initial condition for the long time evolution equation.

4.5.2 The outer solution

Away from the initial layer, the solution can be expanded as the perturbation series

$$u(x,t) = \sum_{n=0}^{\infty} \epsilon^n u_n(x,t) = u_0(x,t) + \epsilon u_1(x,t) + \cdots, \tag{4.43a}$$

$$s(x,t) = \sum_{n=0}^{\infty} \epsilon^n s_n(x,t) = s_0(x,t) + \epsilon s_1(x,t) + \cdots. \tag{4.43b}$$

Substituting these expansions in (4.31ab) and retaining leading order terms yields

$$\frac{\partial^2 u_0}{\partial x^2} + \frac{\partial^2 s_0}{\partial x^2} = 0, \tag{4.44a}$$

$$\frac{\partial s_0}{\partial t} = (c(u_0)s_0 + d(u_0))\frac{\partial u_0}{\partial t} - b(u_0)(s_0 - S(u_0)). \tag{4.44b}$$

If we define a chemical potential [12] function $w(x,t)$ as

$$w(x,t) \equiv u(x,t) + s(x,t), \tag{4.45}$$

(where, from here onward, we will drop the 0 subscripts and work with leading order terms only) then can write (4.44a) as

$$w_{xx} = 0, \tag{4.46}$$

with solution

$$w(x,t) = A(t)(1-x) + B(t)x. \tag{4.47}$$

To determine the functions $A(t)$ and $B(t)$ observe that for Dirichlet boundary conditions on u (4.31c) we can use (4.31b) to determine the surface stresses at $x = 0$ and $x = 1$. Since (4.31b) has no spatial dependence, it is uncoupled from (4.31a) at $x = 0$ and $x = 1$, where u is given for all times. These considerations, along with the initial condition for s (from the initial layer), yield the stresses at the boundaries:

$$s(0,t) = S(r) + (\mathcal{S}(r) - S(r))\mathrm{e}^{-b(r)t}, \tag{4.48a}$$

$$s(1,t) = S(1) + (\mathcal{S}(1) - S(1))\mathrm{e}^{-b(1)t}. \tag{4.48b}$$

Similar results hold if the boundary conditions on u at $x = 0$ and $x = 1$ were time-dependent, or, more generally, if $u(0,t)$ and $u(1,t)$ were given

by the solutions of ordinary differential equations at the boundaries. This allows us to easily extend our analysis to cover problems with time-dependent nonequilibrium boundary conditions [12]. In these more general cases, the functional forms of $s(0,t)$ and $s(1,t)$ may be more complicated, but they can always be evaluated using numerical integration.

Given the stress boundary conditions (4.48a,b), we now determine $w(x,t)$ to be

$$w(x,t) = \left[r + S(r) + (\mathcal{S}(r) - S(r))\mathrm{e}^{-b(r)t}\right](1-x) + \left[1 + S(1) + (\mathcal{S}(1) - S(1))\mathrm{e}^{-b(1)t}\right]x. \tag{4.49}$$

From the definition of w (4.45), we can write $s = w - u$ to eliminate stress from (4.44b) yielding an evolution equation for u,

$$\frac{\partial u}{\partial t} = \frac{\frac{\partial w}{\partial t} + b(u)\left(w(x,t) - u - S(u)\right)}{1 + c(u)(w(x,t) - u) + d(u)}. \tag{4.50}$$

Further structure may be attached to (4.50) by decomposing the chemical potential w into steady-state, relaxational and instantaneous contributions

$$w(x,t) = \overline{w}(x) + \tilde{w}(x,t) + \hat{w}(x,t), \tag{4.51}$$

where the transient stress-relaxation term is

$$\tilde{w}(x,t) = -S(r)\mathrm{e}^{-b(r)t}(1-x) - S(1)\mathrm{e}^{-b(1)t}x, \tag{4.52}$$

the instantaneous stress contribution is

$$\hat{w}(x,t) = \mathcal{S}(r)\mathrm{e}^{-b(r)t}(1-x) + \mathcal{S}(1)\mathrm{e}^{-b(1)t}x, \tag{4.53}$$

and the equilibrium chemical potential distribution is

$$\overline{w}(x) = (r + S(r))(1-x) + (1 + S(1))x. \tag{4.54}$$

From (4.44b), at equilibrium, the stress is given by $s = S(u)$, and from (4.45) we may define an equilibrium chemical potential function by

$$W(u) \equiv u + S(u). \tag{4.55}$$

Then, in terms of W, $\overline{w}$ can be written as

$$\overline{w}(x) = W(r)(1-x) + W(1)x. \tag{4.56}$$

Observe that the chemical potential $w(x,t)$ smoothly evolves from the initial distribution (4.42) to the equilibrium distribution (4.56). Using the above decomposition in (4.50) yields

$$\frac{\partial u}{\partial t} = \tilde{b}(u,x,t)\left[\left(\hat{w} + \frac{1}{b(u)}\frac{\partial \hat{w}}{\partial t}\right) + \left(\tilde{w} + \frac{1}{b(u)}\frac{\partial \tilde{w}}{\partial t}\right) + (\overline{w}(x) - W(u))\right], \tag{4.57}$$

where

$$\tilde{b}(u,x,t) = \frac{b(u)}{1 + c(u)(w-u) + d(u)}. \tag{4.58}$$

This evolution equation governs the long-time asymptotics of u as the system

approaches equilibrium. The terms involving $\tilde{w}$ and $\hat{w}$ in (4.57) are explicit time-dependent forcing terms. Their presence is a consequence of having a variable relaxation times given by $b(u)$. If $b(u)$ were a constant, say $b(u) \equiv b_0$, then the forcing terms would vanish identically. Conversely, the analysis for an inhomogeneous substrate with a given $b(x)$ yields an equation of the same form as (4.57). Note that while neither the equations (4.31a,b) nor the boundary conditions (4.31c) in our model explicitly involve time, the stress relaxation on the boundaries results in explicit forcing in (4.57). The early behavior of (4.57) is dominated by a competition between relaxational and instantaneous forces. However, these influences decay exponentially in time, and the solution will approach an equilibrium at $t \to \infty$. In the next section we will study in detail the influence of variable relaxation-time forcing on the selection of a steady-state solution.

4.6 Shock formation

We will study the dynamics of the evolution equation

$$\frac{\partial u}{\partial t} = b(u)\left[\left(\tilde{w} + \frac{1}{b(u)}\frac{\partial \tilde{w}}{\partial t}\right) + \left(\overline{w}(x) - W(u)\right)\right] \tag{4.59}$$

for the case of a bi-stable medium. The formation of stationary shocks in this problem will be related to the initial conditions and the distribution of relaxation times. We note that (4.59) could also result from a leading-order

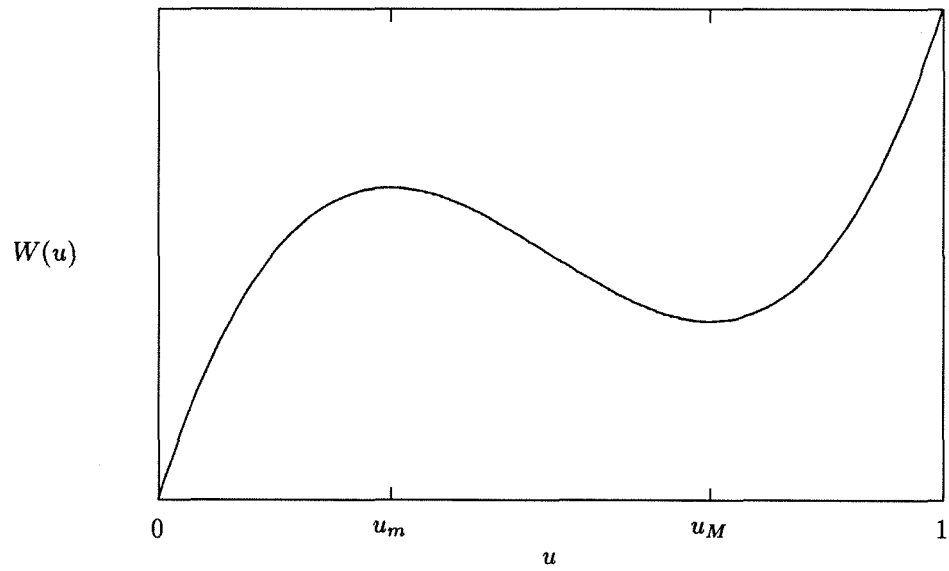

Figure 1: The chemical potential function $W(u)$.

analysis of the inhomogeneous, forced reaction-diffusion system

$$u_t = \epsilon^2 u_{xx} - b(u)(u + s - w(x,t)) + w_t(x,t), \tag{4.60a}$$

$$\epsilon s_t = \epsilon^2 s_{xx} - b(u)(s - S(u)). \tag{4.60b}$$

After a brief discussion of the equilibrium solution of (4.59), we will consider the dynamics of shock formation and go on to note some extensions to more complicated problems.

Equation (4.59) admits steady-state shocks if $W(u)$ is a nonmonotone function; cubic-like potential functions (see Fig. 1) are found in many applications [33], [12], [34]. In terms of the equilibrium stress $S(u)$, this condition requires that $S'(u) < -1$ on some interval $u \in (u_m, u_M)$. As $t \to \infty$, we expect the solution of (4.59) to approach a time-independent equilibrium

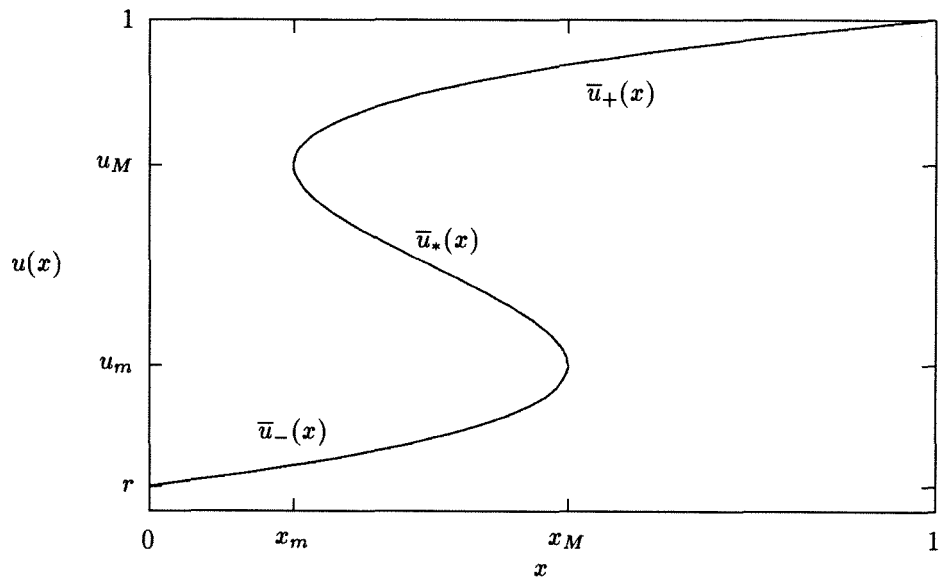

Figure 2: The multivalued, time-independent solution $\overline{x}(\overline{u})$.

solution $\overline{u}(x)$. For long times, the transient terms involving $\tilde{w}$ vanish exponentially, and equilibrium requires that

$$\overline{w}(x) - W(\overline{u}) = 0. \tag{4.61}$$

Substituting (4.54) in (4.61) gives us an implicit representation of the time-independent solution

$$\overline{x}(\overline{u}) = \frac{W(\overline{u}) - W(r)}{W(1) - W(r)}. \tag{4.62}$$

For nonmonotone $W(u)$, (4.62) can not be the steady-state solution of (4.59) for any initial-value problem; (4.62) is a multivalued "S-shaped" curve (see Fig. 2), whereas solutions of (4.59) are necessarily single-valued functions. What is observed in direct simulations of (4.59) is that solutions develop a

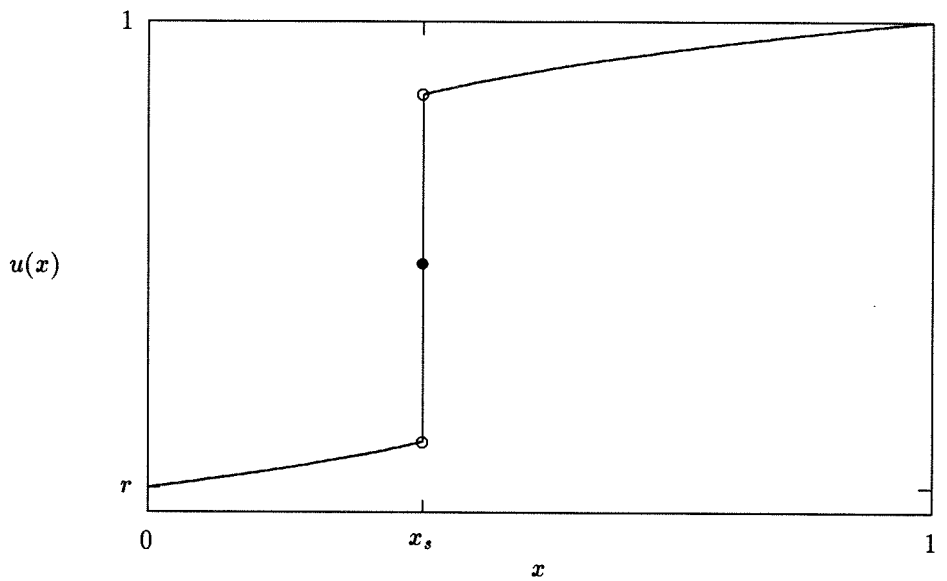

Figure 3: The steady-state shock solution.

shock connecting the upper and lower branches of $\overline{x}(\overline{u})$ (see Fig. 3). Such solutions satisfy the equilibrium condition (4.61) pointwise,

$$\overline{u}(x) = \begin{cases} \overline{u}_-(x) & x < x_s, \\ \overline{u}_*(x) & x = x_s, \\ \overline{u}_+(x) & x > x_s, \end{cases} \tag{4.63}$$

where x_s is the shock position and $\overline{u}_-$, $\overline{u}_*$, and $\overline{u}_+$ are the lower, middle and upper branches of (4.62) (see Fig. 2). There is a continuum of such solutions corresponding to each $x_s \in [x_m, x_M]$ where $\overline{u}_*(x)$ is defined. Which one of these solutions is selected by the system depends on the initial conditions. In the case of (4.59), where there is time-dependent forcing, this becomes a more complicated problem.

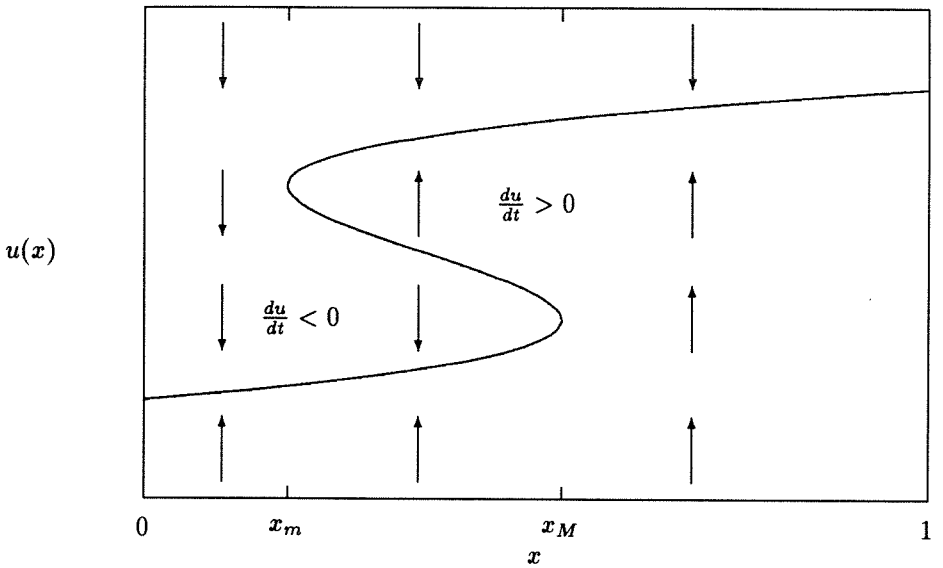

Figure 4: The direction field for (4.64).

In the absence of the forcing terms, (4.59) reduces to

$$\frac{\partial u}{\partial t} = b(u)(\overline{w}(x) - W(u)). \tag{4.64}$$

For this equation, the shock position can be readily determined from the initial data. The curve $\overline{x}(\overline{u})$ corresponds to equilibrium points where $\partial u/\partial t = 0$. Away from this curve $\partial u/\partial t$ is either positive or negative and hence u increases or decreases monotonically until it reaches an equilibrium point (see Fig. 4). Similarly, a linearized stability analysis can be carried out to show that $\overline{u}_*(x)$ is unstable while $\overline{u}_+(x)$ and $\overline{u}_-(x)$ are stable branches of $\overline{x}(\overline{u})$. If the initial data, the curve $\underline{u}(x)$, intersects $\overline{u}_*(x)$ then a shock will occur where $\overline{u}_*(x_s) = \underline{u}(x_s)$. If $\underline{u}(x)$ does not intersect $\overline{u}_*(x)$, then the shock will occur at one of the turning points, $x_s = x_m$ or $x_s = x_M$. These shock

position rules can be summarized by defining a shock origin curve (see Fig. 5)

$$\underline{x}(\underline{u}) = \begin{cases} x_m & \underline{u} > u_M, \\ x & \underline{u} = \overline{u}_*(x), \\ x_M & \underline{u} < u_m. \end{cases} \tag{4.65}$$

The shock position x_s is then defined by the solution of

$$\underline{x}(\underline{u}(x_s)) = x_s. \tag{4.66}$$

The addition of time-dependent forcing in the system makes the study of shock formation more complicated. Several aspects of the arguments given above break down because there are no fixed equilibrium points while the forcing is nonzero. This introduces some subtle changes to the nature of shock formation that will be examined below.

Insight into the behavior of (4.59) can be gained by recasting it as a phase plane system with a bifurcation parameter. Equation (4.59) is purely evolutionary - it contains no spatial coupling. It depends on the position x only parametrically through the functions $\overline{w}(x)$ and $\tilde{w}(x,t)$. Therefore, we will view (4.59) as an ordinary differential equation in time with fixed position x, for all $x \in (0,1)$. By using the change of variables

$$v = \mathrm{e}^{-b(r)t}, \tag{4.67}$$

we can eliminate the explicit time-dependence in (4.59) to yield the au-

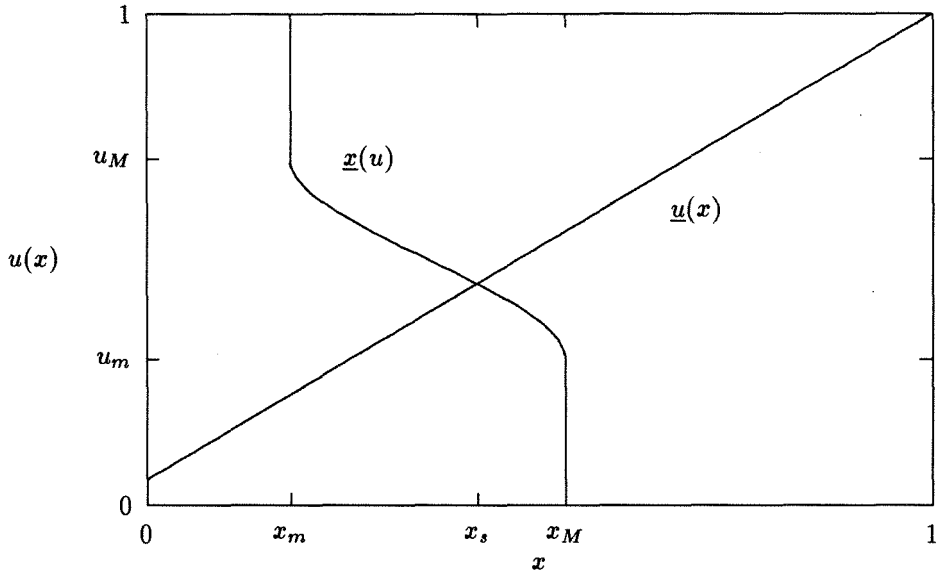

Figure 5: The shock origin curve for shock position determination.

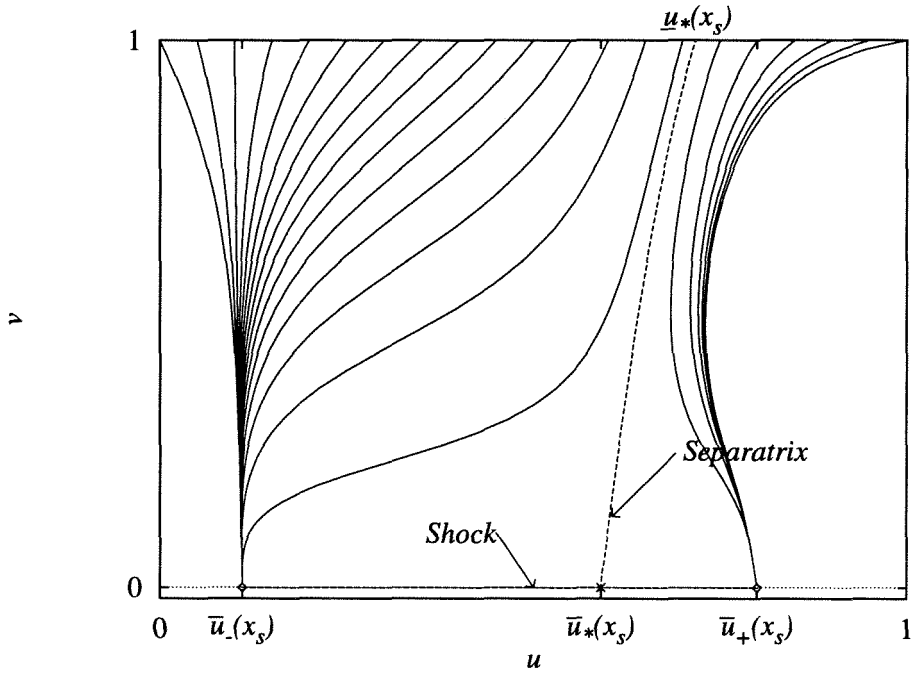

Figure 6: The phase plane representation.

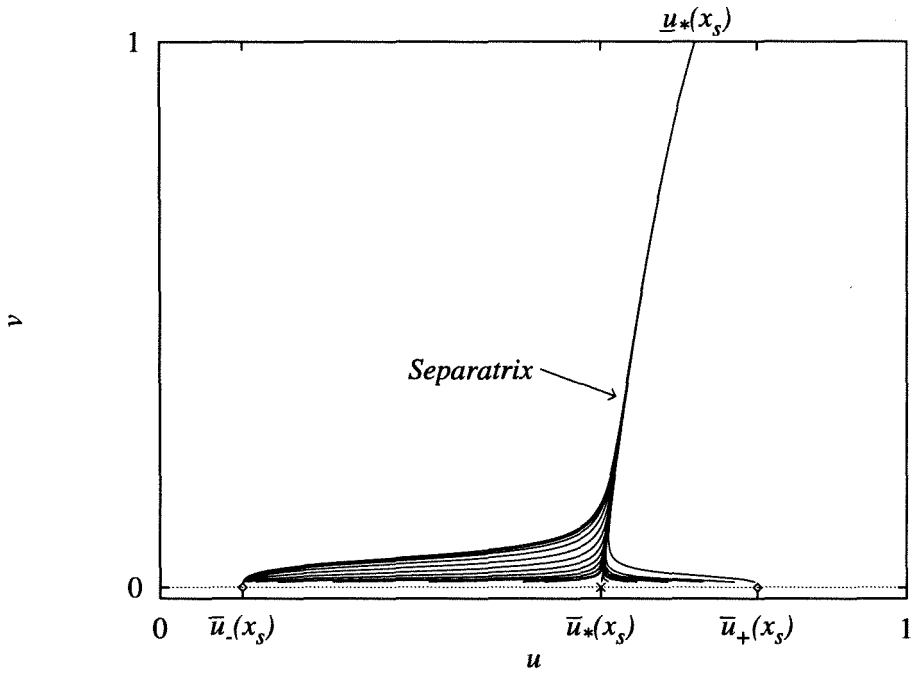

Figure 7: The attracting property of the separatrix as $v \to \infty$.

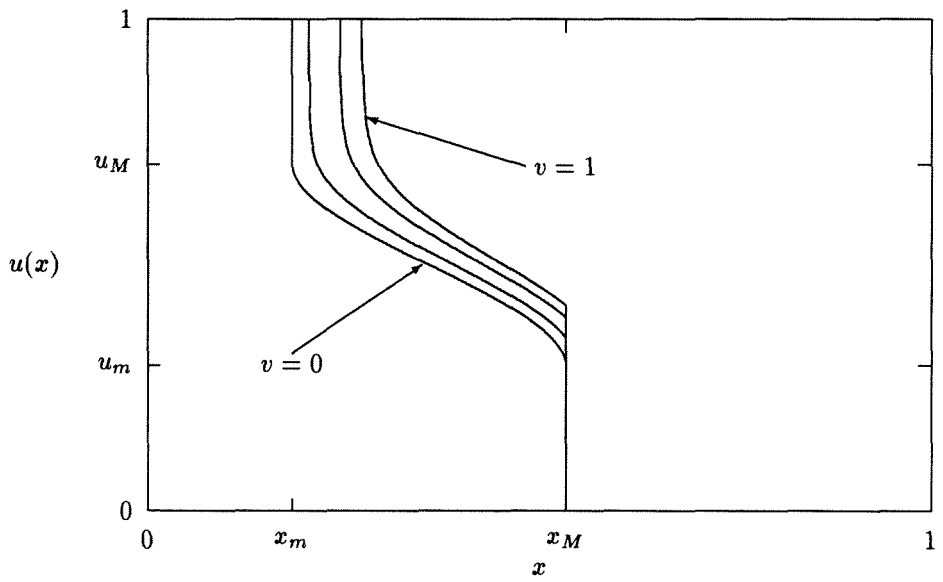

Figure 8: The time evolution of $\underline{x}(\underline{u})$.

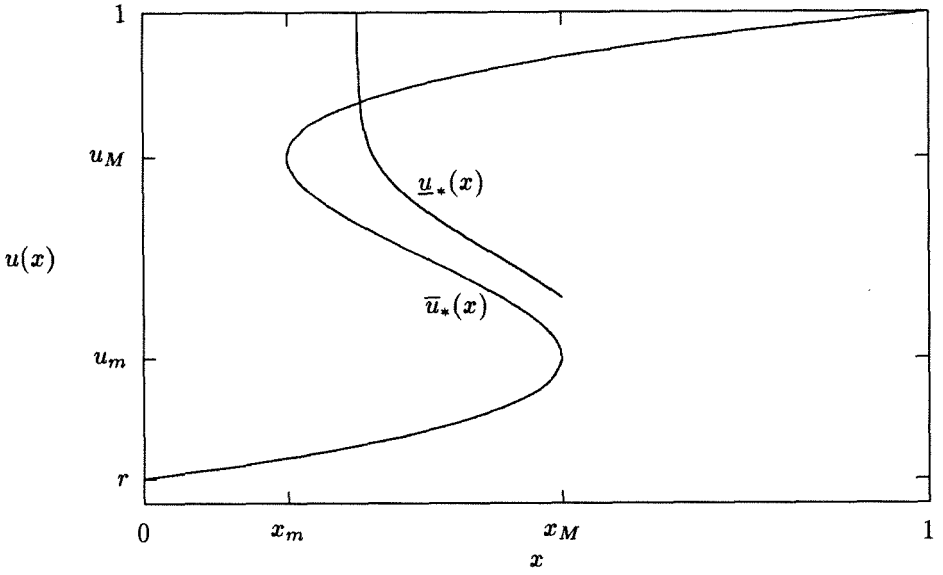

Figure 9: The $\underline{u}_*(x)$ branch.

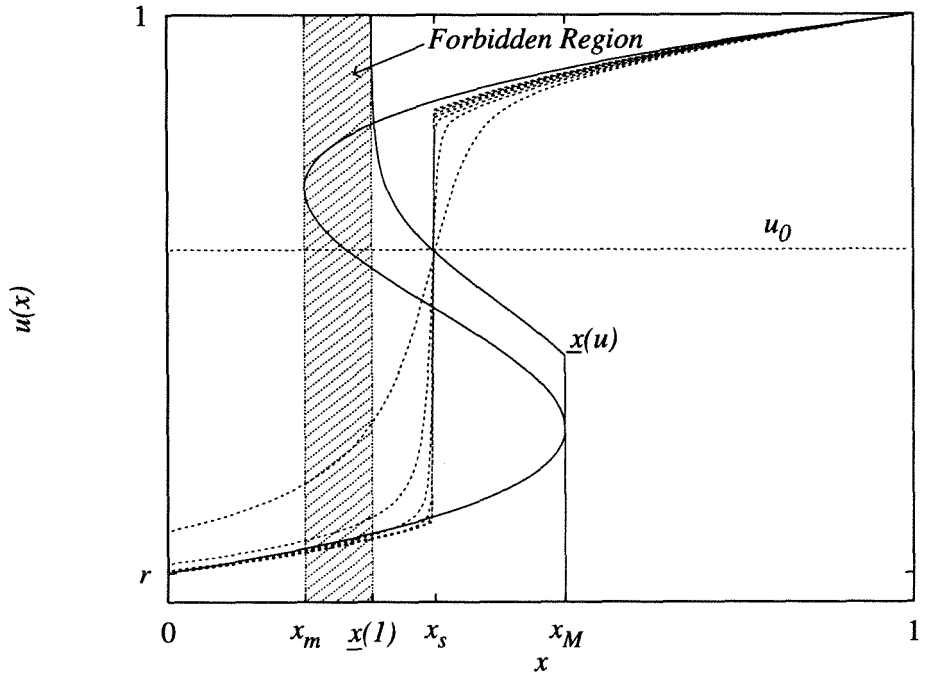

Figure 10: Shock formation from a uniform initial condition $\underline{u}(x) = u_0$.

tonomous phase plane system

$$\frac{du}{dt} = F(u,v;x) \equiv b(u)\left[\left(\tilde{w} + \frac{1}{b(u)}\frac{\partial \tilde{w}}{\partial t}\right) + (\overline{w}(x) - W(u))\right], \qquad (4.68a)$$

$$\frac{dv}{dt} = -b(r)v, \qquad (4.68b)$$

where

$$\tilde{w}(v;x) = -S(r)v(1-x) - S(1)v^{\alpha}x, \qquad \alpha = \frac{b(1)}{b(r)} > 1. \qquad (4.69)$$

System (4.68ab) has equilibrium points at $v = 0$ at the roots of the time-independent equilibrium condition (4.61). Depending on the value of x, there may be one, two or three fixed points. Linear stability analysis yields the exponential growth rates, $\mu_{1,2}$, at the fixed points

$$\mu_1 = \left.\frac{\partial F}{\partial u}\right|_{v=0,\overline{u}} = -b(\overline{u})W'(\overline{u}), \qquad \mu_2 = -b(r) < 0. \qquad (4.70)$$

The eigenvalue μ_1 is the same as in the unforced case (4.64) and μ_2 is a result of the change of variables (4.67). In this representation, $\overline{u}_+$ and $\overline{u}_-$ correspond to stable nodes while $\overline{u}_*$ is an unstable hyperbolic saddle point. For $x < x_m$ and $x > x_M$, the phase plane has a single stable node, corresponding to the unique equilibrium solution of (4.59) in these domains. We will briefly discuss the degenerate behavior at the turning points $x = x_m$ and $x = x_M$ in the appendix, but here we focus on shock formation for $x_m < x < x_M$.

When $\overline{x}(\overline{u})$ is triple-valued, qualitative information about the shock can be gained from an interpretation of behavior in the phase plane. Except for

points on the stable manifold, the separatrix, of the saddle point, all points are on trajectories that will approach one of the two stable nodes as $t \to \infty$ ($v \to 0$). The separatrix is the boundary between the basins of attraction for the two stable nodes. Points on the separatrix will approach the saddle as $t \to \infty$. On the line $v = 0$ are heteroclinic connections from the saddle to the stable nodes; this is the unstable manifold of the saddle, which corresponds to a shock connecting the stable branches of $\overline{x}(\overline{u})$. If the initial condition $u = \underline{u}(x_s)$ at $t = 0$ ($v = 1$) is on the separatrix for the phase plane system at parameter x_s then as $t \to \infty$, u will approach the unstable branch of $\overline{x}(\overline{u})$ and will form a shock at x_s connecting it to the stable branches at infinite time, $v = 0$ (see Fig. 6). This line of argument is consistent with the fact that system (4.31a-d) can not form shocks in finite time [8], [9].

The phase plane can also be used to obtain quantitative information about the influence of the time-dependent forcing. By putting (4.68a,b) in the form

$$\frac{du}{dv} = -\frac{F(u, v; x)}{b(r)v}, \tag{4.71}$$

we can easily obtain the integral curves for the system. If there is no forcing and hence F is independent of v, then the lines $u = \overline{u}_-$, $u = \overline{u}_+$, and $u = \overline{u}_*$ are invariant curves, as for (4.64). The addition of time-dependent forcing makes these curves time-dependent. In the case of the stable nodes $\overline{u}_+$ and $\overline{u}_-$, these curves are typical of a continuous set of trajectories in the plane attracted to the stable equilibria as $t \to \infty$. For the saddle point $\overline{u}_*$, there is a unique trajectory, the separatrix, that approaches $\overline{u}_*$ as $v \to 0$ (see Fig. 6). Moreover, calculation of the separatrix is of interest since, as described

above, it gives the position of the shock. We seek the separatrix at time $t = 0$ ($v = 1$), call it $\underline{u}_*(x)$. The shock position is then given by the position where the initial condition intersects $\underline{u}_*(x)$, $\underline{u}(x_s) = \underline{u}_*(x_s)$. A generalized definition of the shock origin curve is then

$$\underline{x}(\underline{u}) = \begin{cases} x_m & \underline{u} > \underline{u}_*(x_m), \\ x & \underline{u} = \underline{u}_*(x), \\ x_M & \underline{u} < \underline{u}_*(x_M). \end{cases} \tag{4.72}$$

In the unforced case $\underline{u}_*(x) = \overline{u}_*(x)$ and we recover (4.65) from (4.72). The curve $\underline{u}_*(x)$ is defined as $u(v = 1; x)$ for the solution of (4.71) with initial condition $u(v = 0; x) = \overline{u}_*(x)$ for all $x \in [x_m, x_M]$ where $\overline{u}_*(x)$ is defined. The right-hand side of (4.71) is an indefinite form at the saddle point $u = \overline{u}_*(x)$, $v = 0$; but an application of l'Hopital's rule yields an applicable initial condition as $v \to 0$

$$u(v = \Delta v; x) \sim \overline{u}_*(x) + \frac{du}{dv}\Delta v, \tag{4.73}$$

where

$$\left.\frac{du}{dv}\right|_{\overline{u}_*, v=0} = -\frac{\frac{\partial F}{\partial v}}{b(r) + \frac{\partial F}{\partial u}} = -\frac{b(\overline{u}_*) + b(r)S(r)}{b(r) - b(\overline{u}_*)W'(\overline{u}_*)}(1 - x). \tag{4.74}$$

Further, this scheme for computing $\underline{u}_*(x)$ is stable since the separatrix is an attracting set in the phase plane as v increases ($t \to -\infty$) (see Fig. 7). Following this procedure, we observe that at $v = 0$ we begin with the initial condition (4.65), the "steady" shock origin curve. As v increases, the curve

smoothly evolves to (4.72) at $v = 1$ (see Fig. 8). The nature of this evolution process is determined by the function $b(u)$. Some qualitative statements can be made about the effects of the forcing. In (4.71), the time-dependent forcing terms are

$$\mathcal{F}(u,v;x) = \frac{1}{b(r)}\Big((b(u)-b(r))S(r)(1-x)+(b(u)-b(1))S(1)v^{\alpha-1}x\Big). \quad (4.75)$$

By considering the form of $\mathcal{F}$, it can be shown that if $b(u)$ is an increasing function, then $\mathcal{F}$ works to drive the growth of u. Conversely, if $b(u)$ is a decreasing function, then $\mathcal{F}$ opposes the motion of u and serves to damp the evolution of the shock origin curve. In connection with our application [12], we studied increasing $b(u)$ functions and have observed the following behavior: $\underline{u}_*(x_M)$ will generally be different from u_m, but it will remain finite, and, more significantly, as $x \to x_m$, $\underline{u}_*(x)$ appears to diverge (see Fig. 9). This last point is very important since it implies that the time-dependent forcing has effectively reduced the domain on which shocks can form and has created a "forbidden region." To see this consider the general class of smooth initial conditions $\underline{u}(x)$ for (4.59) on $0 \le x \le 1$ bounded by $0 \le \underline{u}(x) \le 1$. As remarked in the discussion of (4.64), in the absence of forcing, this class of initial conditions can yield shocks on $x_s \in [x_m, x_M]$. With forcing, these initial conditions can only yield shocks on the reduced set $x_s \in [\underline{x}(1), x_M]$ (see Fig. 10). Hence shocks can not form in the interval $x_s \in [x_m, \underline{x}(1))$. Since $\mathcal{F}$ is invariant under rescaling of $b(u)$, $b(u) \to kb(u)$, it is not the magnitude of the relaxation time, but rather the variation of $b(u)$ and other properties that govern the formation of forbidden regions.

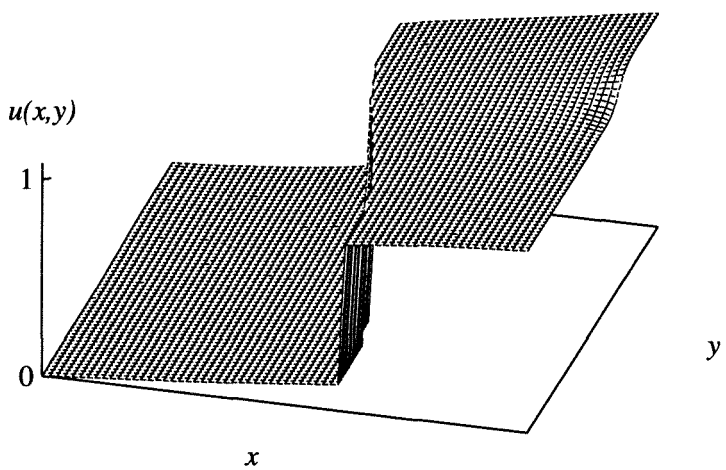

Figure 11: A two-dimensional steady-state solution $u(x, y)$ with a curved shock.

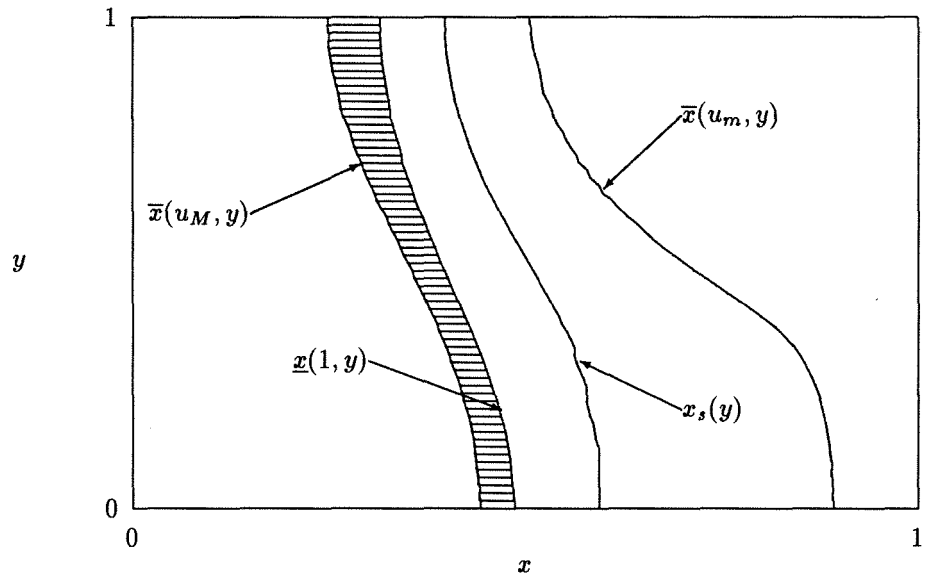

Figure 12: The curved shock $x_s(y)$ and the "forbidden region" (shaded) in the shock formation domain $\overline{x}(u_M, y) \leq x \leq \overline{x}(u_m, y)$.

This work can be extended in several directions to apply to more complex systems. For a two-dimensional extension of the system (4.31a-d) considered in [12], we show that curved shocks are excluded from a region in the unit square (see Figs. 11, 12). There is also considerable interest in systems with many coexisting stable states that support different, competing shocks [33], [11], [35]. These problems have more complicated $W(u)$ potential functions; we present the results for two generic cases of a tri-stable system (see Figs. 13, 14 in which shading indicates forbidden regions for shock formation). Here there are two shock origin curves, one associated with each unstable branch of $\overline{x}(\overline{u})$. For Fig. 13, solutions will always contain two shocks, while for Fig. 14 nearly the entire upper unstable branch is a forbidden region and solutions may have either one or two shocks. We will now conclude with a

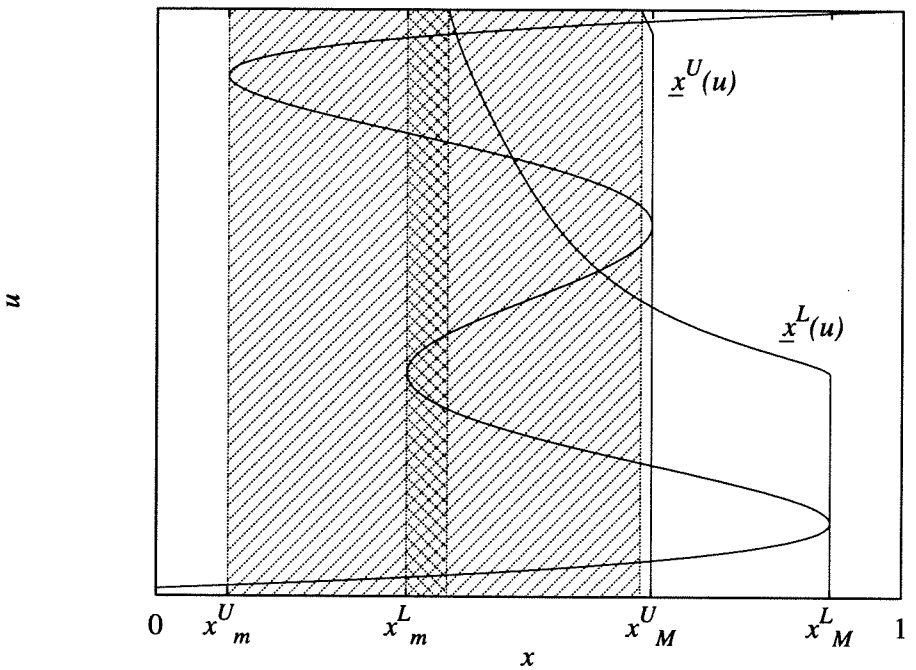

Figure 13: Shock formation for a tri-stable system. Shading indicates forbidden regions for shock formation.

brief discussion of another aspect of the dynamics of shock formation - the evolution of the shock layer thickness.

4.7 Shock-layer thickness

In studying the dynamics of (4.59), we always begin with a smooth initial condition that will yield a steady-state shock profile. Hence, at the shock position x_s, the gradients of u must diverge as $t \to \infty$. Here we give a brief analysis of the effects of time-dependent forcing on this rate of divergence.

For the unforced case (4.64), if we linearize u in the neighborhood of the

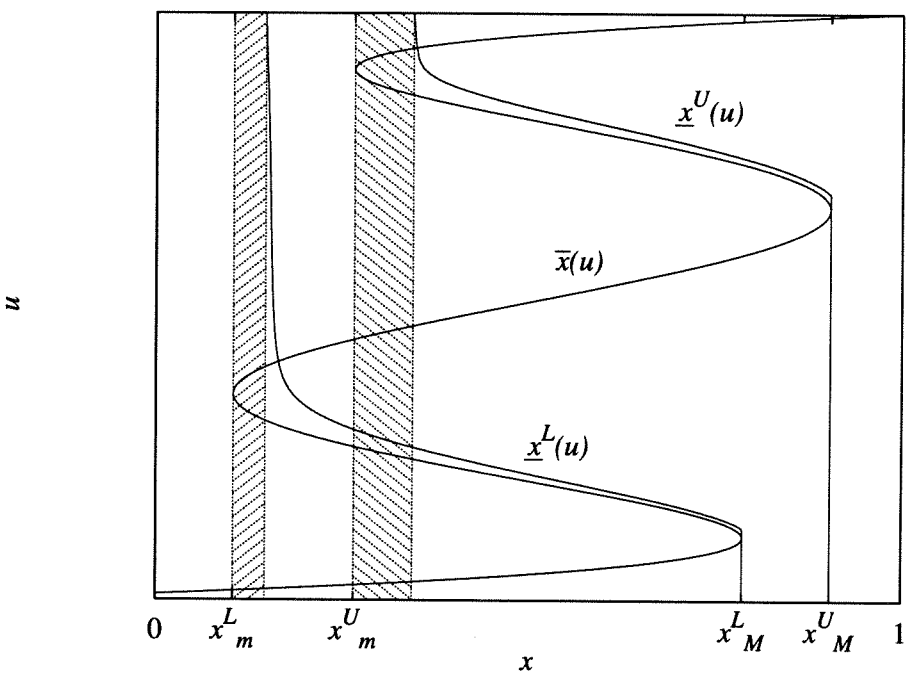

Figure 14: Shock formation for a tri-stable system. Shading indicates forbidden regions for shock formation.

shock

$$u(x_s + \Delta x, t) \sim \overline{u}_*(x_s) + m(t)\Delta x + O(\Delta x^2), \tag{4.76}$$

where $m(t)$ is the local slope and we take $\Delta x \to 0$, then we obtain the linearized equation for slope evolution at $O(\Delta x)$

$$\frac{dm}{dt} = b(\overline{u}_*)(\overline{w}'(x_s) - W'(\overline{u}_*)m). \tag{4.77}$$

Therefore, the long-time behavior of the slope is

$$m(t) = O(\exp[-b(\overline{u}_*)W'(\overline{u}_*)t]), \tag{4.78}$$

where $W'(\overline{u}_*) < 0$. Taking the layer thickness to be inversely proportional to the slope we see that the unforced shock thickness decays exponentially like

$$O(\exp[b(\overline{u}_*)W'(\overline{u}_*)t]). \tag{4.79}$$

In the time-dependent case we proceed similarly. Now we linearize about the time-dependent solution $u_*(x_s, t)$, the trajectory corresponding to the separatrix,

$$u(x_s + \Delta x, t) \sim u_*(x_s, t) + m(t)\Delta x + O(\Delta x^2), \tag{4.80}$$

to yield the slope evolution equation

$$\frac{dm}{dt} = b(u_*)\left[\left(\overline{w}'(x_s) + \frac{\partial \tilde{w}}{\partial x} + \frac{1}{b(u_*)}\frac{\partial^2 \tilde{w}}{\partial x \partial t}\right) - \left(W'(u_*) + \frac{b'(u_*)}{b^2(u_*)}\frac{\partial \tilde{w}}{\partial t}\right)m\right]. \tag{4.81}$$

From our earlier examination of the phase plane system (4.68ab), we know the long-time asymptotics of $u_*(x_s, t)$ are given by

$$u_*(x_s, t) \sim \overline{u}_* - \frac{F_v}{b(r) + F_u} \, \mathrm{e}^{-b(r)t} \qquad t \to \infty. \tag{4.82}$$

A crude estimate of the shock layer thickness as $t \to \infty$ is then

$$O\left(\exp\left[b(\overline{u}_*)\frac{\partial}{\partial u}\left(W(u) - \frac{1}{b(u)}\frac{\partial \tilde{w}}{\partial t}\right)\Big|_{\overline{u}_*} t\right]\right). \tag{4.83}$$

Note that while the time-dependent forcing has had a significant effect in shock placement, it only contributes an exponentially small change to the long-time shock formation rate.

4.8 Mass-uptake characteristics

In polymer-penetrant diffusion experiments observations typically include mass-uptake calculations, measurements of the amount of penetrant absorbed in the polymer film at each instance of time

$$M(t) = \int_0^1 u(x, t)\, dx. \tag{4.84}$$

In the results of Vrentas, Duda and Hou, the mass-uptake curve initially shows a rapid increase, obtains a maximum value, slowly decreases, and then adjusts to a steady-state value; this behavior is called sorption overshoot. We examine how this behavior is manifested in our model. As in [12], we use

the stress evolution equation

$$s_t + b(u)\left(s - \frac{u}{b(u)}\right) = 0, \tag{4.85}$$

where

$$b(u) = \frac{1+\omega}{2} + \frac{1-\omega}{2}\tanh\left(\frac{u-u_{rg}}{\delta}\right), \tag{4.86}$$

(see Fig. 15) to focus on the influence of the phase transition. For penetrant concentrations less than the rubber-glass transition point, u_{rg}, the polymer will be in the glassy state with a slower rate of viscoelastic relaxation $b \sim \omega < 1$. For the polymer in the rubbery state, the relaxation rate is $b \sim 1$. Additionally, we take the equilibrium stress to be

$$S(u) = \frac{u}{b(u)}, \tag{4.87}$$

therefore, at steady state, the glassy state is under more stress than the rubbery state. In this simplified model we will show how the separation in relaxation rates can cause the overshoot behavior.

The observed rapid initial increase and gradual decrease behaviors of $M(t)$ can be readily explained in terms of the two asymptotic regimes used for the model. For a short range of initial times of order ϵ the absorption of the penetrant is governed by the classical heat equation (Fickian diffusion). The analysis of the mass-uptake for this problem is well known [13], [14] and yields the rapid rise on the fast initial time scale τ until the steady state is reached. For large finite times the behavior of the system is dominated by the interaction of the viscoelastic relaxation of the polymer with the fast

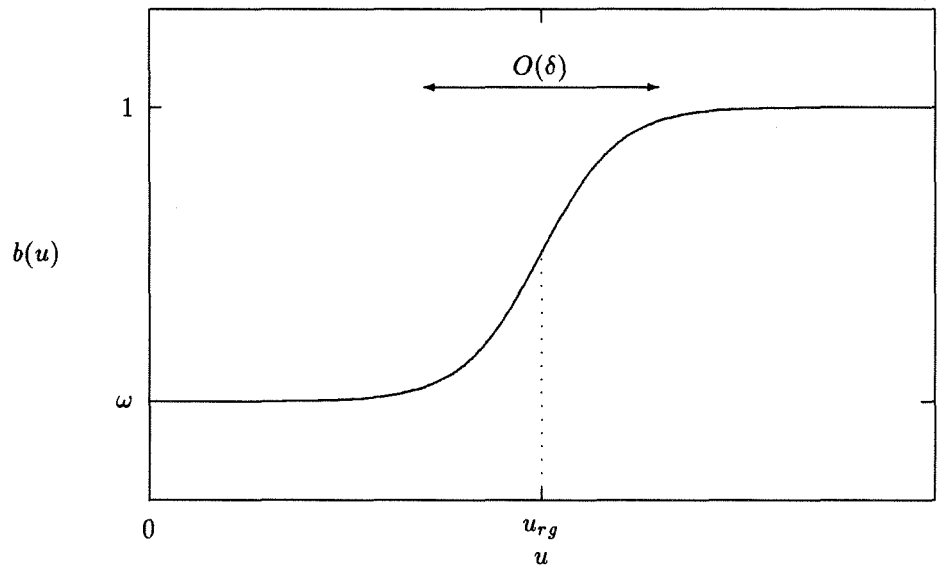

Figure 15: The inverse relaxation time function $b(u)$.

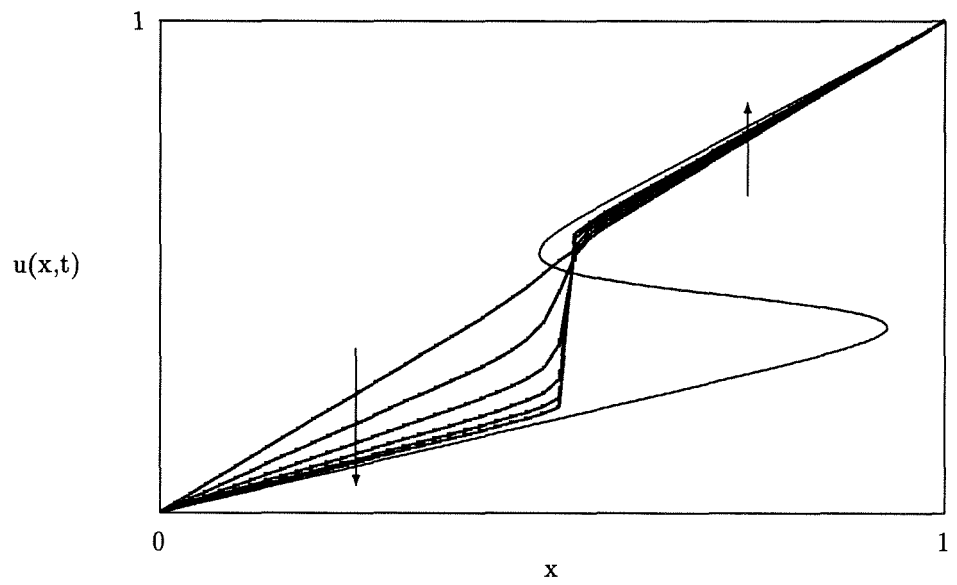

Figure 16: Long-time evolution of the concentration profile.

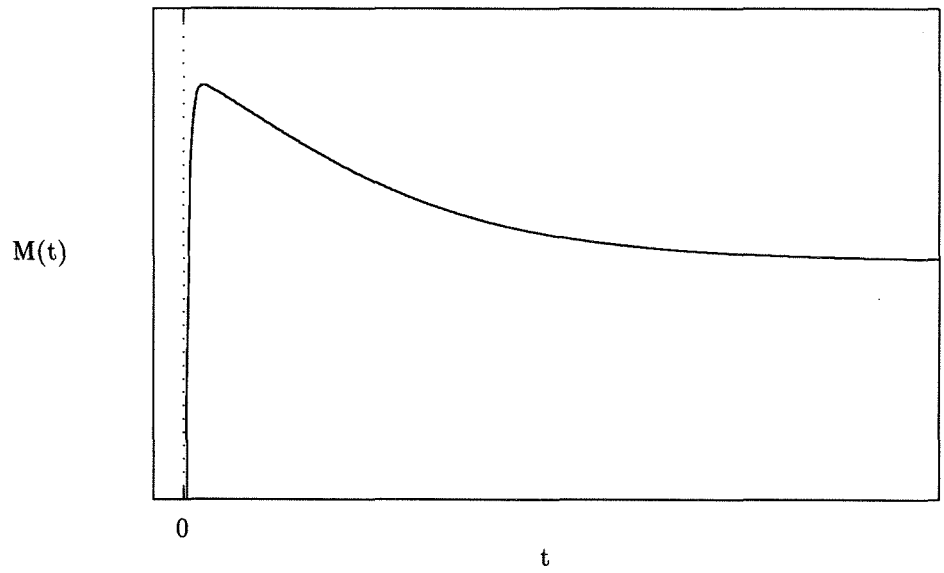

Figure 17: A mass-uptake curve showing overshoot behavior.

diffusive equilibration of the penetrant. The steady-state, $M_\infty = M(t \to \infty)$, is determined by the position of the shock (as given from the results of the previous sections)

$$M_\infty = \int_0^{x_s} \overline{u}_-(x)\,dx + \int_{x_s}^1 \overline{u}_+(x)\,dx. \tag{4.88}$$

To understand the behavior of the outer solution for finite time it is convenient to assume an approximate form for the solution away from the shock and determine how rapidly it converges to the steady-state. The ansatz and consistent approximations used for the following analysis are given by (see Fig. 16)

$$u(x,t) \sim \begin{cases} r(1-x) + k_0(t)x & x \ll x_s, \\ k_1(t)(1-x) + x & x \gg x_s, \end{cases} \tag{4.89}$$

$$\text{away from } x_s \qquad |u - u_{rg}| \gg O(\delta), \tag{4.90}$$

$$x \ll x_s \qquad u \ll u_{rg} \qquad b(u) \sim \omega,$$

$$x \gg x_s \qquad u \gg u_{rg} \qquad b(u) \sim 1.$$

Observe that if $k_0(0) = 1$ and $k_1(0) = r$, then the ansatz satisfies the initial condition (4.31d) and the boundary conditions (4.31c). Combining (4.89), (4.90) with (4.59) yields

$$\frac{dk_0}{dt} \sim -(1+\omega)k_0(t) + 2\omega + (1-\omega)e^{-t}, \tag{4.91a}$$

$$\frac{dk_1}{dt} \sim -2k_1(t) + r(1+1/\omega) + r(1-1/\omega)e^{-\omega t}, \tag{4.91b}$$

and consequently

$$M(t) \sim \frac{1}{2}(k_0(t) + k_1(t) - r - 1)x_s^2 + (r - k_1(t))x_s + \frac{1}{2}(k_1(t) + 1). \tag{4.92}$$

Clearly $k_0(t)$ will have exponential decay rates $1 + \omega$ and 1, and $k_1(t)$ has exponential decay rates ω and 2. From Fig. 16, time-evolution of $k_1(t)$ tends to increase $M(t)$ while evolution of $k_0(t)$ tends to decrease $M(t)$. Therefore, depending on the values of ω, and r, we might observe $M(t)$ to have a local maximum or minimum then decay to a steady-state, or simply monotonically go to a steady-state depending on whether the contributions from $k_0(t)$ and $k_1(t)$ compete or one dominates. Therefore the Cohen-White model yields

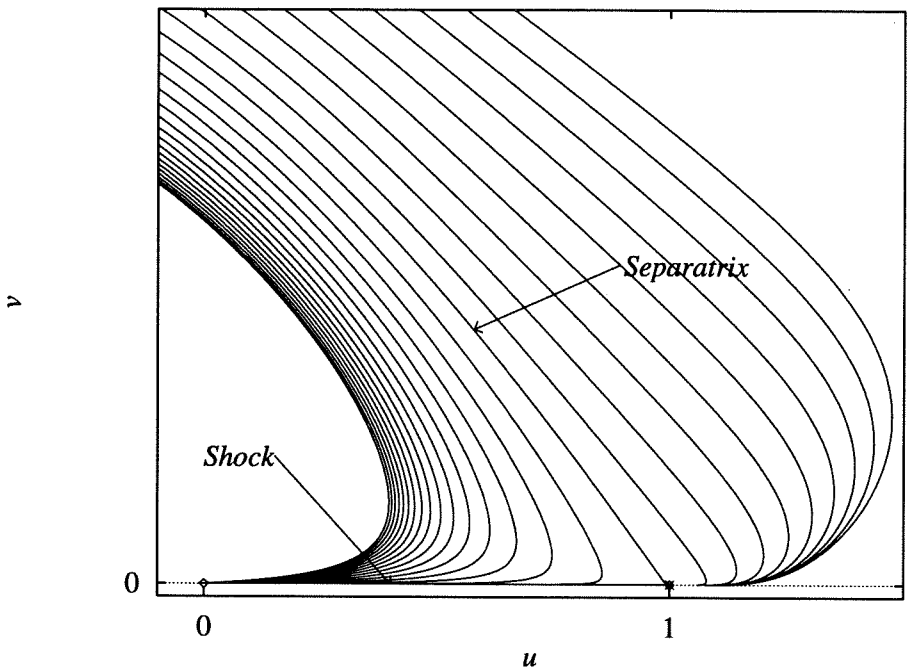

Figure 18: The phase plane at a turning point.

several possible classes of sorption behavior with overshoot being possible in a broad parameter range (see Fig. 17).

4.9 Appendix: shock formation at turning points

At the turning points $x = x_m$ and $x = x_M$ there are some qualitative differences in the phase plane description of shock formation. At $x = x_m$, the two branches $\overline{u}_+(x)$ and $\overline{u}_*(x)$ coincide at $u = u_M$, and $W'(u_M) = 0$, so we have a nonhyperbolic fixed point resulting from the coalescence of a node and a

saddle. The situation at $x = x_M$ is similar, so we will study a simplified model for the behavior at $x = x_m$:

$$\frac{du}{dt} = v + v^2 - u(1-u)^2, \tag{4.93a}$$

$$\frac{dv}{dt} = -bv. \tag{4.93b}$$

Here, the terms in $v = \mathrm{e}^{-bt}$ represents the time-dependent forcing and we have taken $\overline{u}_-(x_m) = 0$ and $u_M = 1$ as the equilibrium points. At $(u, v) = (0, 0)$ we have a stable node with eigenvalues $\mu_1 = -1$, $\mu_2 = -b$. At $(1, 0)$ the eigenvalues are $\mu_1 = 0$, $\mu_2 = -b$. The stable manifold of this equilibrium point, the trajectory with pure μ_2 motion, is a separatrix that separates regions of the plane with different classes of behavior. Pure μ_1 motion on the $v = 0$ axis, the unstable manifold, in the neighborhood of $u = 1$, $u(t) = 1 + z(t)$, is always decreasing since $\dot{z} \sim -z^2 < 0$. The part of the unstable manifold connecting $u = 1$ to $u = 0$ corresponds to a shock connecting $\overline{u}_+(x_m)$ to $\overline{u}_-(x_m)$. Combining these factors, we can give a global description of the phase plane.

Trajectories to the right of the separatrix are attracted to $u = 1$ as $v \to 0$, hence the equilibrium point behaves node-like. Trajectories to the left of the separatrix are attracted to the node at $u = 0$, and $u = 1$ has a saddle-like influence on these orbits. Shocks are formed by all trajectories that are attracted to $u = 1$ as $v \to 0$ (and then connect to $u = 0$ along the unstable manifold). We see that in this case, the separatrix is a limiting case of a continuous set of trajectories that form shocks (see Fig. 18). By comparison,

in the generic case of shock formation on $x_s \in (x_m, x_M)$, the separatrix is the unique trajectory that yields a shock.

Chapter 5

Case II traveling waves

5.1 Introduction

Polymer materials are being used in an increasing number of technological applications. To optimize performance and further extend applications of polymers, their physical properties must be well understood. One area of active research is the study of diffusion of a penetrant liquid in a polymer substrate. This work has applications to many physical problems including the effect of humidity on thin polymer films, the use of polymer materials as liquid seals, and controlled-release pharmaceuticals. We will present a mathematical analysis of Case II polymer diffusion.

The terms "Case II," "non-Fickian," and "anomalous" are commonly used to describe the occurrence of various nontraditional effects that cannot be predicted from classical Fickian diffusion models. For example, for Case II diffusion, experimental studies of polymer sorption behavior show constant

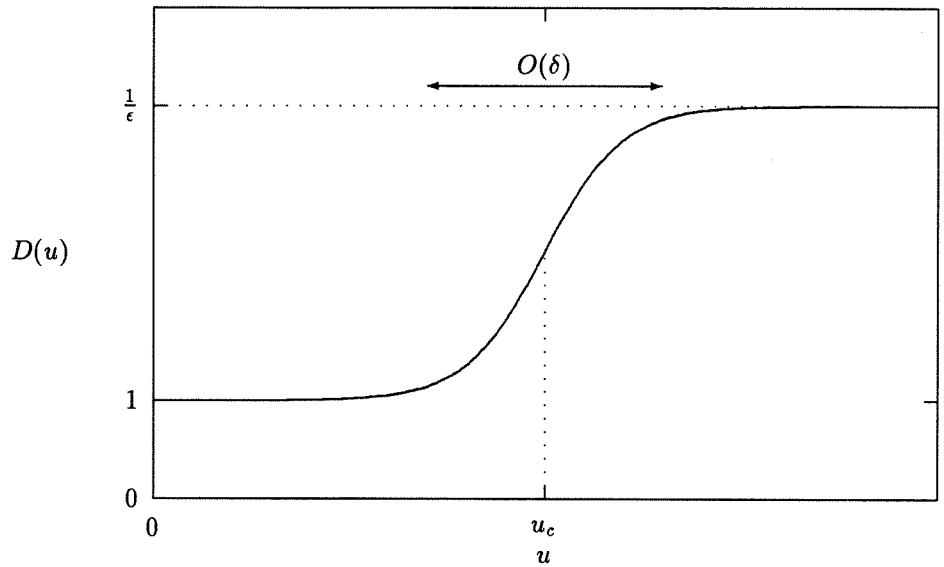

Figure 1: The diffusion coefficient

velocity spreading of the penetrant with a well-defined sharp front. Diffusion models for classical materials do not yield such characteristics. As a result, numerous studies have focused on tying anomalous behaviors to the special material properties of polymers. Since polymers are very long molecules, some effects can have considerable characteristic times [1]. Consequently, incorporation of relaxation effects through viscoelastic models becomes important. Additionally, polymer materials can undergo a phase transition from a relatively inflexible "glassy" state to a more responsive "rubbery" state with corresponding changes in diffusion coefficients and relaxation times. These effects will be incorporated in our model for Case II diffusive transport.

We study the diffusive spreading of a liquid into a one-dimensional semi-infinite layer of initially dry, unstressed polymer material ($0 < x < \infty$). Following a derivation given in [2], [3], we obtain the model for the penetrant

concentration in the polymer,

$$\frac{\partial u}{\partial t} = \frac{\partial}{\partial x}\left[D(u)\left(\frac{\partial u}{\partial x} + E(u)\frac{\partial \sigma}{\partial x}\right)\right], \tag{5.1}$$

where $D(u)$ is a diffusion coefficient, $E(u)$ is a stress coefficient and σ is the stress induced in the polymer material. As in [4], we will take the diffusion coefficient to be

$$D(u) = \frac{1+\epsilon}{2\epsilon} + \frac{1-\epsilon}{2\epsilon}\tanh\left(\frac{u-u_c}{\delta}\right), \tag{5.2}$$

where $0 < \epsilon \ll 1$ is a small parameter corresponding to the large diffusivity of the polymer in the rubbery state (see Fig. 1). The critical penetrant-concentration u_c marks the rubber-glass phase transition in the diffusivity. We will examine this diffusion coefficient in the limit of sharp phase transitions ($\delta = 0$), but we will also consider the influence of moderately steep transitions with $\delta > 0$. Using perturbation methods in the limit of $\epsilon \to 0$, our solution will be a steady-profile traveling wave for the penetrant concentration applicable sufficiently far within the polymer material (see Fig. 2). Namely, we will neglect induction time and surface boundary condition effects and assume that the penetrant concentration far behind the wave front is at equilibrium ($u = u_0$) [2], [5], [6]. The new mathematical presentation of this model given here will include an analytical solution of a simplified Thomas and Windle model [4], [6] as well as analysis of more general viscoelastic stress evolution models.

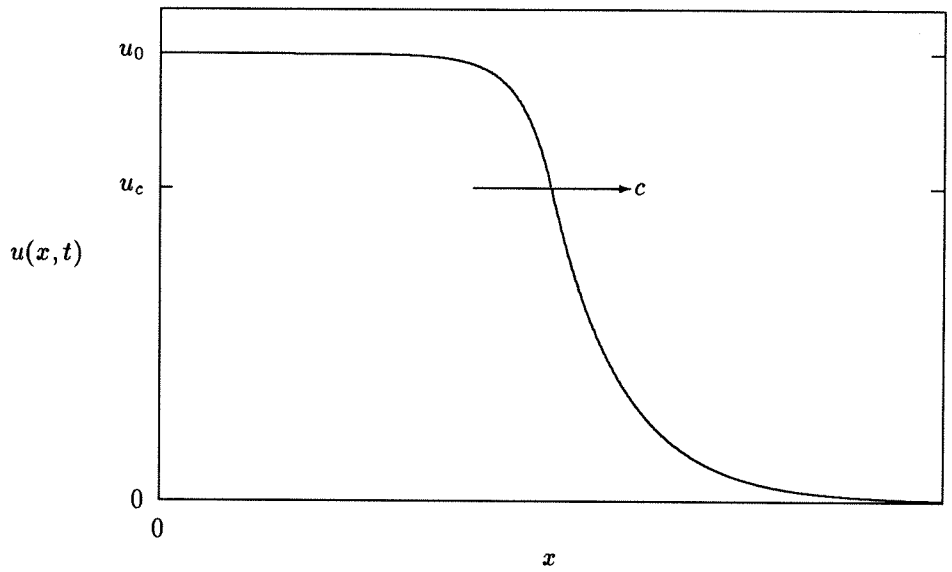

Figure 2: The Case II solution

5.2 The viscous model

In the elastic limit, we may reduce (4.21) to the viscous model [2]

$$\sigma = G(u)\frac{\partial u}{\partial t}, \tag{5.3}$$

where $G(u) = \lambda(u)/\beta(u)$. This stress model yields the diffusion equation

$$\frac{\partial u}{\partial t} = \frac{\partial}{\partial x}\left[D(u)\left(\frac{\partial u}{\partial x} + E(u)\frac{\partial}{\partial x}\left(G(u)\frac{\partial u}{\partial t}\right)\right)\right]. \tag{5.4}$$

This higher-order partial differential equation has been studied as a simplified model of the viscoelastic integro-differential equation (4.23) [2], [4], [5], [6]. We will show that for the problem of Case II traveling waves, both models can be studied in the same framework of phase plane analysis.

Consider a steady-profile traveling wave solution of (5.4) of the form

$$u(x,t) = U(z), \qquad z = x - ct, \tag{5.5}$$

where we require that the solution satisfy limiting behaviors far away from the transition front. Far behind the wave front,

$$u(z \to -\infty) \to u_0 > u_c, \tag{5.6a}$$

where u_0 is the equilibrium concentration, determined from a boundary condition on the chemical potential at the surface of the polymer [2], [6]. Similarly, far ahead of the front, the polymer is dry,

$$u(z \to \infty) \to 0. \tag{5.6b}$$

Observe that the equilibrium concentration is assumed to be greater than the critical phase transition concentration u_c. Hence the wave front marks an interface between wet, rubbery and dry, glassy regions. It will be shown in the analysis that the phase transition for $u_0 > u_c$ is essential for the existence of the traveling wave solution. Substituting form (5.5) into (5.4) yields the ordinary differential equation

$$-c\frac{dU}{dz} = \frac{d}{dz}\left[D(U)\left(\frac{dU}{dz} - cE(U)\frac{d}{dz}\left(G(U)\frac{dU}{dz}\right)\right)\right], \tag{5.7}$$

which may be integrated once, subject to the boundary condition (5.6b), to

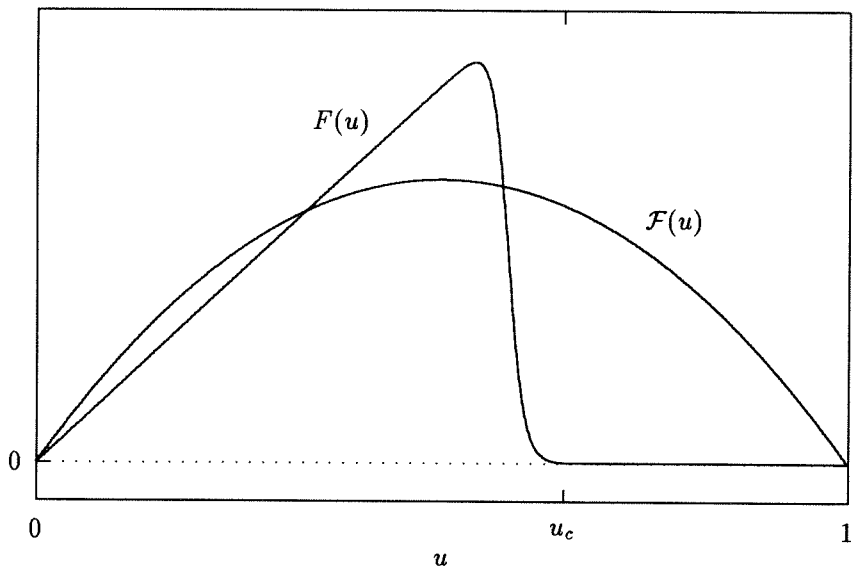

Figure 3: Comparison to Fisher-like nonlinear reaction terms.

yield

$$-cU = D(U)\left(\frac{dU}{dz} - cE(U)\frac{d}{dz}\left(G(U)\frac{dU}{dz}\right)\right). \tag{5.8}$$

Interestingly, we may relate (5.8) to the classical model for traveling waves in reaction-diffusion systems. A well-known model in population dynamics and other applications is Fisher's equation [11], [12],

$$\frac{\partial u}{\partial t} = \frac{\partial}{\partial x}\left(\mathcal{D}(u)\frac{\partial u}{\partial x}\right) + \mathcal{F}(u), \tag{5.9}$$

where $\mathcal{D}(u)$ is a diffusion coefficient and $\mathcal{F}(u)$ is a nonlinear reaction term of a specified form [13]. This equation has traveling wave solutions connecting homogeneous, isolated solutions of $\mathcal{F}(u) = 0$ (for example $u = 0$ and $u = 1$, see Fig. 3). The corresponding traveling wave ordinary differential equation

for Fisher's equation is

$$\frac{d}{dz}\left(\mathcal{D}(U)\frac{dU}{dz}\right)+c\frac{dU}{dz}+\mathcal{F}(U)=0, \tag{5.10}$$

for u given by (5.5). Our model for stress-driven traveling waves, (5.8), may be put in a similar form,

$$\frac{d}{dz}\left(G(U)\frac{dU}{dz}\right)-\frac{1}{cE(U)}\frac{dU}{dz}+\frac{U}{D(U)E(U)}=0. \tag{5.11}$$

In this form we note that the elastic modulus $G(U)$ takes the role of the diffusivity in (5.10) whereas the diffusion coefficient $D(U)$ appears only in the nonlinear reaction term

$$F(U)=\frac{U}{D(U)E(U)}. \tag{5.12}$$

There are, however, some significant differences between (5.10) and (5.11). For $\epsilon \to 0$, the reaction term $F(U)$ in (5.11) vanishes to leading order for all $U > u_c$; this characteristic will lead to the determination of a unique wave velocity for Case II diffusion, whereas the same is not possible for Fisher's equation. Mathematically, this arises from differences in the nature of the singular boundary value problem defining the traveling wave [14].

We can write (5.8) in the form of an autonomous phase plane system by defining the traveling wave stress profile $S(z)$ as

$$S=-cG(U)\frac{dU}{dz}, \tag{5.13a}$$

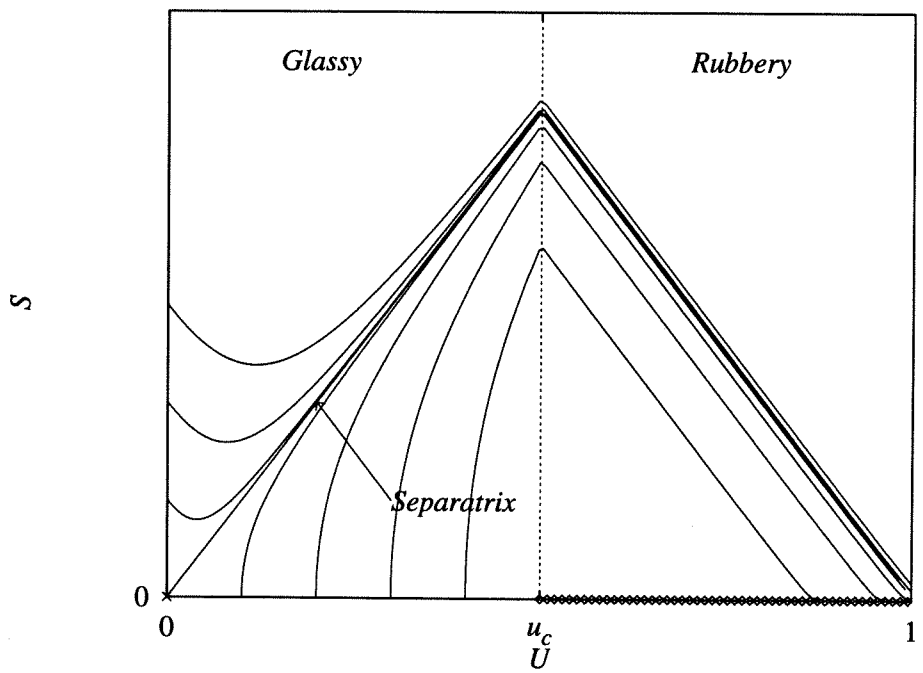

Figure 4: The phase plane for the viscous model.

then (5.8) becomes

$$\frac{dS}{dz} = \frac{S}{cE(U)G(U)} - \frac{cU}{E(U)D(U)}, \tag{5.13b}$$

and (5.13a,b) is the phase plane system. A complete asymptotic analysis for a similar system is studied in [12]. Here we will study the solution to this system away from the phase transition layer at $U = u_c$. For definiteness, we will assume that the transition occurs at $z = 0$, $U(z = 0) = u_c$. Solving in the outer regions, for $U > u_c$, $z < 0$ with $D \sim \epsilon^{-1}$ yields the equations

$$\frac{dU}{dz} = -\frac{S}{cG(U)}, \tag{5.14a}$$

$$\frac{dS}{dz} = \frac{S}{cE(U)G(U)} - \epsilon\frac{cU}{E(U)}, \tag{5.14b}$$

and for $U < u_c$, $z > 0$ with $D \sim 1$

$$\frac{dU}{dz} = -\frac{S}{cG(U)}, \tag{5.15a}$$

$$\frac{dS}{dz} = \frac{S}{cE(U)G(U)} - \frac{cU}{E(U)}. \tag{5.15b}$$

Our solution procedure will consist of solving the two phase plane systems above to leading order in ϵ and then matching the solutions together through the transition layer.

We will first solve the problem for the simplified, but illustrative, case of

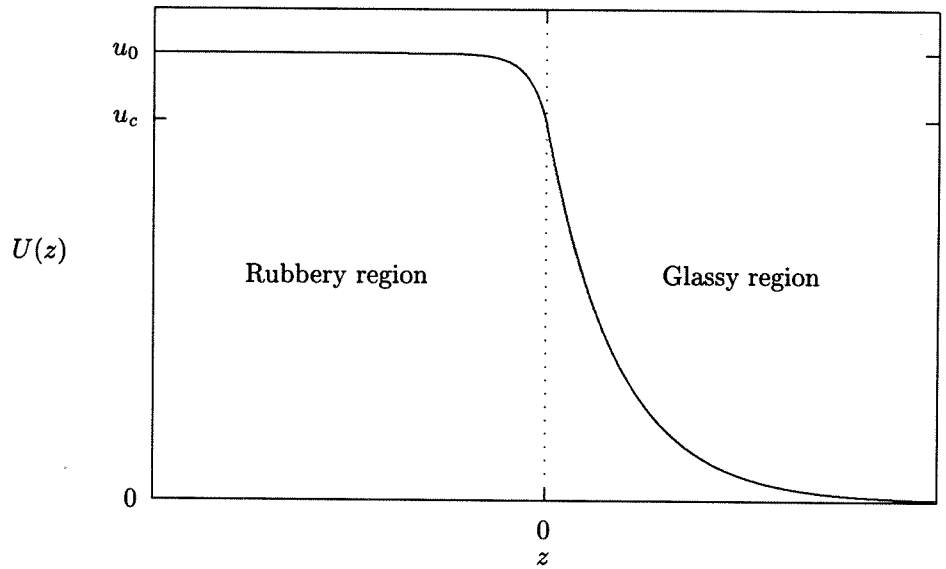

Figure 5: The traveling wave solution $U(z)$.

constant coefficients with

$$E(U) \equiv E, \qquad G(U) \equiv G. \tag{5.16}$$

To account for the significant effects of the rubber-glass transition on the viscoelastic properties of the polymer material, a much more realistic model for $G(U)$ is

$$G(U) = \begin{cases} G_R & U > u_c, \\ G_G & U < u_c, \end{cases} \tag{5.17}$$

as in the model (5.2) for $D(U)$. This piecewise constant model for $G(U)$ is handled by our phase plane system in exactly the same way as (5.16) and yields a solution of the form given below, though with a slightly more complicated dependence on the parameters G_R and G_G for the velocity c

than (5.23). The desired traveling wave solution is a separatrix connecting fixed points in the phase plane (see Fig. 4). The glassy system (5.15a,b) has a saddle point at $U = 0$, $S = 0$. The rubbery system (5.14a,b) however has a continuum of fixed points at $S = 0$ for all $U > u_c$. Significantly this means that phase transition traveling waves connecting dry polymer ($U = 0$) to rubbery polymer ($U = u_0 > u_c$) can exist for all values of u_0 greater than u_c. Hence, there is no problem satisfying the equilibrium surface boundary condition, and this analysis might be extended to also cover non-equilibrium surface conditions [6]. In fact, this problem is a linear system with the closed-form outer solution (see Fig. 5)

$$U(z) \sim \begin{cases} u_0 + (u_c - u_0)\mathrm{e}^{z/(cEG_R)} & z < 0, \\ u_c \mathrm{e}^{mz} & z > 0, \end{cases} \tag{5.18}$$

where

$$m = \frac{1 - \sqrt{1 + 4c^2 EG_G}}{2cEG_G} < 0. \tag{5.19}$$

At this point, our solution is completely specified except for the velocity c, which will be determined from considerations of the transition layer.

Solving (5.13a,b) for general $E(U)$ and $G(U)$ requires more sophisticated analysis, but yields qualitatively similar results. The derivation of the model given in section 2 suggests that $E(U)$ should be of the order $O(U)$ as $U \to 0$. This change, however, makes system (5.15a,b) singular at the origin. We can eliminate this problem by using the coordinate transformation

$$\frac{d}{d\hat{z}} = E(U)\frac{d}{dz}, \tag{5.20}$$

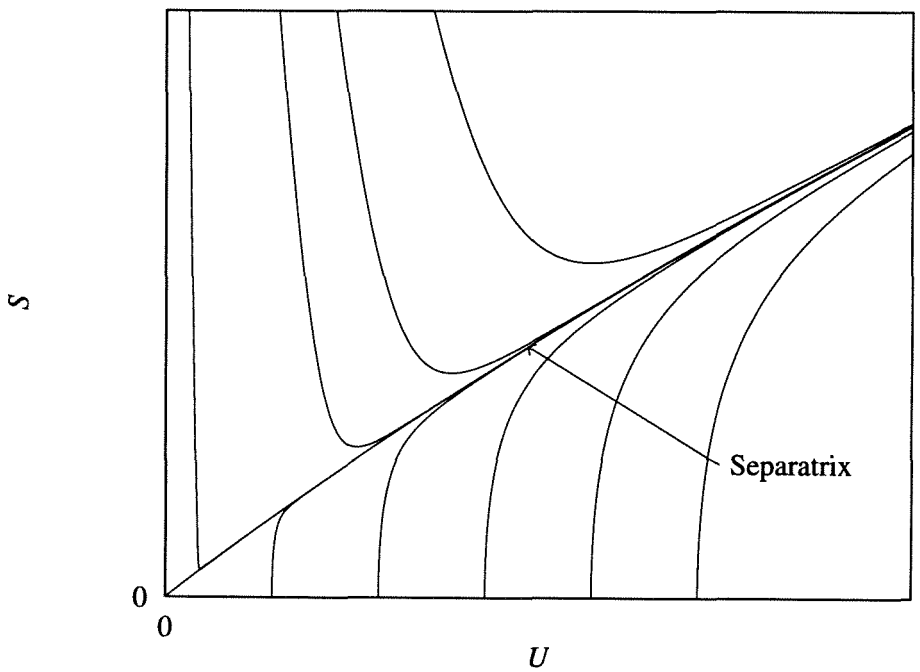

Figure 6: Phase plane for the nonlinear saddle point.

suggested by Murray [11], to yield the new, non-singular, glassy system

$$\frac{dU}{d\hat{z}} = -\frac{E(U)S}{cG(U)}, \tag{5.21a}$$

$$\frac{dS}{d\hat{z}} = \frac{S}{cG(U)} - cU. \tag{5.21b}$$

Like (5.15a,b), (5.21a,b) has a saddle point at the origin with a separatrix corresponding to a unique traveling wave solution (see Fig. 6); however, in this case it is a nonlinear (non-hyperbolic) saddle point which is more complicated to analyze mathematically.

5.3 Transition-layer behavior

In the phase transition region, the form of the diffusion coefficient $D(U)$ becomes important for determining the structure of the solution. We will study the limit of sharp transitions in $D(U)$ as $\delta \to 0$. This analysis will yield some observations about the stress, as well as the traveling wave velocity c.

For studying the transition region, it becomes useful to represent the phase plane system (5.13a,b) as

$$\frac{dS}{dU} = \frac{c^2 G(U)U}{E(U)D(U)S} - \frac{1}{E(U)}. \tag{5.22}$$

This is a first-order ordinary differential equation for the stress as a function of the concentration. In the transition region, $S > 0$ and it can be shown that the terms in (5.22) are non-singular and bounded. Hence we can conclude that the stress is continuous. If the transition is very sharp ($\delta \sim 0$), then the

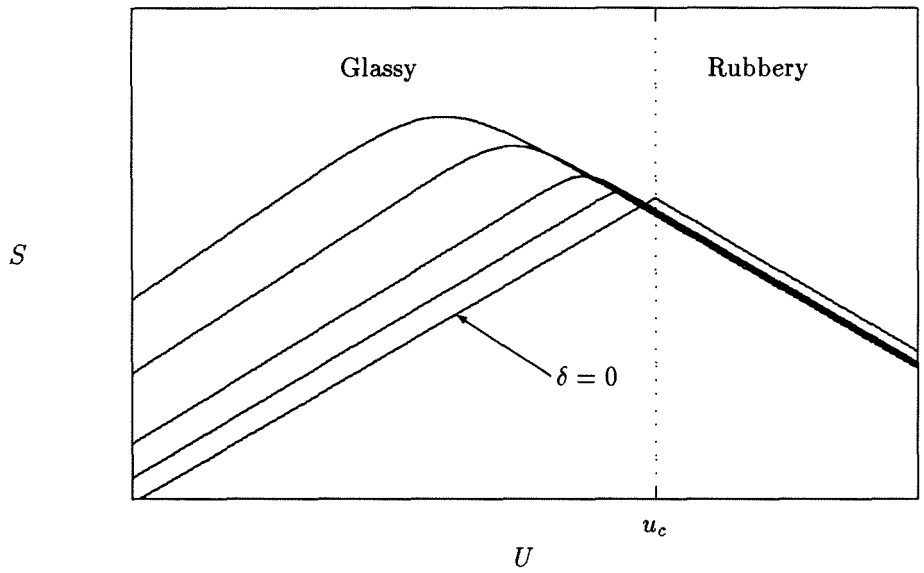

Figure 7: Transition layer dependence on δ in the phase plane.

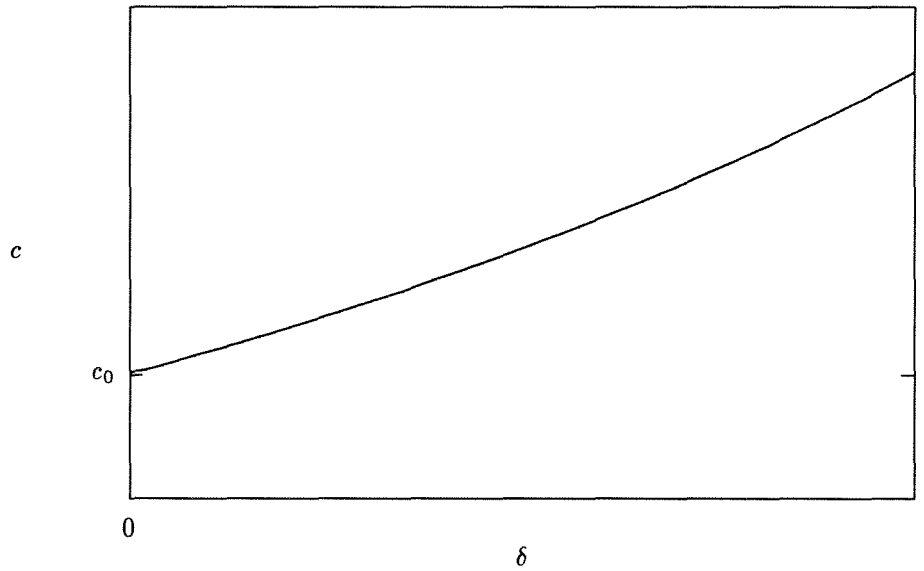

Figure 8: Velocity dependence on δ.

stress will be roughly constant across the interval. Continuity of the stress can then be enforced by matching together the solutions in the rubbery and glassy regions. For our linear constant-coefficient problem, (5.16), with $\delta = 0$ we simply make the first derivative of (5.18) continuous at $z = 0$. This condition yields the velocity

$$c_0 = c(\gamma) = \frac{1}{2\gamma}\sqrt{\frac{(2-\gamma)^2 - \gamma^2}{EG}}, \tag{5.23}$$

where the concentration ratio is $\gamma = u_c/u_0 < 1$. When the transition layer has finite thickness, $\delta > 0$, then (5.22) must be integrated directly to obtain the stress, and the form of the diffusion coefficient will modify the velocity and the outer solutions. Significantly, we note several trends that occur as the transition layer thickness increases: the maximum stress increases, and it becomes broader and occurs *ahead* of the front, in the glassy region (see Fig. 7), and the traveling wave velocity c increases (see Fig. 8).

5.4 The viscoelastic model

We will now show how the phase plane method can be applied to more general stress evolution models. General viscoelastic models can be written as single integro-differential equations of the form (4.23), however we will use the coupled form

$$\frac{\partial u}{\partial t} = \frac{\partial}{\partial x}\left[D(u)\left(\frac{\partial u}{\partial x} + E(u)\frac{\partial \sigma}{\partial x}\right)\right], \tag{5.24a}$$

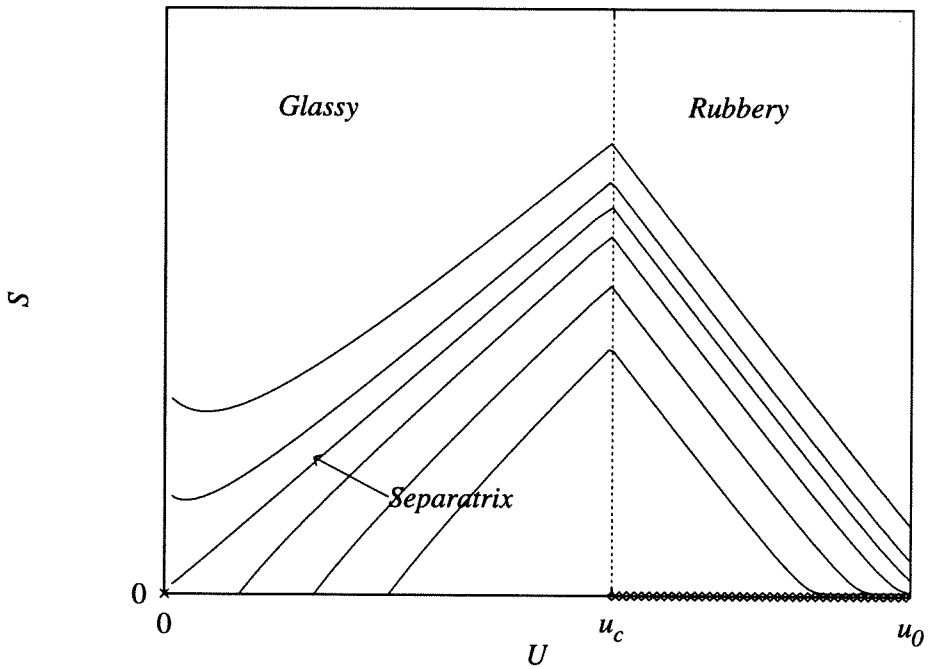

Figure 9: The phase plane for the viscoelastic traveling wave solution.

$$\frac{\partial \sigma}{\partial t} + \beta(u)\sigma = \lambda(u)\frac{\partial u}{\partial t}. \tag{5.24b}$$

We consider a Maxwell model (5.24b) for our analysis, however the approach is very similar for other equations, such as Durning's model (4.25).

Again, searching for steady-profile traveling wave solutions moving into dry, unstressed polymer material, let

$$u(x,t) = U(z), \qquad \sigma(x,t) = S(z), \qquad z = x - ct, \tag{5.25}$$

then (5.24a,b), subject to boundary condition (5.6b), become

$$-cU = D(U)\left(\frac{dU}{dz} + E(U)\frac{dS}{dz}\right) \tag{5.26a}$$

$$\frac{dS}{dz} - \frac{\beta(U)}{c}S = \lambda(U)\frac{dU}{dz} \tag{5.26b}$$

or in a more standard form

$$\frac{dU}{dz} = -P(U)U - E(U)Q(U)S, \tag{5.27a}$$

$$\frac{dS}{dz} = -\lambda(U)P(U)U + Q(U)S, \tag{5.27b}$$

where

$$P(U) = \frac{R(U)}{D(U)}, \qquad Q(U) = \frac{1}{c^2}\beta(U)R(U), \tag{5.28}$$

and

$$R(U) = \frac{c}{1 + \lambda(U)E(U)}. \tag{5.29}$$

In this representation, the influences of diffusion and stress-relaxation are given respectively by the functions $P(U)$ and $Q(U)$. As in the viscous model, in the limit of a sharp transition, we can separate (5.27a,b) into two simpler phase plane systems. In the rubbery region for $z < 0$, $U > u_c$,

$$\frac{dU}{dz} = -E(U)Q(U)S - \epsilon R(U)U, \tag{5.30a}$$

$$\frac{dS}{dz} = Q(U)S - \epsilon\lambda(U)R(U)U, \tag{5.30b}$$

and in the glassy region for $z > 0$, $U < u_c$,

$$\frac{dU}{dz} = -R(U)U - E(U)Q(U)S, \tag{5.31a}$$

$$\frac{dS}{dz} = -\lambda(U)R(U)U + Q(U)S. \tag{5.31b}$$

These systems of equations are more complicated than in the viscous case but they share the same qualitative characteristics. Like (5.15a,b), (5.31a,b) has a saddle point at the origin. Unlike the viscous model, for (5.31a,b), the origin is always a linear saddle point independent of the form of the stress coefficient $E(U)$. Similarly, as $\epsilon \to 0$, system (5.30a) has fundamentally the same dynamics as (5.14a,b). Not surprisingly, we obtain a very similar phase plane plot for (5.27a,b) (see Fig 9). However, there are significant qualitative differences in the traveling wave profile.

To better understand the influence of some of the physical effects on the solution we again study a simplified constant-coefficient model with

$$E(U) \equiv E, \qquad \beta(U) \equiv \beta, \qquad \lambda(U) \equiv \lambda. \tag{5.32}$$

As in the case of the viscous model studied in the previous section, to properly describe the influence of the rubber-glass transition on the viscoelastic properties of the polymer material, $\beta(U)$ and $\lambda(U)$ should be piecewise constant in the rubbery and glassy regions. Again, the solution of this extended problem has the same form as that of the solution with (5.32), except for a more complicated parameter dependence in c (5.38). This model can be expected to capture most of the qualitative properties of the general model,

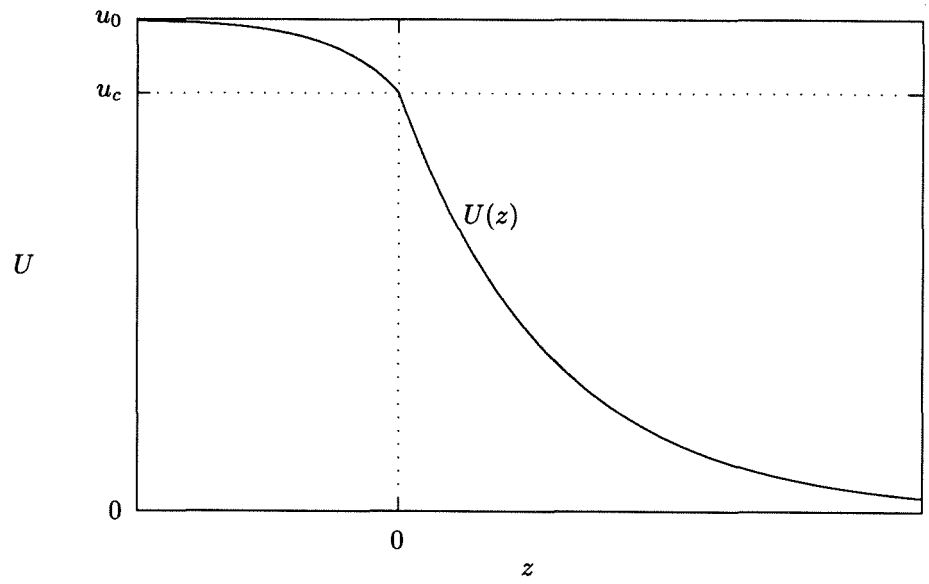

Figure 10: The viscoelastic traveling wave profile.

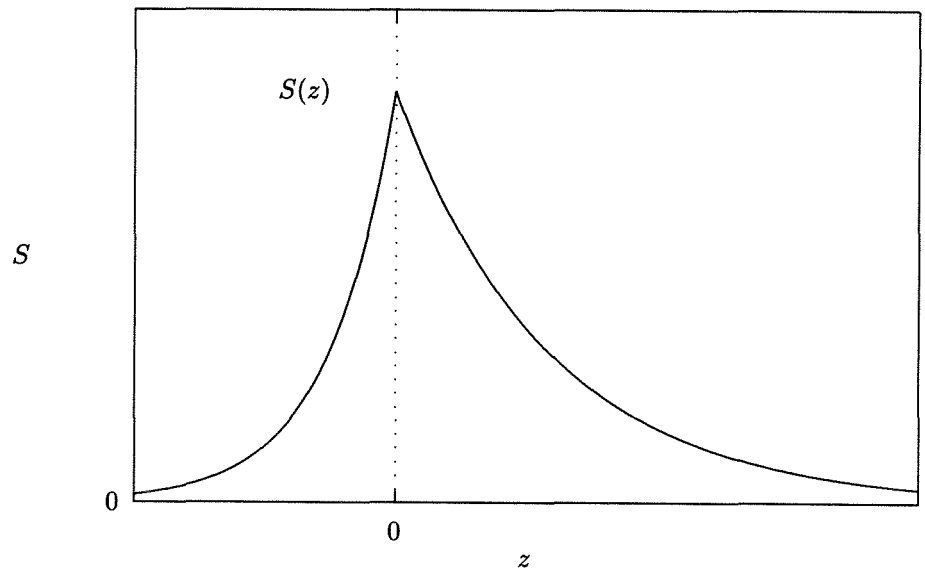

Figure 11: The corresponding viscoelastic stress profile.

and it also admits the closed-form analytic solution

$$U(z) \sim \begin{cases} u_0 + (u_c - u_0)\mathrm{e}^{Qz} & z < 0 \\ u_c \mathrm{e}^{mRz} & z > 0 \end{cases} \tag{5.33}$$

where

$$m = \frac{\beta_R - c^2 - \sqrt{(\beta_R + c^2)^2 + 4\beta_R c^2 \lambda_R E}}{2c^2} < 0, \tag{5.34}$$

$$Q = \frac{\beta_G}{c(1 + \lambda_G E)}, \qquad R = \frac{c}{1 + \lambda_R E}. \tag{5.35}$$

The form of (5.33) is the same as the viscous solution (5.18), but differences in the nature of the stress yield a significantly different penetrant profile (see Figs 10, 11). The structure of the wave front is governed by the wave velocity c, which is determined by matching the stress across the transition layer. From the phase plane systems (5.30a,b) and (5.31a,b), the stress can be expressed as a function of $U(z)$. In the rubbery region

$$S(z) = -\frac{1}{EQ}\frac{dU}{dz}, \tag{5.36}$$

and in the glassy region

$$S(z) = -\frac{c^2}{\beta E}U - \frac{1}{EQ}\frac{dU}{dz}. \tag{5.37}$$

Observe that in the rubbery region, the stress (5.36) is of the form (5.13a), suggesting that a viscous model is sufficient to describe the penetrant behavior in the rubbery polymer. However, the glassy stress (5.37) shows that a full viscoelastic model is needed in general. At the rubber-glass transition,

we have $U(z = 0) = u_c$ and matching stresses (5.36) and (5.37) yields a formula for the wave velocity with $\delta = 0$

$$c_0 = c(\gamma) = \sqrt{\frac{1-\gamma}{\gamma((1+\lambda E)\gamma - 1)}}, \tag{5.38}$$

where $\gamma = u_c/u_0$. We note that the characteristics of this wave profile strongly resemble results obtained from numerical simulations [2], [6] and from experimental observations [15]. In particular, below are results from the numerical computations done by Fu and Durning for a Case II transport initial-boundary value problem (see Figs. 12–14). Their calculations suggest that the penetrant concentration profile is a slowly evolving (nearly steady) traveling wave. Comparing corresponding figures (10 and 12), (11 and 13), (9 and 14) shows that our very simple analytical model has a very good level of qualitative agreement with the solution of the general nonlinear transport equation.

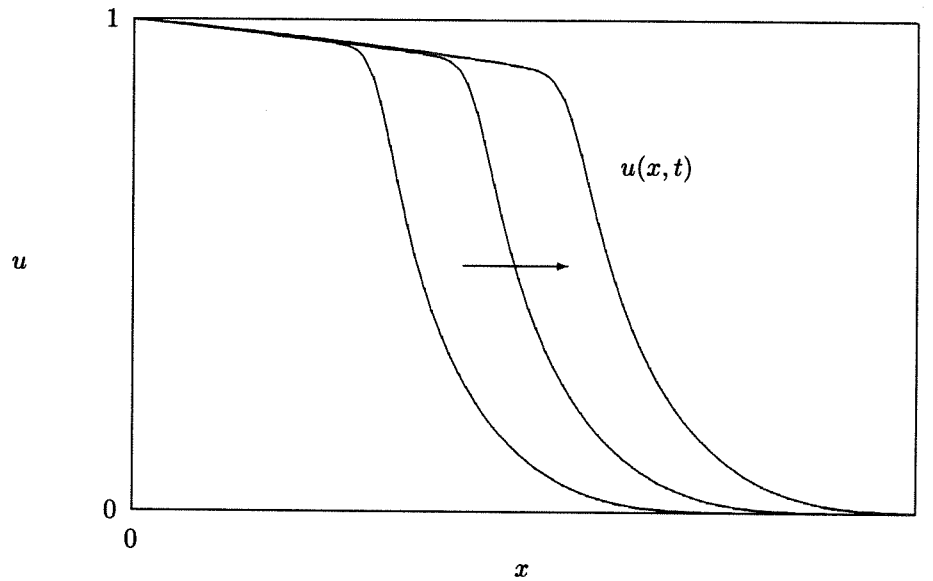

Figure 12: The Fu and Durning numerical concentration profile.

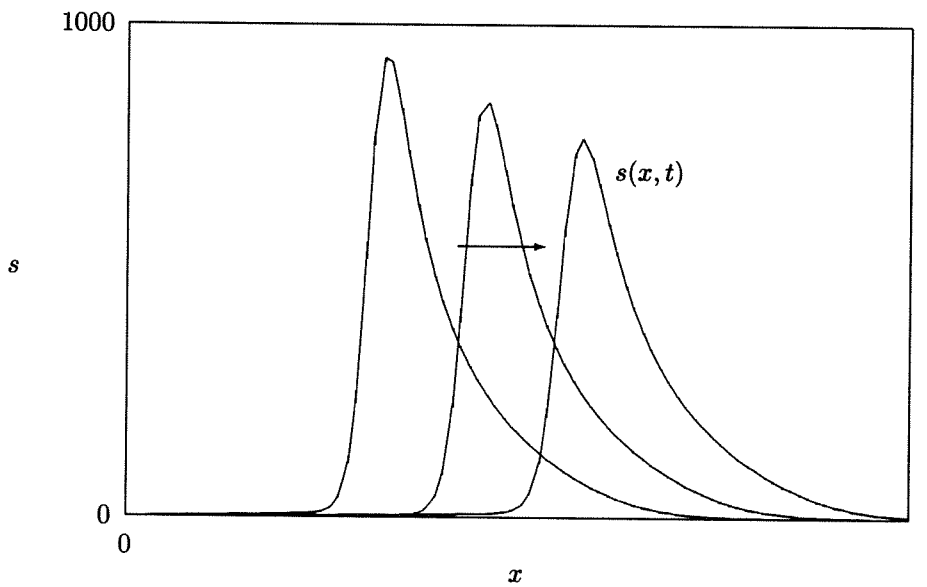

Figure 13: The Fu and Durning numerical stress profile.

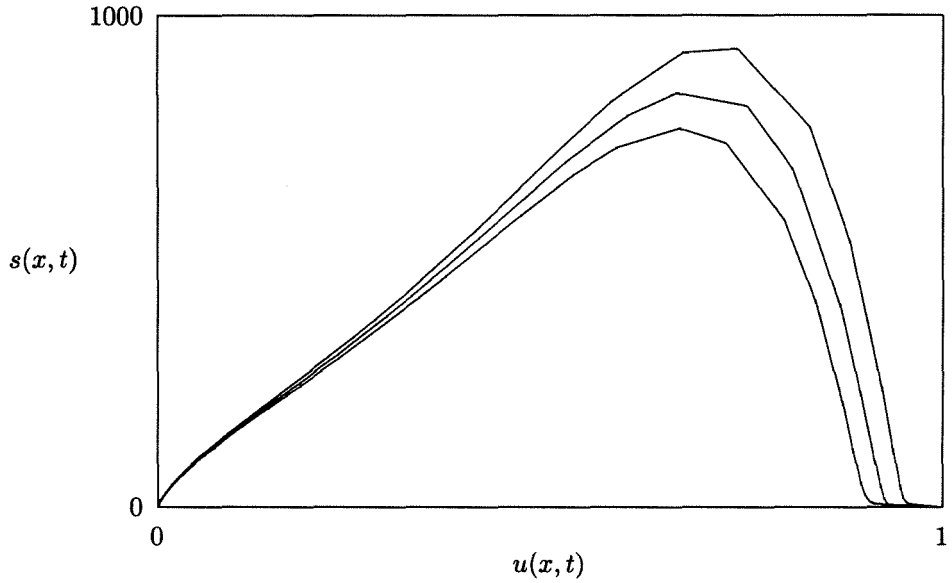

Figure 14: The Fu and Durning numerical approximate phase plane.

References: Chapter 1

[1] M. ABRAMOWITZ AND I. A. STEGUN, *Handbook of Mathematical Functions*, Dover, New York, 1965.

[2] W. F. AMES, *Nonlinear Partial Differential Equations in Engineering*, vol. 1, Academic Press, New York, 1965.

[3] S. ANGENET, *Large time asymptotics for the porous media equation*, in Nonlinear Diffusion Equations and their Equilibrium States I, W. M. Ni, et. al eds., Springer-Verlag, New York, 1988.

[4] D. G. ARONSON, *Regularity of flows in porous media: A survey*, in Nonlinear Diffusion Equations and their Equilibrium States I, W. M. Ni, et. al eds., Springer-Verlag, New York, 1988.

[5] B. K. BABU AND M. T. VAN GENUCHTEN, *A similarity solution to a nonlinear diffusion equation of singular type*, Quarterly of Applied Math., April (1979), pp. 11–21.

[6] G. I. BARENBLATT, *Similarity, Self-Similarity and Intermediate Asymptotics*, Consultants Bureau, New York, 1979.

[7] C. M. BENDER AND S. A. ORSZAG, *Advanced Mathematical Methods for Scientists and Engineers*, Mc Graw-Hill, New York, 1978.

[8] W. BRUTSAERT, *Some exact solutions for nonlinear desorptive diffusion*, Z. angew Math. Phys., **33** (1982), pp. 540–546.

[9] J. BUCKMASTER, *Viscous sheets advancing over dry beds*, Journal of Fluid Mechanics, 81 (1977), pp. 735–756.

[10] G. F. CARRIER, M. KROOK AND C. E. PEARSON, *Functions of a Complex Variable*, Hod Books, Ithaca, 1983.

[11] H. S. CARSLAW AND J. C. JAEGER, *Conduction of Heat in Solids*, 2nd ed., Oxford University Press, Oxford, 1959.

[12] I. CHANG, *Navier-Stokes solutions at large distances from a finite body*, Journal of Mathematics and Mechanics, 10 (1961), pp. 811–875.

[13] D. S. COHEN AND J. D. MURRAY, *A generalized diffusion model for growth and dispersal in a population*, J. Math. Biology, 12 (1981), pp. 237–249.

[14] J. KEVORKIAN AND J. D. COLE, *Perturbation Methods in Applied Mathematics*, Springer-Verlag, New York, 1981.

[15] J. CRANK, *The Mathematics of Diffusion*, 2nd ed., Oxford University Press, Oxford, 1975.

[16] R. C. DIX AND J. CIZEK, *The isotherm migration method for transient heat conduction analysis*, in Heat Transfer 1970, vol. 1, U. Grigull and E. Hahne eds., Elsevier, Amsterdam, 1970.

[17] L. DRESNER, *Similarity solutions of nonlinear partial differential equations*, Pitman, Boston, 1983.

[18] C. M. ELLIOTT, M. A. HERRERO, J. R. KING, AND J. R. OCKENDON, *The mesa problem diffusion patterns for* $u_t = \nabla \cdot (u^m \nabla u)$ *as* $m \to \infty$, IMA Journal of Applied Mathematics, **37** (1986), pp. 147–154.

[19] C. M. ELLIOTT AND J. R. OCKENDON, *Weak and Variational Methods for Moving Boundary Problems* (Pitman, Boston, 1982).

[20] J. M. HILL, *Similarity solutions for nonlinear diffusion - a new integration procedure*, Journal of Engineering Mathematics, 23 (1989), pp. 141–155.

[21] S. KAMIN, *Asymptotic behavior of the porous media equation with absorption*, in Nonlinear Diffusion Equations and their Equilibrium States I, W. M. Ni, et. al eds., Springer-Verlag, New York, 1988.

[22] W. L. KATH AND D. S. COHEN, *Waiting-time behavior in a nonlinear diffusion equation*, Studies in Applied Math., 67 (1982), pp. 79–105.

[23] A. A. LACEY, J. R. OCKENDON AND A. B. TAYLER, *"Waiting-time" solutions of a nonlinear diffusion equation*, SIAM Journal of Applied Mathematics, 42 (1982), pp. 1252–1264.

[24] P. A. LAGERSTROM, *Matched Asymptotic Expansions*, Springer-Verlag, New York, 1988.

[25] I. G. LISLE AND Y. P. PARLANGE, *Analytical Reduction for a concentration dependent diffusion problem*, Z. angew Math. Phys., 44 (1993), pp. 85–118.

[26] J. R. PHILIP, *General method of exact solution of the concentration dependent diffusion equation*, Australian J. Phys., 13 (1960) pp. 1–12.

[27] J. R. PHILIP, *Theory of infiltration*, Adv. in Hydroscience, 5 (1969), pp. 215–296.

[28] D. W. SCHWENDEMAN, *Nonlinear diffusion of impurities in semiconductors*, Z. angew Math. Phys., 41 (1990), pp. 607–621.

References: Chapter 2

[1] D. G. ARONSON, *Density-dependent interaction-diffusion systems*, in Dynamics and Modelling of Reactive Systems, W. E. Stewart. et al. eds., Academic Press, New York, 1980.

[2] D. G. ARONSON, *Regularity of flows in porous media: A survey*, in Nonlinear Diffusion Equations and their Equilibrium States I, W. M. Ni, et al. eds., Springer-Verlag, New York, 1988.

[3] C. M. BENDER AND S. A. ORSZAG, *Advanced Mathematical Methods for Scientists and Engineers*, McGraw-Hill, New York, 1978.

[4] J. CANOSA, *On a nonlinear diffusion equation describing population growth*, IBM J. Res. & Dev., 17 (1973), pp. 307–313.

[5] M. C. CROSS AND P. C. HOHENBERG, *Pattern formation outside of equilibrium*, Rev. Mod. Phys., 65, 3 (1993).

[6] H. T. DAVIS, *Introduction to Nonlinear Differential and Integral Equations*, Dover, New York, 1962.

[7] W. S. C. GURNEY AND R. M. NISBET, *The regulation of inhomogeneous populations*, J. Theor. Biol., 52 (1975), pp. 441–457.

[8] W. L. KATH AND D. S. COHEN, *Waiting-time behavior in a nonlinear diffusion equation*, Studies in Applied Math., 67 (1982), pp. 79–105.

[9] A. KOLMOGOROV, I. PETROVSKY AND N. PISCOUNOFF, *Study of the diffusion equation with growth of the quantity of matter and its application to a biology problem*, in Dynamics of Curved Fronts, Pelce, P. ed., Academic Press, Boston, 1988.

[10] A. A. LACEY, J. R. OCKENDON AND A. B. TAYLER, *"Waiting-time" solutions of a nonlinear diffusion equation*, SIAM Journal of Applied Mathematics, 42 (1982), pp. 1252–1264.

[11] C. C. LIN AND L. A. SEGEL, *Mathematics Applied to Deterministic Problems in the Natural Sciences*, SIAM, Philadelphia, 1988.

[12] J. D. MURRAY, *Mathematical Biology*, Springer-Verlag, Berlin, 1990.

[13] W. I. NEWMAN, *Some exact solutions to a nonlinear diffusion problem in population genetics and combustion*, J. Theor. Biol., 85 (1980), pp. 325–334.

[14] W. I. NEWMAN, *The long-time behavior of the solution to a non-linear diffusion problem in population genetics and combustion*, J. Theor. Biol., 104 (1983), pp. 473-484.

[15] T. P. WITELSKI, *An asymptotic solution for traveling waves of a nonlinear-diffusion Fisher's equation*, J. Math. Biol., 33 (1994), pp. 1–16.

[16] T. P. WITELSKI, *Stopping and merging problems for the porous media equation*, IMA J. Appl. Math., (to appear).

References: Chapter 3

[1] H. W. Alt and I. Pawlow, *A mathematical model of dynamics of nonisothermal phase-separation*, Physica D, 59 (1992), pp. 389–416.

[2] W. F. Ames, *Numerical Methods for Partial Differential Equations*, 3rd ed., Academic Press, New York, 1992.

[3] D. G. Aronson, *Regularity of flows in porous media: A survey*, in *Nonlinear Diffusion Equations and their Equilibrium States I*, W. M. Ni, et al. eds., Springer-Verlag, New York, 1988.

[4] D. K. Babu, *Infiltration analysis and perturbation methods. 2. Horizontal absorption*, Water Resources Research, 12 (1976), pp. 1013–1018.

[5] B. K. Babu and M. T. van Genuchten, *A similarity solution to a nonlinear diffusion equation of singular type*, Quarterly of Applied Math., April (1979), pp. 11–21.

[6] P. W. Bates and P. C. Fife, *The dynamics of nucleation for the Cahn-Hilliard equation*, SIAM J. Appl. Math., 53 (1993), pp. 990–1008.

[7] W. BRUTSAERT, *Some exact solutions for nonlinear desorptive diffusion*, Z. angew Math. Phys., **33** (1982), pp. 540–546.

[8] J. W. CAHN AND J. E. HILLIARD, *Free energy of a nonuniform system. 1. Interfacial free energy*, J. Chem. Phys., 28 (1958), pp. 258–267.

[9] J. CRANK, *The Mathematics of Diffusion*, 2nd ed., Oxford University Press, Oxford, 1975.

[10] D. S. COHEN AND R. ALEXANDER, *Chemical reactor theory and problems in diffusion*, Physica D, 20 (1986), pp. 122–141.

[11] D. S. COHEN AND J. D. MURRAY, *A generalized diffusion model for growth and dispersal in a population*, J. Math. Biology, 12 (1981), pp. 237–249.

[12] E. A. COUTSIAS AND J. C. NEU, *The aging of nuclei in a binary mixture*, Physica D, 12 (1984), pp. 295–302.

[13] C. M. ELLIOTT AND D. A. FRENCH, *Numerical studies of the Cahn-Hilliard equation for phase separation*, IMA J. Appl. Math., 38 (1987), pp. 97–128.

[14] P. S. HAGAN AND D. S. COHEN, *Stratified layer formation in particle suspensions*, Physica D, 17 (1985), pp. 54–62.

[15] W. L. KATH AND D. S. COHEN, *Waiting-time behavior in a nonlinear diffusion equation*, Studies in Applied Math., 67 (1982), pp. 79–105.

[16] E. LIVNE AND A. GLASNER, *A finite difference scheme for the heat-conduction equation*, J. Comp. Physics, 58 (1985), pp. 59–66.

[17] A. NOVICK-COHEN AND L. A. SEGEL, *Nonlinear aspects of the Cahn-Hilliard equation*, Physica D, 10 (1984), pp. 277–298.

[18] J. Y. PARLANGE, *Theory of water movement in soils. 1. one dimensional absorption*, Soil Science, 111 (1971), pp. 134–137.

[19] R. L. PEGO, *Front migration in the nonlinear Cahn-Hilliard equation*, Proc. R. Soc. Lond. A, 422 (1989), pp. 261–278.

[20] J. R. PHILIP, *General method of exact solution of the concentration dependent diffusion equation*, Australian J. Phys., 13 (1960) pp. 1–12.

[21] J. R. PHILIP, *Theory of infiltration*, Adv. in Hydroscience, 5 (1969), pp. 215–296.

[22] G. B. WHITHAM, *Linear and Nonlinear Waves* John Wiley, New York, 1974.

References: Chapter 4

[1] G. F. Billovits and C. J. Durning, *Polymer material coordinates for mutual diffusion in polymer-penetrant system*, Chem. Eng. Comm., 82 (1989), pp. 21–44.

[2] G. F. Billovits and C. J. Durning, *Linear viscoelastic diffusion in the poly(styrene)-ethylbenzene system: Comparison between theory and experiment*, (to appear).

[3] C. J. Durning and K. N. Morman, Jr., *Nonlinear swelling of polymer gels*, J. Chem. Phys., 98 (1993), pp. 4275–4293.

[4] S. Govindjee and J. C. Simo, *Coupled stress-diffusion: Case II*, J. Mech. Phys. Solids, 41 (1993), pp. 863–887.

[5] See Chapter 3.

[6] D. D. Joseph, *Fluid Dynamics of Viscoelastic Liquids*, Springer-Verlag, New York, 1990.

[7] C. J. Durning and T. Z. Fu, *Numerical simulation of Case-II transport*, AIChE Journal, 39 (1993), pp. 1030–1044.

[8] H. AMANN, *Nonhomogeneous linear and quasilinear elliptic and parabolic boundary value problems*, in Function Spaces, Differential Operators and Nonlinear Analysis, H. Triebel and H. J. Schmeiszer eds., Teubner, Liepzig, 1993.

[9] ——, *Highly degenerate quasilinear parabolic systems*, Scuola Normale Superiore, 43 (1991), pp. 135–166.

[10] D. S. COHEN AND A. B. WHITE JR., *Sharp fronts due to diffusion and stress at the glass transition in polymers*, J. Polymer Sci. B: Polymer Physics, 27 (1989), pp. 1731–1747.

[11] ——, *Sharp fronts due to diffusion and viscoelastic relaxation in polymers*, SIAM J. Appl. Math., 51 (1991), pp. 472–483.

[12] D. S. COHEN, A. B. WHITE JR. AND T. P. WITELSKI *Shock formation in a multi-dimensional viscoelastic diffusive system*, SIAM J. Appl. Math, 55 (1995), pp. 348–368.

[13] J. CRANK, *The Mathematics of Diffusion*, 2nd ed., Oxford University Press, Oxford, 1975.

[14] J. CRANK AND G. S. PARK, *Diffusion in Polymers*, Academic Press, London, 1968.

[15] C. J. DURNING, *Differential sorption in viscoelastic-fluids*, J. Polymer Sci. B: Polymer Physics, 23 (1985), pp. 1831–1855.

[16] C. K. HAYES AND D. S. COHEN, *The evolution of steep fronts in non-Fickian polymer-penetrant systems*, J. Polymer Sci. B: Polymer Physics, 30 (1992), pp. 145–161.

[17] C. K. HAYES, *Diffusion and stress driven flow in polymers*, Ph.D. thesis, California Institute of Technology, 1990.

[18] R. W. COX AND D. S. COHEN, *A mathematical model for stress-driven diffusion in polymers*, J. Polymer Sci. B: Polymer Physics, 27 (1989), pp. 589–602.

[19] R. W. COX, *A model for stress-driven diffusion in polymers*, Ph.D. thesis, California Institute of Technology, 1988.

[20] ——, *Shocks in a model for stress-driven diffusion*, SIAM J. Appl. Math., 50 (1990), pp. 1284–1299.

[21] H. L. FRISCH, *Sorption and transport in glassy polymers - a review*, Polymer Engr. and Sci., 20 (1980), pp. 2–13.

[22] T. L. SMITH AND R. E. ADAM, *Effect of tensile deformations on gas transport in glassy polymer films*, Polymer, 22 (1981), pp. 299–304.

[23] D. A. EDWARDS, *Heavily stressed polymer-penetrant system exhibiting two fronts*, Ph.D. thesis. California Institute of Technology, 1994.

[24] C. J. DURNING, D. S. COHEN, AND D. A. EDWARDS, *Perturbation analysis of Thomas' and Windle's model of Case II diffusion*, to appear.

[25] P. C. FIFE, *Singular perturbation and wave front techniques in reaction diffusion problems*, in SIAM-AMS Proceedings, Symposium on Asymptotic Methods and Singular Perturbations, New York, 1976.

[26] ——, *Dynamics of internal layers and diffusive interfaces*, Society for Industrial and Applied Mathematics, Philadelphia, (1988).

[27] W. FLUGGE, *Viscoelasticity*, Springer-Verlag, New York, 1975.

[28] W. G. KNAUSS AND V. H. KENNER, *On the hygrothermomechanical characterization of polyvinyl acetate*, J. Appl. Physics, 51 (1980), pp. 5131–5136.

[29] N. L. THOMAS AND A. H. WINDLE, *A theory of Case II diffusion*, Polymer, 23 (1982), pp. 529–542.

[30] J. S. VRENTAS, J. L. DUDA AND A. C. HOU, *Anomalous sorption in poly(ethyl methacrylate)*, J. Appl. Polymer Sci., 29 (1984), pp. 399–406.

[31] C. Y. Hui, K. C. Wu, R. C. Lasky and E. J. Kramer, *Case-II diffusion in polymers. II. Steady-state front motion*, J. Appl. Phys., 61, 11 (1987), pp. 5137–5149.

[32] J. C. Wu and N. A. Peppas, *Numerical simulation of anomalous penetrant diffusion in polymers*, J. of Applied Polymer Science, 49 (1993), pp. 1845–1856.

[33] D. S. COHEN AND R. ALEXANDER, *Chemical reactor theory and problems in diffusion*, Physica D, 20 (1986), pp. 122–141.

[34] R. L. PEGO, *Phase Transitions in one-dimensional nonlinear viscoelasticity: admissibility and stability*, in Dynamical Problems in Continuum Physics, J. L. Bona et al. eds., Springer-Verlag, New York, 1987.

[35] J. RUBINSTEIN, P. STERNBERG AND J. B. KELLER, *Front interaction and nonhomogeneous equilibria for tristable reaction-diffusion equations*, SIAM J. Appl. Math., 53 (1993), pp. 1669–1685.

References: Chapter 5

[1] J. S. VRENTAS, J. L. DUDA AND A. C. HOU, *Anomalous sorption in poly(ethyl methacrylate)*, J. Appl. Polymer Sci., 29 (1984), pp. 399–406.

[2] J. C. WU AND N. A. PEPPAS, *Numerical simulation of anomalous penetrant diffusion in polymers*, J. of Applied Polymer Science, 49 (1993), pp. 1845–1856.

[3] J. C. WU AND N. A. PEPPAS, *Modeling of penetrant diffusion in glassy polymers with an integral sorption Deborah number*, J. Polymer Sci B: Polymer Physics, 31 (1993), pp. 1503–1518.

[4] C. Y. HUI, K. C. WU, R. C. LASKY AND E. J. KRAMER, *Case-II diffusion in polymers. II. Steady-state front motion*, J. Appl. Phys., 61 (1987), pp. 5137–5149.

[5] T. Z. FU AND C. J. DURNING, *Numerical simulation of Case II transport*, AIChE Journal, 39 (1993), pp. 1080–1044.

[6] C. J. DURNING, D. S. COHEN, AND D. A. EDWARDS, *Perturbation analysis of Thomas' and Windle's model of Case II diffusion*, to appear.

[7] D. S. COHEN AND A. B. WHITE JR., *Sharp fronts due to diffusion and stress at the glass transition in polymers*, J. Polymer Sci. B: Polymer Physics, 27 (1989), pp. 1731–1747.

[8] ——, *Sharp fronts due to diffusion and viscoelastic relaxation in polymers*, SIAM J. Appl. Math., 51 (1991), pp. 472–483.

[9] D. S. COHEN, A. B. WHITE JR. AND T. P. WITELSKI *Shock formation in a multi-dimensional viscoelastic diffusive system*, SIAM J. Appl. Math, 55 (1995), pp. 348–368.

[10] D. D. JOSEPH, *Fluid Dynamics of Viscoelastic Liquids*, Springer-Verlag, New York, 1990.

[11] J. D. MURRAY, *Mathematical Biology*, Springer-Verlag, New York, 1990.

[12] T. P. WITELSKI, *An Asymptotic solution for traveling waves of a nonlinear-diffusion Fisher's equation*, Journal of Mathematical Biology, 33 (1994), pp. 1–16.

[13] A. KOLMOGOROV, I. PETROVSKY AND N. PISCOUNOFF, *Study of the diffusion equation with growth of the quantity of matter and its application to a biology problem*, in Dynamics of Curved Fronts, Pelce, P. ed., Academic Press, Boston, 1988.

[14] I. STAKGOLD, *Green's functions and boundary value problems*, J. Wiley, New York, 1979.

[15] N. L. THOMAS AND A. H. WINDLE, *A theory of Case II diffusion*, Polymer, 23 (1982), pp. 529–542.